THESIS

DEVELOPMENT OF A SOLID HUMAN WASTE SEMIGASIFIER BURNER FOR USE IN DEVELOPING COUNTRIES

Submitted by

Nathan Loveldi

Department of Mechanical Engineering

In partial fulfillment of the requirements

For the Degree of Master of Science

Colorado State University

Fort Collins, Colorado

Summer 2014

Master's Committee:

Advisor: Anthony J. Marchese
Co-Advisor: Morgan DeFoort

Sybil Sharvelle

ABSTRACT

DEVELOPMENT OF A SOLID HUMAN WASTE SEMIGASIFIER BURNER FOR USE IN DEVELOPING COUNTRIES

Recent estimates suggest that approximately 40% of the world's population does not have access to an adequate sanitation system. This lack of access is one of the major causes of child mortality, mainly due to diarrhea. In an attempt to increase access to sanitation, the Bill and Melinda Gates Foundation proposed a program called the Reinvent the Toilet Challenge. The challenge is to develop sustainable toilets that can be used in areas without an electrical grid or sanitary plumbing. These criteria allow the toilet to be placed in rural areas without access to an electrical grid and in environments where water is scarce.

This thesis describes the design and development of a solid human waste semi-gasifier burner for use in developing countries that was developed in response to the Reinvent the Toilet Challenge. The incineration process was chosen because the high operating temperature ensures the elimination of pathogens. The device was developed by understanding the fundamentals of fecal material combustion. Several design iterations were constructed to systematically optimize the critical variables. Those variables include char production, air flow rate requirement, ignition sequence, and power source requirement.

The result is a prototype powered by a single 12 Volt battery that can incinerate solid waste. A thermoelectric generator is used to harvest the heat from combustion and convert the heat back into electricity. The exhaust gas from the combustion is used for drying of fecal material. Both the thermoelectric generator and exhaust gas usage provide a sustainable energy source for the toilet.

ACKNOWLEDGEMENTS

First of all, I would like to thank God for His guidance throughout my life as the lamp unto my feet. Secondly, I would like to thank Dr. Morgan DeFoort, Dr. Anthony Marchese, John Mizia, and Dr. Sybil Sharvelle for the guidance and support on this wonderful project. I would like to give special thanks to John Mizia for guiding me every day from the first day I came to the lab. Now I can say that I have irreplaceable time to work under his wing. I would like to recognize my coworkers that have helped me for their caring and help including Jason Prapas, Sean Babbs, James Tillotson, Evan Hoffman, Andrew Andraski, Annie Lelek, Mark Kollash, Andrew Thompson, and Marc Baumgardner. I would like to thank the sponsors of the research, which include Colorado State University, the Bill and Melinda Gates Foundation, and the Research Triangle Institute, for their support on the pursuit of global sanitation. I hope that this thesis can be a reflection of everyone's contribution for the greater good of this world.

TABLE OF CONTENTS

LIST OF FIGURES

LIST OF TABLES

1. MOTIVATION

1.1 Motivation

In the year 2000, the United Nations created a Millennium Declaration which stated that, by the year of 2015, it would reduce children's mortality by approximately 60%, and provide access to clean water to 50% of the people who currently do not have clean water [1]. A major issue that intertwines both goals is sanitation. Sanitation is an issue that contributes to both children's mortality and preventing the access to clean water. Currently, the lack of sanitation access is experienced by 2.4 billion people worldwide [2]. Out of the 2.4 billion, there are approximately 1.5 million child deaths due to diarrhea every year which are attributable to poor sanitation [3]. The situation is caused by the fact that 90% of sewage in developing countries is discharged untreated, often times directly into water ways.

The Bill and Melinda Gates Foundation decided to focus on this issue. They started a project called the Reinvent the Toilet Challenge (RTTC). Colorado State University decided to take part in this challenge in conjunction with the Research Triangle Institute (RTI). CSU approached this challenge by building a toilet that sanitizes the waste completely through incineration. The proposed toilet would be able to sanitize the waste without any external power or water source. If successfully implemented, such a device would increase the access to a sanitation system for the billions of people who currently lack such access.

1.2 Toilets in Developing Countries

As previously stated, roughly 90% of the sewage in developing countries is discharged untreated with the majority being disposed of by two conventional methods [4]. The first method is to drain it to a river (or other body of water) untreated with pathogens contained in the solid waste. In most developing countries, for example, one village along the river will take their drinking water from upstream in the river, have a bath, and create a toilet that dumps the waste straight to the river downstream. They may not consider that there are other villages downstream who will also take the water from the now contaminated river. The second method commonly used to treat sewage is to drop it into a large pit [4]. While this approach does not provide great improvement, the soil does act to remove nutrients and pathogen. This treatment imposes a risk when wastewater contaminates the ground water. Concrete land pits have been developed but these pits require regular cleaning. The person whose job it is to clean the pit is shown in Figure 1 [5]. A highly un-sanitized work environment might influence the health of the people who work in the pit.

Figure 1. A "frogman" cleans out a latrine put in Tanzania [4].

1.3 Problem with Conventional Toilet and Sewage System

A solution to the sanitation problems in rural areas cannot be achieved with a conventional toilet system. The innovations for conventional toilets have not been pushed since the early 19th century [5], shown in Figure 2. The basic technology used for current day toilet requires massive infrastructure for plumbing and power, which have not changed since the early 19th century. The cost to build the infrastructure of the wastewater system is enormous, and beyond the capability of the very people that needs sanitation access. The infrastructure includes wastewater collection, transport, and treatment, with each one cost significant capital investment. The conveyance of the waste in developed country is conducted on city scale where the waste is transported to the wastewater treatment facility in the city, which does not exist in developing countries.

Figure 2. Modern flush toilet on the late 19th century and current design of Toto.

1.4 Approach of this Application

CSU has been in a research field of developing biomass cook-stoves for the past decade. This knowledge in biomass combustion can be applied into developing incineration toilet. Incineration is one method that can be applied to sanitize the waste by increasing the waste temperature. When waste reaches flame temperature, pathogens in the fuel can be killed. Incineration is a favorable method because of two reasons. First, the operating temperature of the burner is high, and therefore the heat can be used for various purposes, such as exhaust gas channeling, in a thermoelectric generator, or heating device. Second, the rate of sanitation of this design is relatively fast since the waste can be incinerated and sanitized within hours. A faster sanitation rate means that a smaller device can be used when compared with slower sanitation methods. For example, the composting toilet requires about a week residence time until the waste is sanitized [13], which means that it requires a larger design.

2. THEORETICAL BACKGROUND

The incineration method to treat waste has been commonly applied in industry. However, the common method is viapropane combustion, which requires a propane tank. To develop this design as a self-sustaining burner, propane cannot be used. Rather, the waste itself can be used as a fuel. This implies that for the best fit technology for this application is significantly different than common incineration toilet.

The general overview of solid waste sanitation process is shown in Figure 3. The waste is first fed into a dryer to reduce the waste's moisture content. The dried mass is then conveyed into a combustion chamber where the biomass is ignited and incinerated. The heat developed from this process is used to produce electricity by using TEG (Thermoelectric Generator). On the other hand, the exhaust gas from the combustion will be channeled to the dryer. This exhaust gas has a temperature above $300^{o}C$, which can be used as heat source for to accelerate drying process.

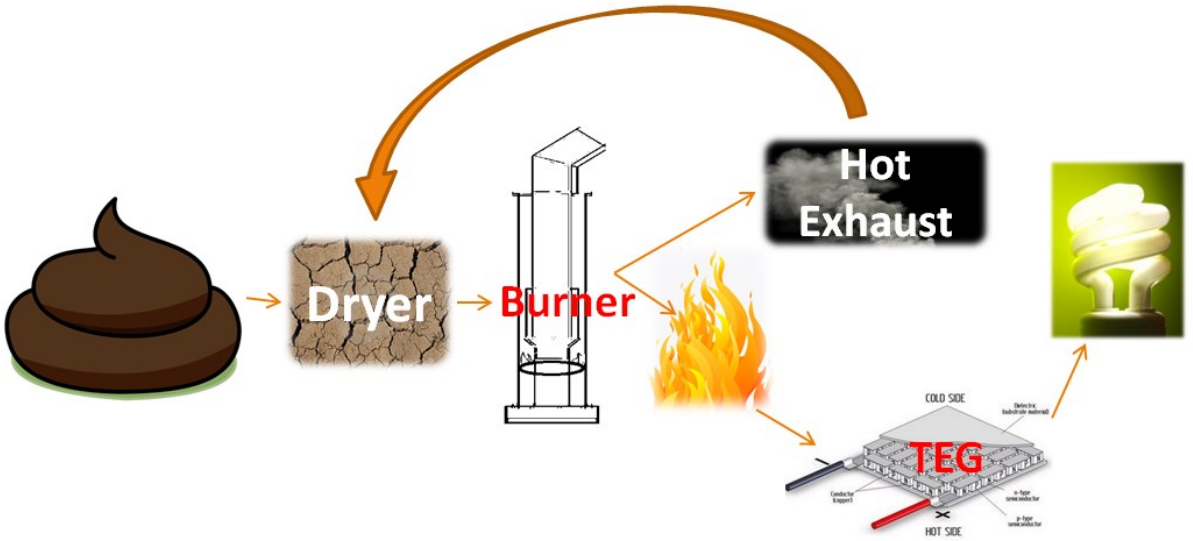

Figure 3. Solid waste overall treatment process.

Each component on Figure 3 can be expanded further to understand the theoretical backgrounds that are needed to understand this thesis. Phenomena such as feces composition, drying, pyrolysis, gasification, and combustion will be discussed in the following few sections. The final section of this chapter will discuss different methods to apply the theoretical backgrounds through selections of gasifier systems.

2.1 Properties and Composition of Human Feces as Solid Fuel

2.1.1 **Shape**

Human waste can be characterized by several criteria such as color, shape, and texture. Lewis (1997), University of Bristol, developed the Bristol stool form scale [17]. This scale is used to categorize stools using everyday words. The scale goes from one to seven: one as a very hard, nut shaped lump, and seven as liquid. The scale plays an important role for the scope of

this application, because the large individual shape of the waste will clog the burner. A pelletized shape waste is desired for this application because the wastes can combust more efficiently without clogging the burner. However, to determine the optimum pellet size for combustion is difficult due to the transient nature of the burns.

2.1.2 **Heating Value**

Heating value can be defined as energy content per unit weight, measured in MJ/kg. Heating value is very essential in any burner system, because heating value is an indication of the fuel quality. There are two types of heating values that can be measured for solid fuel: Higher Heating Value (HHV) and Lower Heating Value (LHV) [19]. The main difference between those two values is the water production. HHV is measured by assuming that the water that comes from combustion product condenses, and therefore, adding energy. The LHV considers that water from the combustion product evaporates, and therefore, subtracts energy out of the output. The relationship between HHV and LHV is shown in equation 1:

(1) $$HHV = LHV + \frac{m_{H2O}}{m_{total}} * h_v$$

where HHV is the higher heating value, LHV is the lower heating value, m_{H2O} is the mass of water produced by combustion, m_{total} is the total mass of the fuel, and h_v is the heat of vaporization. A previous study by the Energy Research Centre of Netherlands (ECN) (2009) [18] suggests that the dry feces has a HHV of 15.1 MJ/kg and LHV of 14.03 MJ/kg.

2.1.3 **Composition**

The measurement of C, H, and O percentage determines the fuel characteristic. Based on Barneto, 2009 [19], human waste consists of 27.16 % C, 4.62 % H, 4.91% N, 1% S and 22.37 % O. All these percentages are in dry matter basis. When the dry waste is incinerated, the C, H, and O will react with air and converted into combustion products. The residue after incineration is ash ranging from 40~55% and is comprised of mostly inorganic element. Comparing data from Barneto, ECN (Energy Research Centre of Netherlands) [17] stated that human waste contains 30.63% C, 4.41% H, 4.23% N, 1.17% S, and 18.03% O. The difference between the data is the percentage of C and O. The difference is likely due to diet and geographic differences of the samples. Taking the average of the two data, human waste can be written as $CH_2N_{0.1}S_{0.01}O_{0.6}$. However, only C, H, and O reactions are important in this molecule, because the percentage of S and N reactions is low (0.01% and 0.06%) [28].

2.1.4 **Fuel Surrogates**

Because of the regulations and the practicality, using human waste as an experiment fuel is not feasible. Therefore, fuel surrogates were used during the early stage of the project, which are wood pellets and dog waste. Wood pellet was used to simulate dry human waste because it has similar lower heating values to human waste. The LHV of wood pellets is 16.2 MJ/kg [20]. Dog waste was used due to the similarity in diet with humans, which implied that the waste should have similar composition. In addition to the characteristic of the fuel, the following section will discuss the phenomena that are related within the scope of this application.

2.2 Drying Process

As previously discussed, wet human waste are not capable of producing combustion, which implies that the drying is required. Biomass drying can be separated into two different steps. They are the evaporation of water from solid material and the removal of the water vapor with the flow of air. The flow of air is required to regulate the vapor pressure around the material as saturated air around the material will prevent evaporation. Luboschik, 1999 [23], explained the case of sewage sludge by solar drying in two stages. The first stage of drying is done mechanically with a screen belt until moisture level drops to 80% wet basis, and then the sludge is applied to intensive aeration. Mathinoudakis, 2009 [24] performed an extended period of solar drying to study the effect of seasonal change on drying performance. Based on his paper, drying with solar energy requires at least 7 days. Deng, 2009 [25] utilized a contact drying where the heat was supplied with a hot surface, and the convective air current took the moisture away.

The main indication of drying is moisture content. There are two different ways to define moisture content within each material: dry basis or wet basis. Indicating moisture content on wet and dry bases is shown on equation 2. MC is moisture content (%), m_{wet} is the initial mass of the material and m_{dry} is the final mass of material after it is completely dried. In this application, all the moisture content data will be expressed in wet basis. [27] Dry basis is not used because if mass of water is greater than the dry mass, the expression might exceed 100%, which is confusing for reader.

(2) $$MC_{dry} = \frac{m_{wet} - m_{dry}}{m_{dry}} \qquad MC_{wet} = \frac{m_{wet} - m_{dry}}{m_{wet}}$$

2.3 Pyrolysis

The drying process described in the previous section is only relevant up to approximately 100^{o}C. As the temperature reaches 300^{o}C, Pyrolysis process becomes more important than drying. The pyrolysis process is a very complicated process, and the detail of the process is beyond the scope of this thesis. This section will only discuss an overview on pyrolysis. The name pyrolysis consists of the word *pyro* which means heat and the word *lysis* which means degradation. Pyrolysis means a thermochemical process where a degradation of biomass by heat occurs in the absence of air.

The application of pyrolysis is usually designed for solid organic compounds that contain hydrocarbon chains. Overall, pyrolysis has several processes as seen in Figure 4. When heat is applied, the hydrocarbon bonds are broken, which then produces two types of products. The first product is volatile compounds. Volatile compounds are usually desired because they can be the fuel for combustion in the form of tar and syngas. Tar is a highly viscous liquid fuel that is unstable in nature, where syngas is a combustible gas that consists of mostly methane, CO, and H_2. Whether the volatile will form into gas or tar depends on the certain conditions, such as pyrolysis temperature, pyrolysis heating rate, and heat loss rate [27]. The second product of pyrolysis is char. Char is the leftover after all the volatiles leave the biomass. Char consists mostly of carbon, and burns like charcoal.

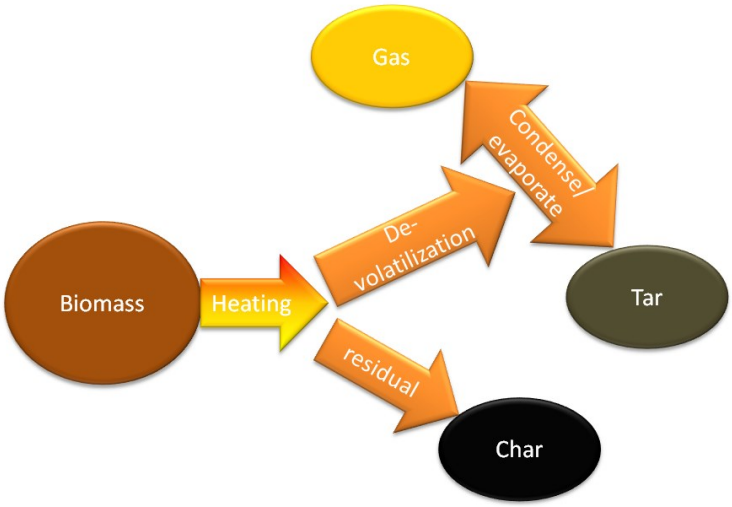

Figure 4. Pyrolysis Overall process.

2.4 Gasification

Because pyrolysis occurs at high temperature, it can sanitize the waste. However, pyrolysis is inherently an endothermic process, and it requires energy as an input. This energy can come via gasification. The Gasification process can be defined as the addition of less than stoichiometric oxidizer to the hot zone of pyrolysis. By adding oxidizer to the hot zone of pyrolysis, exothermic reactions can occur and produce an energy feedback for the pyrolysis. The exothermic reactions create sustainable operations to the overall process, which means that gasification does not require outside energy source as long as the air is supplied. On top of that, higher operating temperature of gasification results in char gasification and tar evaporation. All the processes produce gaseous products. Gaseous products are more desirable for this application, because they are more easily treated.

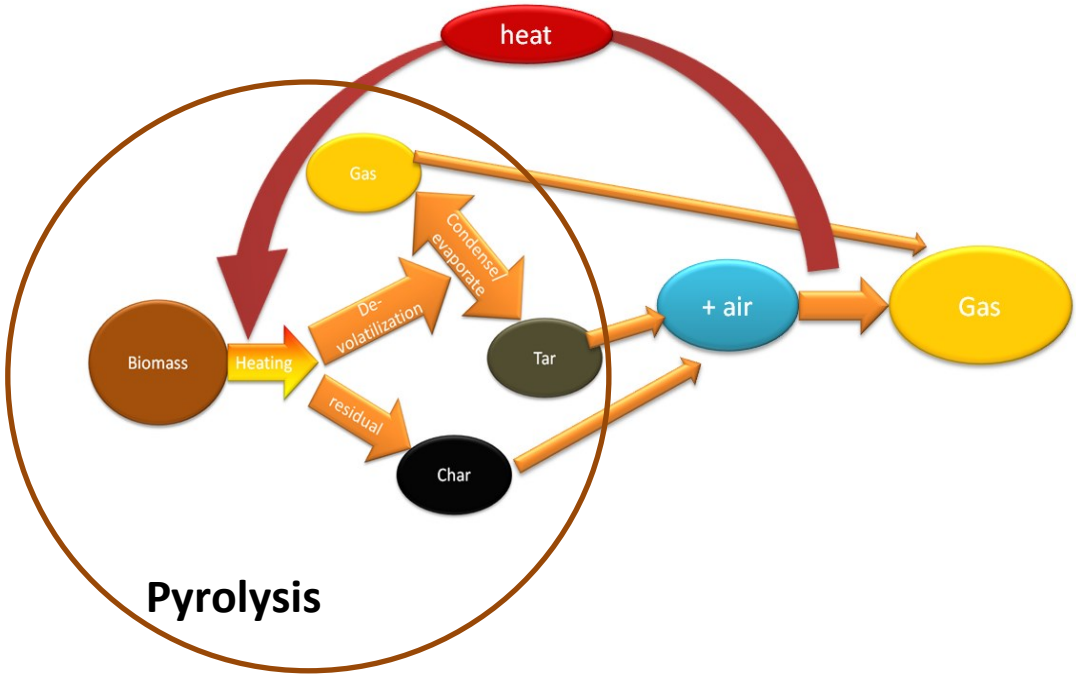

Figure 5. gasification overall schematic process.

2.4.1 **Gasification Chemical Kinetics**

The previous discussion explained the overall process of gasification and the advantages of the gasification process. This section will explain more in depth the gasification process. An ideal one step reaction of gasification is shown in equation 3.

(3) $$CH_{1.4}O_{0.6} + 0.2\ O_2 \rightarrow CO + 0.7\ H_2 \qquad \Delta H = 0\,\frac{kJ}{mol}$$

Typical biomass ($CH_{1.4}O_{0.6}$) [28] reacts with O_2 to produce CO and H_2 with the net change of enthalpy is equal to zero. Unlike complete combustion that produces CO_2 and H_2O, the amount of oxidizer in this reaction is below stoichiometric conditions, which implies that the reaction is oxygen deprived. The reactions do not produce flame, but instead, produces syngas. The kinetics

of the reactions are complicated; however, a further discussion can be conducted from major processes in gasification. Some of them to be discussed are:

1. Pyrolysis
2. Exothermic reactions
3. Tar cracking
4. Char gasification process

These processes are the major process within the overall gasification scheme. Pyrolysis needs to occur before other reactions to produce the initial syngas. When the initial syngas is produced, primary combustion can be produced by introduction of primary air. Complete combustion products, such as CO_2 and H_2O are produced from the primary combustion, which then is reduced back to CO and H_2 through char gasification. The last process that occurs is the tar cracking, in which the tar is vaporized by the energy from exothermic reactions.

2.4.2 **Exothermic Reactions**

The previous section discussed the process of pyrolysis and therefore, the following sections will only discuss the other three processes, starting from exothermic reactions. Exothermic reactions occur when the fuel makes contact with air, which occurs upstream of the other two processes. The four overall exothermic reactions are shown in Table 1. All the enthalpy of reactions in Table 1 have negative values, which indicate that energy is produced. The energy from these reactions is supplied to the endothermic pyrolysis reactions. The products of these reactions are CO_2 and H_2O, which is why these reactions are commonly called primary combustion.

Table 1. Exothermic reactions in gasification [37,38].

Oxidation molecules	Chemical reactions	Enthalpy of reactions (kJ/mol)
Carbon	$C + O_2 \leftrightarrow CO_2$	-394
Carbon Monoxide	$CO + 0.5\ O_2 \leftrightarrow CO_2$	-284
Methane	$CH_4 + 2\ O_2 \leftrightarrow CO_2 + 2\ H_2O$	-803
Hydrogen	$H_2 + 0.5\ O_2 \leftrightarrow H_2O$	-242

2.4.3 **Tar Cracking**

Tar is a mixture of condensable hydrocarbons [27]. Tar is sticky and viscous liquid, which is produced by pyrolysis when the gas temperature decreases below dew point. The production of tar is not a commonly desirable for several reasons. First, tar has low energy content, and is not suitable to be used as fuel. Second, it is unstable in nature due to the concentration difference of each hydrocarbon species in the mixture. Third, it is highly viscous and sticky which causes the gasifier to clog. These reasons lead to the need for tar elimination.

There are several methods of tar elimination. The methods are post reduction and in-situ reduction. The post reduction method requires extra equipment that is relatively more expensive than the in-situ cleaning. In-situ cleaning is a preferable method for this application, and can be accomplished by modifying the operation conditions, which are pressure and temperature. An increase of pressure in gasification reduces the production of tar in general [33]. However, elevation of pressure is difficult to accomplish with limited power supply. Temperature is an easier operating condition to adjust than pressure. As stated before, the hydrocarbons condense and form tar at the temperature below 500^{o}C. Therefore, an operating temperature higher than 500^{o}C will vaporize the tar.

2.4.4 **Char Gasification**

Char is the leftover of the pyrolysis process, which consists of mostly carbon. In the char gasification process that occurs downstream of the primary combustion, char is further gasified with oxidizer to form syngas. The products of primary combustion, which are CO_2 and H_2O, are converted back to CO and H_2. These conversions are shown in Table 2. The reactions in this table are based on air gasification, which will be a different if the gasification medium is steam or pure oxygen.

Table 2. Char Gasification Reactions [36, 37].

Reaction Type	Chemical Overall Reactions	Enthalpy of reactions (kJ/mol)
Boudouard reaction	$C + CO_2 \leftrightarrow 2\,CO$	+172
Water-gas reaction	$C + H_2O \leftrightarrow CO + H_2$	+131
Hydrogasification reaction	$C + 2\,H_2 \leftrightarrow CH_4$	-74.8
Char Reaction 4	$C + 0.5\,O_2 \leftrightarrow CO$	-111
Char Reaction 5	$C + O_2 \leftrightarrow CO_2$	-394

Examining the table, Bouduard reaction occurs for converting back the CO_2 into CO. Boudouard reaction is considered a fundamental reaction that produces CO. Some other literatures [28] have stated that it is also called reduction reaction. Water-gas reaction is an important reaction that produces CO and H_2 from water and char. The final reaction that occurs is hydrogasification reaction, converting hydrogen to methane.

2.4.5 **Gasification Summary**

These sections are not meant to be a detail discussion about gasification. Nonetheless, some points can be taken from these sections.

a. Gasification produces syngas, which consists of mostly CO and H_2 with the basis of pyrolysis reactions.
b. Addition of air is needed to oxidize a small percentage of syngas to provide the energy back to the endothermic pyrolysis reactions. Gasification is a self-sustaining process as long as adequate oxidizer present inside the gasifier.
c. Tar production can be reduced by increasing the temperature of the vessel to above 800^oC. With temperature above 800^oC, tar is cracked and vaporized.
d. Char gasification reactions can further converted char into pyrolysis gas, such as CO, H_2, and small amount of CH_4.
e. The amount of oxidizer in gasification is lower than stoichiometric condition, and therefore gasification produces incomplete combustion products.

2.5 Semi-Gasification Combustion

As previously discussed gasification produces a syngas from solid biomass, which can ultimately be used as a fuel in a burner. Combustion of syngas after it exits the gasifier is called secondary combustion. Due to the multiple species contained in syngas, chemical kinetic of syngas combustion is complicated, therefore only CO and H_2 would be taken into consideration, because they have the highest concentration in syngas.

2.5.1 **Carbon Monoxide Oxidation**

Some of the important reactions of CO oxidation are shown in Table 3.

Table 3. CO oxidation reactions [42,43].

Reaction	Chemical Overall Reactions	Enthalpy of reactions (kJ/mol)
1	$CO + O_2 \leftrightarrow CO_2 + O$	+47.69
2	$O + H_2O \leftrightarrow OH + OH$	+13.40
3	$CO + OH \leftrightarrow CO_2 + H$	-0.765
4	$H + O_2 \leftrightarrow OH + O$	+16.44
5	$CO + O + M \leftrightarrow CO_2 + M$	-4.54

Inherently, Carbon monoxide does not have the capability to produce ignition. If CO and O_2 are mixed without any other species present (shown in reaction 1), the reaction does not create branching radicals [42]. Without branching radicals, combustion cannot be sustained. However, if there is any hydrogen molecule present, branching reactions can occur with H molecules as catalyst. Reaction 2 and 4 are the branching reactions with H molecules present.

2.5.2 **Hydrogen Oxidation**

Hydrogen combustion is the most basic combustion mechanism, because it has the least amount of species in comparison with other molecule mechanism. The full understanding of the mechanism can be found in paper published by Fred. Dryer, 2004 [45].

A discussion has been conducted about the related physical phenomena. To further understand the implication of these phenomena, a discussion can be conducted on the gasifier systems. These systems are different approaches that have been conducted to apply these physical phenomena.

2.6 Pyrolyzer

Pyrolyzer is a device that produces pyrolysis in its chamber. The device usually consists of a sealed chamber, and heating element. The biomass inside the pyrolyzer will be converted into syngas, tar, and char. Depending on the need of the user, the products yield can be adjusted. Due to the endothermic nature of pyrolysis, it is impossible to create a pyrolyzer that is energy neutral; therefore, a pyrolyzer is usually used on research application in order to give a better understanding of the pyrolysis process. An improved pyrolyzer by Tyden-Ericsson [46] is an example of a pyrolyzer used for research.

2.7 Gasifier System

Gasifier has been used extensively for about 200 years. It is attractive because its syngas can be produced from abundantly available biomass. With high efficiency, gasifiers are able to convert the biomass energy to be used for natural gas engines. Deciding on which design will

produce the efficiency needed for this application require some understanding of different gasifier types, shown in Figure 6.

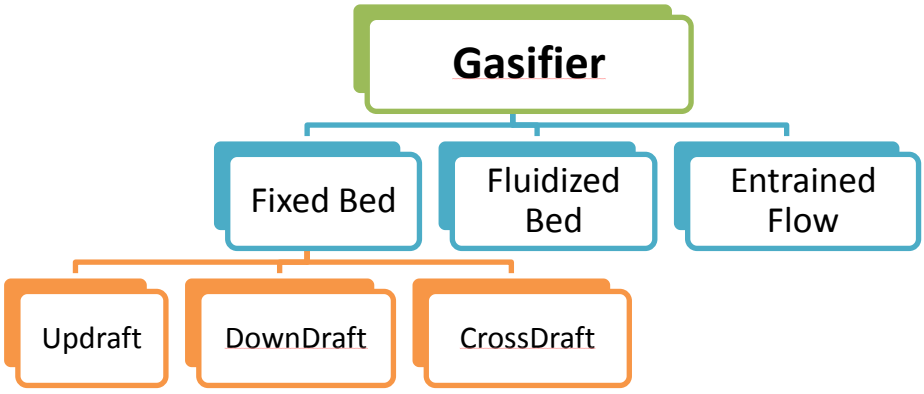

Figure 6. Different Gasifier Systems.

Each type of gasifier is used for different applications due to different characteristics. The gasifier systems in this section are updraft, downdraft, crossdraft, and fluidized bed. For the scope of this application, the entrained flow gasifier will not be discussed due to their high thermal output [27].

2.7.1 **Updraft Gasifier**

Updraft gasifier, as the name suggest, indicates an upward flow of syngas. The biomass is fed from the top and the air comes from the bottom. The air that is introduced at the bottom produce the exothermic reactions that heats up the reduction and pyrolysis zones, which produce the hot gas. The hot gas then passes through the drying section and flows out of the gasifier. The process of the updraft gasifier is shown in Figure 7 [27,28]

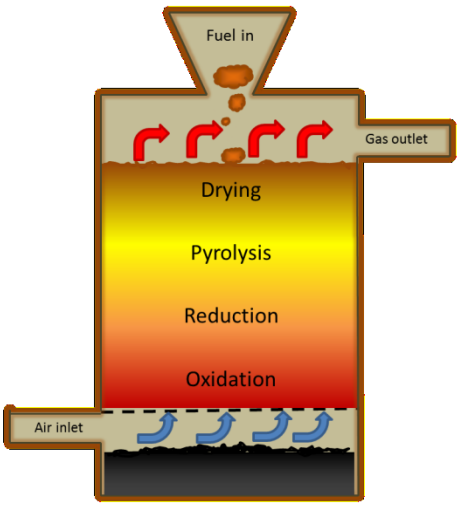

Figure 7. Updraft Gasifier.

There are several advantages of an updraft gasifier. First, the design of updraft gasifier is simple. The simplicity comes from the fact that the updraft only requires a chamber to hold the fuel. Second, updraft gasifier is very susceptible to various fuel; even the fuel low volatility and high ash content. Third, the thermal efficiency of updraft gasifier is relatively high. The gas that is flowing upwards will heat the incoming fuel, which implied a small heat loss to the outside of gasifier.

On the other hand, an updraft gasifier also has some disadvantages. First, the tar production in updraft gasfier is high. The temperature of syngas that is heating the incoming fuel might drop below the dew point. Condensation might occur as the gas temperature goes below dew point. Second, the temperature at the grate has to be limited. With oxidation region at the grate, the energy release from exothermic reaction might damage the grate. Third, updraft gasifier produces higher charcoal leftover in comparison to other gasifiers. High volume of charcoal means that the conversion efficiency from the biomass to gas is low.

2.7.2 **Downdraft Gasifier**

A downdraft gasifier is indicated with a downward flow of syngas. Like the updraft, the biomass in a downdraft gasifier is still fed from the top, but the air is introduced downstream. The air oxidizes the biomass downstream and forces the gas to flow downwards. As it is shown in Figure 8, the combustion zone (oxidation) and reduction zone in downdraft are flipped from the updraft. The reduction zone in a downdraft is below the combustion zone, which implied that the gas production from the reduction went straight out of the gasifier instead of passing through the fuel bed like in the updraft.

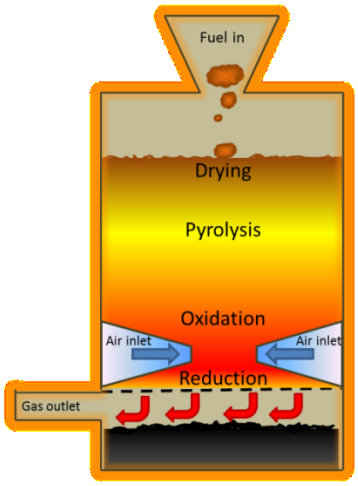

Figure 8. Downdraft Gasifier.

There are some advantages to a downdraft gasifier. First, the tar production of downdraft gasifier is low. The gas that is produced in the reduction zone exits downwards while the temperature is still high. The high temperature will prevent the gas from condensing and allows tart to stay in vapor form. Downdraft gasifier usually does not require significant maintanace due to low tar production. Second, all the hot reactions are located further downstream from the inlet. The addition of fuel upstream of a downdraft gasifier will not affect the process further

downstream. This allows for continuous feed into the gasifier. Third, a downdraft gasifier is ignited faster than other types of gasifier, because of the throat. With faster ignition, downdraft gasifier would require less ignition energy.

The disadvantages of the downdraft gasifier are counterparts of the updraft gasifier. First, the downdraft gasifier is not thermally efficient for drying the incoming fuel. Second, the downdraft gasifier cannot operate on various shape of fuel. The performance is only optimized on pelletized fuel. The moisture content of incoming fuel is also limited to ~30% [28]. Third, the gas that is produced contains high concentration of ash. Gas cleaning devices are commonly attached to a gasifier to increase the purity of the gas. Additional components will raise the cost of the device.

2.7.3 **Cross-draft Gasifier**

As its name suggests, a crossdraft gasifier has a process that is flowing horizontally. The schematic of a crossdraft gasifier is shown in Figure 9. Crossdraft gasifiers have not been widely applied throughout history, and there have not been many literatures that show the development of crossdraft gasifier. This gasifier is not favorable for application because there are no clear boundaries on where the drying, pyrolysis, or combustion zones are.

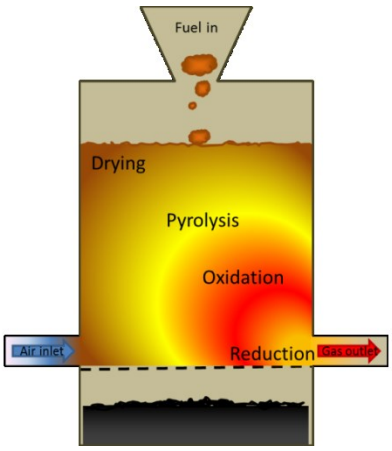

Figure 9. Crossdraft Gasifier.

2.7.4 **Fluidized Bed Gasifier**

A Fluidized Bed Gasifier is a system with air supplied from the bottom and fuel is fed from the top, shown in Figure 10. The fuel for fluidized bed gasifier is commonly had been pelletized. Inside the gasifier, the fuel landed on top of the bed of inert particles, such as sand. The inert materials are used as heating mass medium for the fuel. Air is supplied from the bottom at high velocity such that the fuel and inert material mixture is suspended in the air. High mixing occurs due to the suspension of this mixture, which increase the gasification rate. Unlike the previous gasifier, there is no clear zone in which the fuel is being dried, pyrolized, oxidized, or reduced. Constant mixing of the suspended bed causes different zones to occur within each fuel particle. The sum of surface area of each particle is much larger than other gasifiers. Increase of surface area results in the increase of gasification rate, which is beneficial to the user.

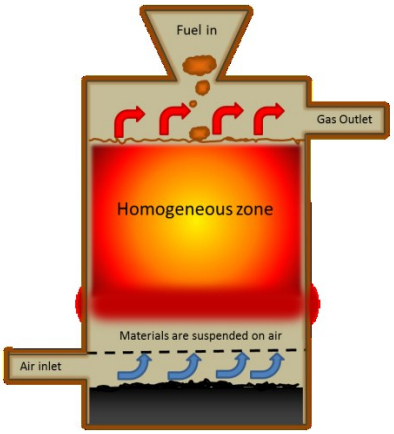

Figure 10. Fuidized Bed gasifier.

Fluidized bed gasifiers are not suitable for small energy burner. The construction of this gasifier is more complex than other gasifiers, because it requires high air velocity to suspend the fuel and inert particles in the air. To have enough air pressure to fluidize the bed, the gasifier requires a large air compressor which is not in favor of energy neutrality.

Morris, 1998 [14] developed a plant scale gasifier to recover energy from solid human waste with engine or gas turbine. The system was able to consume 600 tons of solid waste per day with the power output of 26.5 MW. Kim, 2013 [49] developed a fluidized bed gasifier and experimented with different equivalence ratios for one hour time periods.

2.8 Pros/Cons of gasifier

A table of pros and cons for each gasifier system was created to choose which system fits the criteria of this project.

Table 4. Pros/Cons of Gasifier Systems.

Gasifier system	Pros	Cons
Updraft gasifier	1. Simple 2. High thermal efficiency 3. Take on high moisture fuel	1. Low LHV gas 2. High Tar 3. Material limitation on grate
Downdraft gasifier	1. Low tar 2. Low maintenance 3. Fast ignition 4. Consistent process as fuel is added	1. Thermally inefficient 2. Need shaped and dried fuel 3. High ash exhaust
Crossdraft gasifier	1. Good for micro application	1. Has not been developed properly 2. Vague zones area
Fluidized bed gasifier	1. High mixing 2. High surface area of reactions 3. Homogeneous 4. Stable temperature	1. High energy requirement 2. Need to be built on big scale 3. High number of extra components 4. Slow ignition

2.9 Manure gasifiers

Manure has been one of the most extensively used biomass for gasification application. With the abundance of supply in the farm, the gasifiers for manure have been well established as a product. Some of the manure gasifiers also incorporated a combustion chamber that combust the pyrolysis gas. These system sanitize similar waste with RTTC application, however there are two major differences, which are waste composition and gasifier size. The waste composition of manure is different from human feces due to the high fiber content. The diet that is taken by the animals consists of mostly grass, which results in a high fiber waste. If the manure gasifiers are designed to burn high fibrous biomass, it would not operate efficiently with a low fiber human waste. The manure gasifiers also have a very large size. These gasifiers are meant to input waste in an order magnitude higher than RTTC application. The size drives the cost of production to be high, which would not be feasible for developing countries buying power.

2.10 Semi-gasification Burner

A semi-gasifier burner is a burner that uses a gasifier at its base. The following Figure shows a schematic of semi-gasifier burner. The primary air comes from the bottom and reacted with biomass to produce the syngas. Unlike gasifier, the burner does not channel the gas out, but instead, combust the gas. The gas temperature from the gasifier is high enough, such that when it is mixed with a newly introduced oxidizer, called secondary air, the gas would combust. The combustion of syngas at this stage is called secondary combustion.

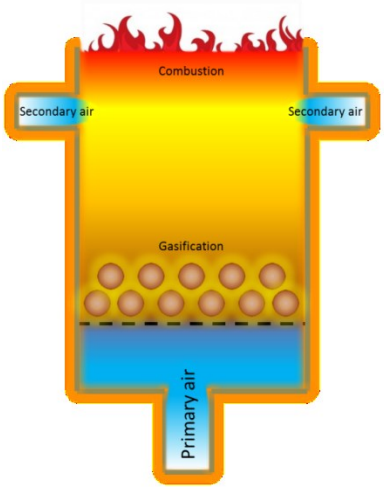

Figure 11. Semi-gasification burner.

The concept of semi-gasification is attractive to a lot of people because of some advantages. First, by burning the biomass with semi-gasification, it is possible to reach combustion efficiency that is higher than the traditional biomass burner [51]. Harmful CO production is reduced with higher combustion efficiency. Second, the burner is usually shrouded with the secondary air gap. Some of the combustion energy is used to heat the gap. With a pre-heated secondary air, combustion efficiency can be further increased. Third, when it is used for cooking, it is able to achieve higher stove efficiency than other wood stoves that burn the wood by using natural draft. Higher stoves efficiency for the stove means that it consumes less wood for a given cooking application. Fourth, in comparison with the gasifier, the burner operates at much higher temperatures. With higher temperature in the chamber, the burner has enough energy to vaporize most of the tar. There are, however, some disadvantages to the semi-gasification process. First, the syngas that is being combusted consists of a high concentration of carbon monoxide. If the secondary air configuration is inappropriate, the CO will be exhausted to the atmosphere. Too low of secondary air will cause oxygen deprivation within the chamber, and

the CO will not be oxidized into CO_2. Too high of secondary air flow will cools down the chamber due and resulted in an exponentially lower reaction rate of CO.

2.11 Design for this Application

The design for this application is ultimately called a downdraft semi-gasifier burner. The design would a hybrid of dowdraft gasifier and semi-gasification burner. The downdraft produces the gas at the bottom section, and secondary air is introduced at that section. The addition of secondary air implies the technology of semi-gasification burner. There are three reasons why this design is developed. First, the downdraft gasifier has consistent flame during fuel addition. Even when fuel is added at the top, it will not affect the performance of the burner. Second, the syngas is combusted at much faster rate. Downdraft gasifier produces higher gas temperature in comparison to other gasifier designs. The hot gas that just exits the reduction zone is mixed with secondary air, which resulted in higher CO oxidation rate than colder gas.

3. DESIGN AND EXPERIMENTAL BACKGROUND

Previous chapter focused on the theoretical background, but this chapter will focus on directing the theory to the respective development. This chapter will discuss the scope for this project to focus the development within a required boundary. The scope for this project is to only develop the burner; therefore more effort was spent more on combustion process than drying process. After the scope was determined, requirements were determined as a goal of the scope. Some of the requirements include MCE, Energy source, Firepower, etc. The requirements from this burner intertwine each other, which makes it difficult to measure development. Therefore, Technology Readiness Level (TRL) is used to segregate the development. The final section of this chapter will discuss the experimental apparatus to reach the goal.

3.1 Task Scope

The primary task for this project is to design a device that will process human feces into a non-hazardous material. Although drying is an important aspect, the task that was specified does not include the drying process. The burner was meant only to incinerate human feces that have been dried and pelletized. The scope indicates that the usage of fuel surrogates is acceptable. An additional task was given to the burner before the development started that the burner has to supply the energy it produces to power the dryer and TEG. The energy form needed by the dryer is the exhaust gas, while the energy for TEG is the heat. Therefore, the design of the burner was adjusted to fit these secondary tasks.

3.2 Design Criteria

Typical burners are usually used as a heat source, to fulfill some energy applications. The application may be cooking or space heating. However, the burner for this project is not designed for energy application. Since the goal is different, the criteria of the burning process are also different. The criteria are developed from several questions that are developed from the task scope. Those questions include:

1. Can the waste be sanitized?
2. How many active users per day?
3. How can we reduce the energy consumption?
4. Can you produce clean combustion?
5. What rate should the waste is sanitized?

To properly measure the sanitation performance of this burner, the leftover of the combustion should be put through a lab test for pathogen colonies. Since there will be numerous experiments conducted in developing this prototype, measurement through the lab will take long and tedious process. Therefore, some assumptions need to be made on the measurement scale. The most common bacteria found on feces are *Eschericia coli*. These bacteria will be killed at the temperature above 350 K [50]. This temperature is much lower than any combustion temperature, and hence, the feces can be sanitized.

After sanitation, a requirement was pre-determined on how many people would use this toilet daily. The requirement was for the toilet to able to contain five waste loads at any given time. Each waste load was determined to be an average dry feces mass each person produce at a

given day. Each people produce about 0.4 kg of wet feces everyday [1], and with an assumed moisture content of 70%, each person would produce about 0.12 kg of dry feces. With five loads of dry fecal material, the fuel hopper of the burner was designed to hold about 600 grams at any given time.

As stated before, the whole toilet has to be able to sustain itself during operations. However, to obtain this energy neutrality is not the requirement that was given to CSU. The energy requirement for the burner is to operate with low power input. Electric fans and Electric igniter are the two largest energy inputs to the burner that were optimized. The final goal that was achieved from the development was a burner that consumes energy only from a 12 Volt battery, with both igniters and fans are powered through the battery. However, the early stages of development will not attempt to fulfill this criterion, because the early development will focus on more fundamental criteria, such as emission and fire power.

Waste treatment using semi-gasification method has some inherent risk in the process. The fuel for secondary combustion contains a high percentage of CO, which is harmful to human. A criterion was determined in terms on how the emission of the burner should be. One way to characterize CO emission is Modified Combustion Efficiency. Modified combustion efficiency is defined as CO_2 concentration divided by the sum of CO_2 and CO concentration. The definition of modified combustion efficiency is shown on equation 4.

(4) $$MCE(\%) = \frac{[CO_2]}{[CO_2]+[CO]}$$

Where $[CO_2]$ is the concentration of CO_2 and [CO] is the concentration of CO. The last requirement for the burner is the fire power. Fire Power represents the amount of energy release

per time. This term is comparable to the heat release rate on the internal combustion engine. Fire power can be defined by the amount of fuel consumed for each period of time multiplied by the Lower Heating Value of the fuel, seen in equation 5.

(5) $$Fire\ Power\ (kW) = \dot{m}_{fuel} * LHV_{fuel}$$

Where Fire power is the energy release rate, $\dot{m}_{fuel}$ is the fuel consumption rate, and LHV_{fuel} is the lower heating value of the fuel. The Lower Heating Value (LHV) term in this equation was referenced by articles, or by a bomb calorimeter. On the other hand, measuring the fuel consumption rate was obtained by employing a carbon balance. In this section, the method of calculating firepower and the carbon balance from CO and CO_2 emissions is presented. The carbon-balance is based on conservation of carbon (C) species. Given the percent of carbon in the fuel, which is roughly 50% [13], the mass flow rate of the fuel could be obtained by measuring the CO and CO_2 in the exhaust. The firepower is then determined by multiplying the fuel mass flow rate multiplied by the fuel heating values. The volume ratio of CO is given by:

(6) $$\frac{Vol_{CO}}{Vol_{air}} = \left(PPM_{CO} - PPM_{CO_{amb}}\right) * 10^6$$

Where Vol_{CO} is the Carbon monoxide volume, Vol_{air} is the total volume of air, PPM_{CO} is the measured mole fraction of CO in parts per million, and PPM_{CO_amb} is the ambient mole fraction of CO . The partial density of CO is given by ideal gas law

(7) $$\rho_{CO} = \frac{P_{amb}}{R_{CO} * T_{amb}}$$

Where ρ_{CO} is the density of CO, P_{amb} is the ambient pressure, R_{CO} is the CO gas constant, and T_{amb} the ambient temperature. The mass flow rate of CO can then be calculated from:

(8) $$\dot{m}_{CO} = \frac{Vol_{CO}}{Vol_{air}} * \dot{m}_{blower} * \frac{\rho_{CO}}{\rho_{air}}$$

Where $\dot{m}_{CO}$ the mass flow rate of CO, Vol_{CO}/Vol_{air} is is the volumetric ratio from equation 6, $\dot{m}_{blower}$ is the mass flow rate of blower, ρ_{CO} is the density of CO, and ρ_{air} is the air density. A similar equation was used for the mass flow rate of CO_2. Having calculated the CO and CO_2 mass flow rates, it is possible to calculate the carbon consumption rate as follows:

(9) $$\dot{m}_C = \dot{m}_{CO} * \frac{MW_C}{MW_{CO}} + \dot{m}_{CO_2} * \frac{MW_C}{MW_{CO_2}}$$

Where $\dot{m}_C$ is the mass flow rate of carbon, $\dot{m}_{CO}$ and $\dot{m}_{CO_2}$ are mass flow rate of CO and CO_2, and MW indicates molecular weight of a respective molecule. Finally, the fuel consumption rate can be calculated from:

(10) $$\dot{m}_{fuel} = \dot{m}_C / \%C_{fuel}$$

Where $\dot{m}_{fuel}$ is the fuel consumption rate, $\dot{m}_C$ is the carbon mass flow rate, and $\%C_{fuel}$ is the percentage of carbon in the biomass molecule. The associated firepower can be calculated from equation 10.

(5) $$Fire\ Power\ (KW) = \dot{m}_{fuel} * LHV_{fuel}$$

The following data were used for all of the calculations

- PPM_{CO_amb} = 0.3 PPM (measured)
- P_{amb} = 12 psi (measured)
- T_{amb} = 28 C (measured)
- R_{CO} = 297 J/kg*K
- R_{CO2} = 189 J/kg*K
- Q_{Blower} = 0.1 kg/s (measured)
- ρ_{air} = 1.2 kg/m^3
- MW_C ,MW_{CO},MW_{CO2} = 12, 28, 44g/mol

The above calculations assume that the fuel would be entirely converted into gas and all the charcoal consumed, because the amount of char remaining was observed to be insignificant compared to the CO and CO2 production.

3.3 Technology Readiness Level (TRL)

One way to measure prototype development is by using Technology Readiness Level. Department of Energy (DOE) TRL will be used as classification. The following criteria for each TRL number is shown in Table 4. This classification is beneficial to organize thought to focus on one aspect at a time.

Table 4. TRL Description.

TRL number	Criteria
1	Basic scientific phenomena Research
2	Brainstorming
3	Start prototyping to learn more about the process
4	Basic process are integrated into prototype that works
5	Integration throughout the system of one or more
6	Prototypes are tested in simulated environment in the lab
7	Field Testing
8	Technology is proven to work
9	Products in final form

3.4 Emission Fume Hood

Throughout the development of this prototype, emission fume hood were used as a measurement device. All experiments were conducted inside the hood. The hood captured the whole emission of the burner, and measured it using NDIR gas analysis. The NDIR are capable of measuring CO and CO_2 emission through non-dispersive infrared. Emission measurement was conducted to display the performance of each prototype. Along with emission analyzer, the hood is also accompanied with temperature measurement and LabView interface. Thermocouples are located inside the fume hood that sends the data straight to LabView. The LabView interface is capable of recording temperature and emission in real time.

Figure 12. Emission fume hood.

4. DEVELOPMENT OF PROTOTYPE AND CORRESPONDING DATA

This chapter is meant to be the results chapter of the thesis. The chapter is divided into six sections, with each section corresponds to one TRL. In each TRL, a goal will be laid out to understand the motivation of each TRL. Afterwards, the design considerations are discussed, which are based on previous TRL observations. The design was then reviewed and fabricated for testing. Some modifications were made from test observation in order to troubleshoot the design. Iterative approach was taken during this development to approach a production level prototype.

4.1 TRL 1

Starting with TRL 1, fundamental understanding of fuel behavior is the goal for this TRL. The first question that emerged was how well human waste combust. To ignite any combustible material, the "fire triangle" needs to be present. The fire triangle consists of fuel, oxidizer, and heat. Among three components, fuel components in this project are conventional and need to be studied further. Combustion chamber was designed to study the waste combustion by ensuring all the components of fire triangle are present. The design employed for the first chamber was obtained from the stainless steel cylinder with grate in the middle. A heating element is placed above the grate to ignite the fuel. For TRL 1, the prototype is designed to be an updraft burner for simplicity. The first combustion chamber can be seen in Figure 13.

Figure 13. TRL 1 combustion chamber.

The insulation of the chamber was made by two layers. The first layer was made from a very high thermal resistant ceramic fiber called INSULFRAX®, and the second layer was a heavy duty aluminum foil that acts as a radiation shield. The chamber was also equipped with a fan to supply the air upwards as if it were in updraft burner. The force draft would be able to provide more oxidization than natural draft. The fan for the experiment is shown in Figure 14, with a rating of 6 volt and 10 CFM flow rate.

Figure 14. Nidec Fan as air supply.

4.1.1 **Initial Solid Waste Experiment**

An experiment was conducted using TRL 1 chamber. The purpose of this experiment is to study how well the waste combust within TRL 1 chamber. Experiment setup was designed to incorporate TRL1 chamber, shown in Figure 15; from the left are the combustion chamber, igniter block, DC power supply, and variac AC converter. With a completed setup, an experiment was carried out by turning on the fans and igniters.

Figure 15. Initial Solid Waste experiment.

Heavy smoke was visible the first two minutes after the igniter was turned on. After another minute, the flame started and grew rapidly. The visual result can be seen in Figure 16. The flame was seen to be a mixture of premixed flame and diffusion flame. The premixed flame was produced by the forced draft of the fan, while the diffusion flame was produced by exposure of the gas to the surrounding air. After the burn, a significant batch of charcoal was left in the chamber, which can be seen in Figure 17. The experiment also showed that it was possible to combust solid waste. However, the time required to ignite the waste was relatively long. In order

for the fuel to be ignited, all the moisture content had to be completely evaporated, which was taken from the igniters. Therefore, the igniters have to first vaporize the moisture content before it can ignite the fuel, which create a delayed ignition.

Figure 16. Ignition from solid dog waste.

Figure 17. Charcoal leftover.

4.1.2 **Shape and Moisture Modification**

Charcoal leftover is not necessarily a favorable condition, because charcoal is quite difficult to re-ignite. One method that could possibly achieve less charcoal production was shape modification. Shape modification was conducted with a purpose to increase the surface area of combustion. An increase in surface area would increase the reaction rate, which ultimately resulted in less charcoal production. Using a meat grinder in Figure 18, the shape was reduced and surface area increased. A dehydrator was used to dry the waste that came out of the meat grinder.

Figure 18. Shape modification process.

4.2 TRL 2

The purpose of TRL 2 was to create more consistent burning, and to reduce the charcoal production. As it was specified in section 3.3, TRL 2 was meant to be a brainstorming session to generate ideas. Rapid experiments were conducted, and the results of the experiments were recorded. The information was used to guide TRL improvement.

The design of TRL 2 chamber in Figure 19 was an updraft burner that was similar to TRL 1. An Inconel chamber with a height of 14 inches and a diameter of 3 inches was used as TRL 2 chamber. The chamber was incorporated with important components, such as fans at the bottom and igniter above the fuel bed. An igniter was placed carefully from the top of the burner, such that there was no short circuit to the chamber wall.

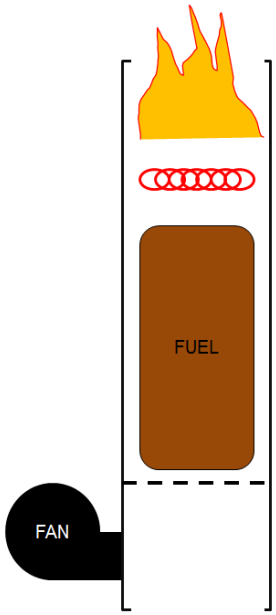

Figure 19. Schematic design of TRL 2.

4.2.1 TRL 2 Combustion Experiment

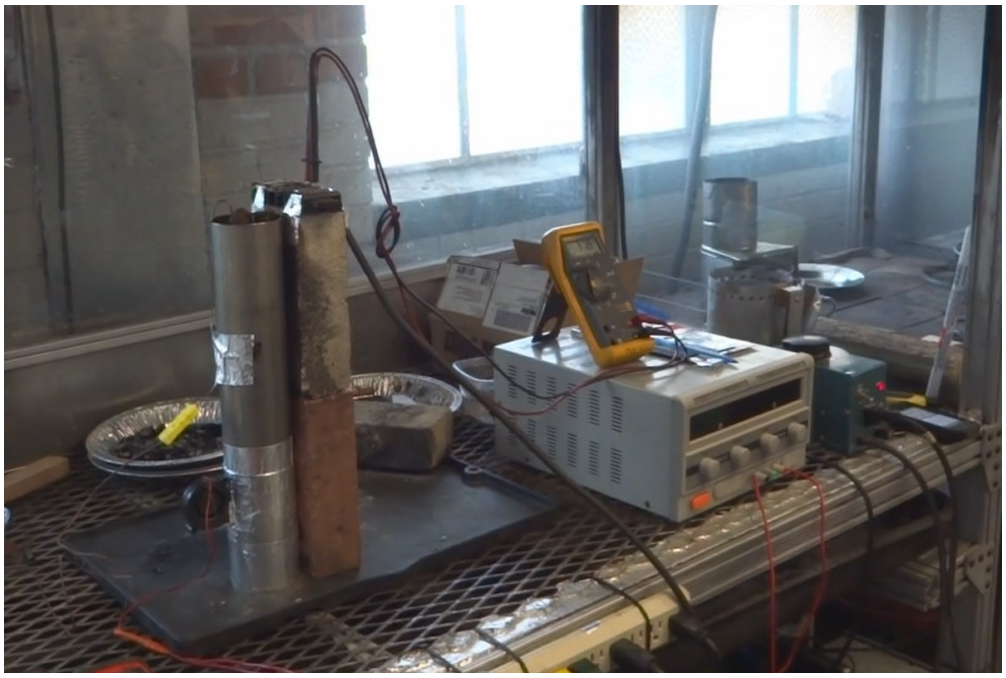

Figure 20. TRL 2 experimental setup.

The experiment was conducted with a new chamber with the expectation of less heat loss. Less heat loss in startup phase would benefit the burns with faster ignition and higher charcoal oxidation. Faster ignition can be achieved by raising the gas temperature to auto ignition as quickly as possible, and charcoal production was predicted to decrease with higher temperature. With experimental setup shown in Figure 20, the experiment was conducted in similar procedure to TRL 1, with an input of 100 grams dry fecal material.

The experiment ran for approximately 5 minutes until the fuel was totally consumed. However, the ignition took place at about 2 minutes, with smoke being produced before the ignition. With igniter on during the first 2 minutes, the syngas that were being produced cools down because the body of the burner was still cold. Gas temperature further decreased with the introduction of air flow at ambient temperature. The product of the first two minutes of the experiment was unburned mixture of syngas and air, which was resulted from the cooling down process.

Figure 21. TRL 2 Combustion experiment.

After the fuel was ignited, the experiment was shown to undergo thermal runaway. Thermal runaway was indicated by fire power flame that kept increasing as experiments went by. Taking an observation from Figure 21, a section of the chamber glowed red at the bottom. The height of the glow was roughly equal to the height of fuel bed inside the chamber, which implied that the whole stack of fuel was consumed at the same time. Before the thermal runaway occurs,

After the burning was completed, the charcoal leftover was found to be significant despite the fuel's shape modification. However, the average individual charcoal size in TRL 2 was found to be smaller than TRL 1 charcoal. Problem might occurs if a new batch of fuel is feed on top of the cold charcoal. The chamber might be filled up with charcoal after couple runs, which can be considered as fuel bridging. The desired prototype would be the one that would force all the charcoal to be consumed completely.

4.2.2 **Secondary Igniters Concept**

Learning from the previous section, ignition did not occur until two minutes mark. Before ignition, the chamber produced high volume of unburned syngas mixture. Going back to the concept of fire triangle, mixture of unburned syngas and air lacks the heating element. If heat can be introduced to the mixture, fire triangle can be completed. This concept started the idea of secondary igniter, which was made in similar fashion to the primary igniter, but placed on top of the burner. To ensure all the components of fire triangle present at the same location, a reducer was placed at the secondary igniter location to channel all the mixture to pass through secondary igniter. The detail view of secondary igniter is shown in Figure 22.

Figure 22. Secondary Igniter concept experiment setup.

Secondary igniter was added with the same setup as previous experiment. As the experiment was started, both igniters were turned on at the same time. Ignition occurred at about 15 seconds mark during this experiment, which was relatively faster than 2 minutes. During the experiment, it was also observed that the reducer behaved as a chimney which increased the secondary air flow. Operational observations can be seen in Figure 23 and 24

Figure 23. Flame out of the combustor during startup.

Figure 24. Air gap that behaves like a chimney effect.

4.3 TRL 3

TRL 3 was developed as the first functional test bed. The main areas of focus included development of downdraft gasifier to assist the problems that were encounter in TRL 2. Some of those problems were high firepower and high volume of charcoal leftover. The solution for those problems was proven through the result of the conducted experiments. The increasing number of experiments put constrain on the current fuel surrogates, dog waste. Preparation of dog waste to be used or experiment was long and tedious process. For practicality, fuel surrogates were changed to wood pellets.

4.3.1 **TRL 3 Design**

The TRL 3 design experienced significant change from TRL 2. The burner design was flipped upside down to produce a downdraft semi-gasifier burner. Downdraft design, as the previously discussed, has more consistent gas production than updraft design. Consistent gas production was predicted to create a steady combustion, which would not cause thermal runaway. Charcoal production was also predicted to be reduced because the all the charcoal had to pass through the oxidation zone in downdraft design. With charcoal temperature raised in oxidation zone, it can be oxidized thoroughly.

The design of the burner is shown on Figure 25 and its legend is shown in Table 5. The burner operates by adding the fuel through the top (1), and then the chamber is sealed with a cap. Primary air, which is an equivalent to the TRL 2 air supply, is supplied through copper tubing (2). The fuel meets the air at the grate (3). The mixture is then heated by the glow plug (4) to produce syngas. After the syngas is produced, it is combusted with a mixing of secondary air (5).

The exhaust will then exit through the concentric exhaust around the fuel chamber as a heat exchanger to pre-heat the fuel.

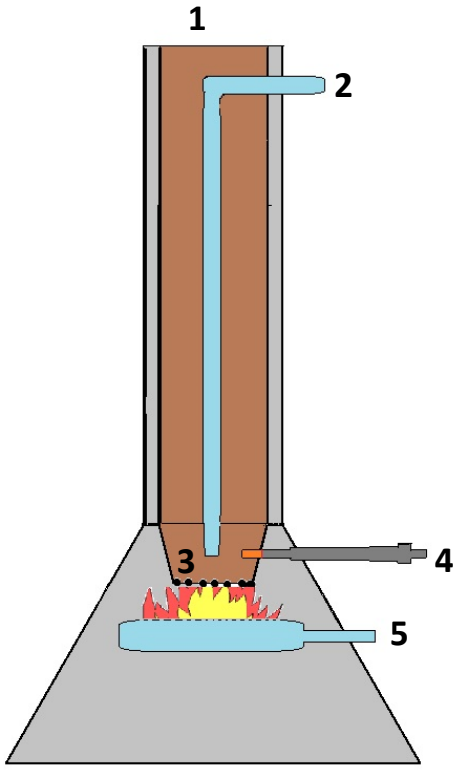

Figure 25. TRL 3 Downdraft Burner schematic.

Table 5. Downdraft Burner Components.

Component Number	Explanation
1	Fuel inlet and cap
2	Primary air inlet
3	High temperature grate
4	Diesel Glow Plug
5	Secondary air Inlet

The fabrication of the parts was conducted with TIG welding using 22nd gauge thick stainless steel sheet metal. However, the major components were not welded together because detachable parts add the flexibility to the design to be modified. The fabricated parts are shown in Figure 26. From the left in the pictures are primary air inlet, exhaust chamber, fuel chamber, combustion chamber with the secondary air inlet, and circular section in the bottom. The device was implemented with 8 thermocouples. There were four thermocouple attached to the primary air tube to measure the temperature of the fuel bed. Three thermocouples were welded to the exhaust chamber to measure the exhaust temperature. The last thermocouple was placed on the conical section to measure the flame right under the secondary air manifold.

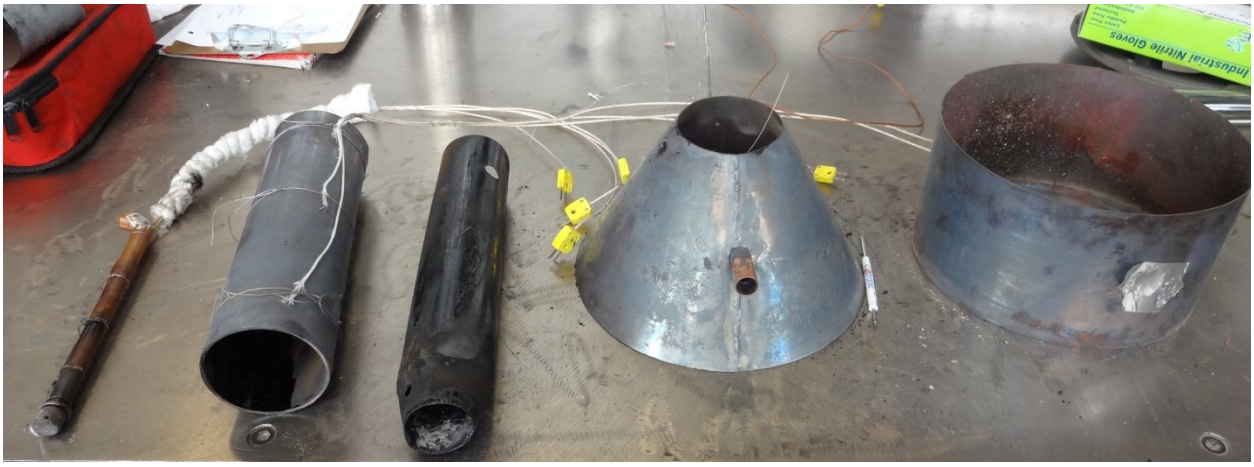

Figure 26. Components for TRL 3 prototype.

Figure 27. Secondary air manifold.

The secondary air manifold is shown in Figure 27. The manifold was fabricated using copper tubing with drilled holes every half an inch. With the manifold design on copper tubing, DC electric fans were no longer adequate to supply the air, and therefore the air supply was changed into compressed air. To adjust the flow of the compressed air, rotameters were implemented to the device for both air flows. The unit indicated by the rotameter scale is in CFM (cubic feet per minute).

Primary Igniter in this prototype was switched into glow plug. Glow plug is a part of diesel engine that is used to preheat the diesel chamber during the engine cold start. In TRL 2, nichrome igniter had to be placed very carefully such that short circuit wouldn't occur, but that method couldn't be used for downdraft design because grate separates the fuel and the igniter. The grate is an electrical conductor which would cause short circuit every time the igniter is turned on. Glow plug's body on the other hand is the ground, which will not cause any short circuit. The glow plug used for TRL 3 is shown in Figure 28.

Figure 28. Glow plug with 12V battery.

4.3.2 **TRL 3 Experiment**

The experimental setup is shown in Figure 29. The setup of the experiment was designed to freely adjust the airflow of the prototype. Rotameters were implemented to adjust primary and secondary air source. With controlled flow rate, desired air to fuel ratio can be achieved. TRL 3 fuel chamber was also designed to hold 500 grams of fuel, which would be the fuel load for this experiment. In the setup, two igniters were used, which are glow plug and propane torch. During TRL 3, implementation of secondary igniter had not been completed. Propane torch was used to simulate the electric secondary igniter. With the setup completed, the experiment was started by turning on the igniter, and the experiment ran for a total time of 90 minutes. During the first 20 minutes of the experiment, it was visually observed that a high firepower was produced by the burner. After 20 minutes passed, unlike TRL 2 where the burner cools down, TRL 3 burns the charcoal for a period of 70 minutes, and then cools down to room temperature. In this

experiment, to accompany the visual result, thermocouples were implemented. The placement of those thermocouples can be seen in Figure 30.

Figure 29. Combustion experiment with TRL 3.

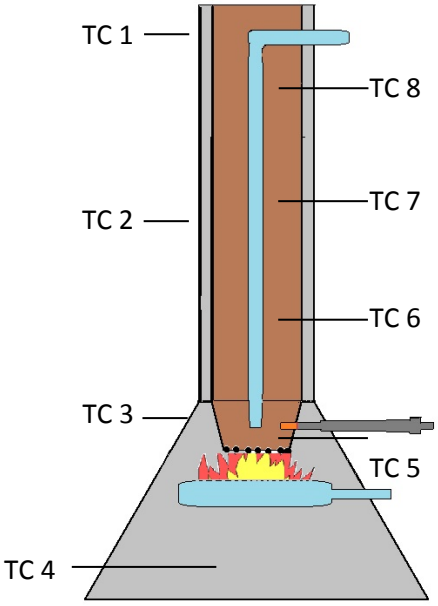

Figure 30. TC placement on TRL 3.

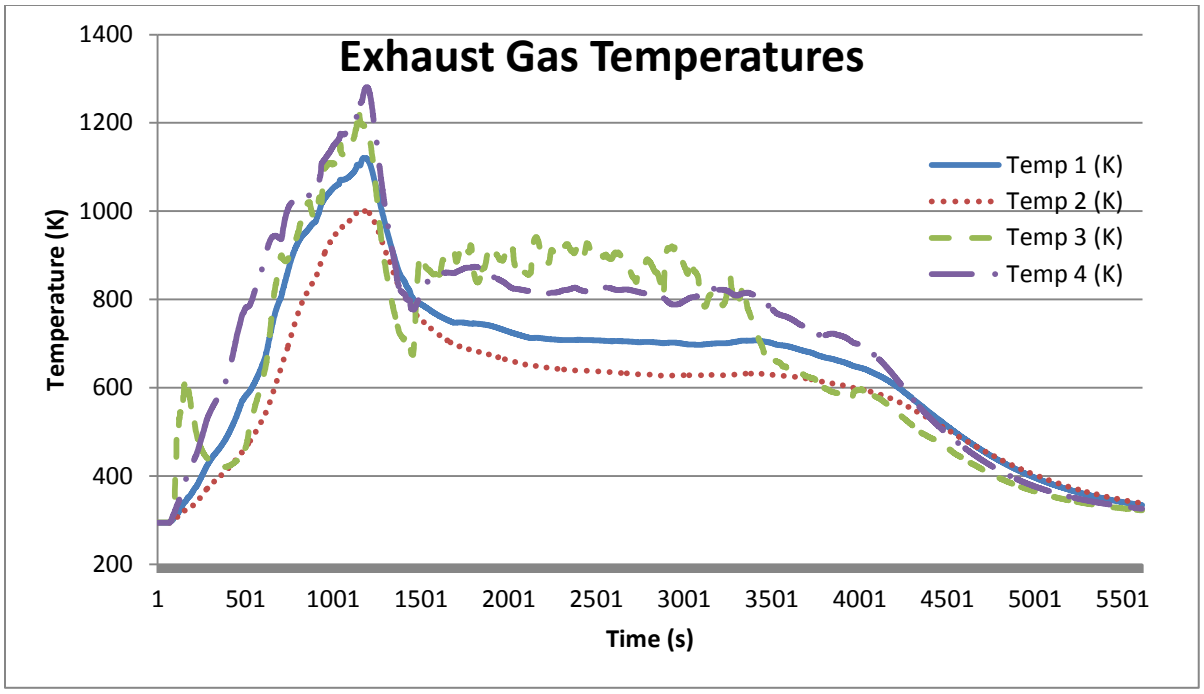

Figure 31. TC 1-4 of TRL 3.

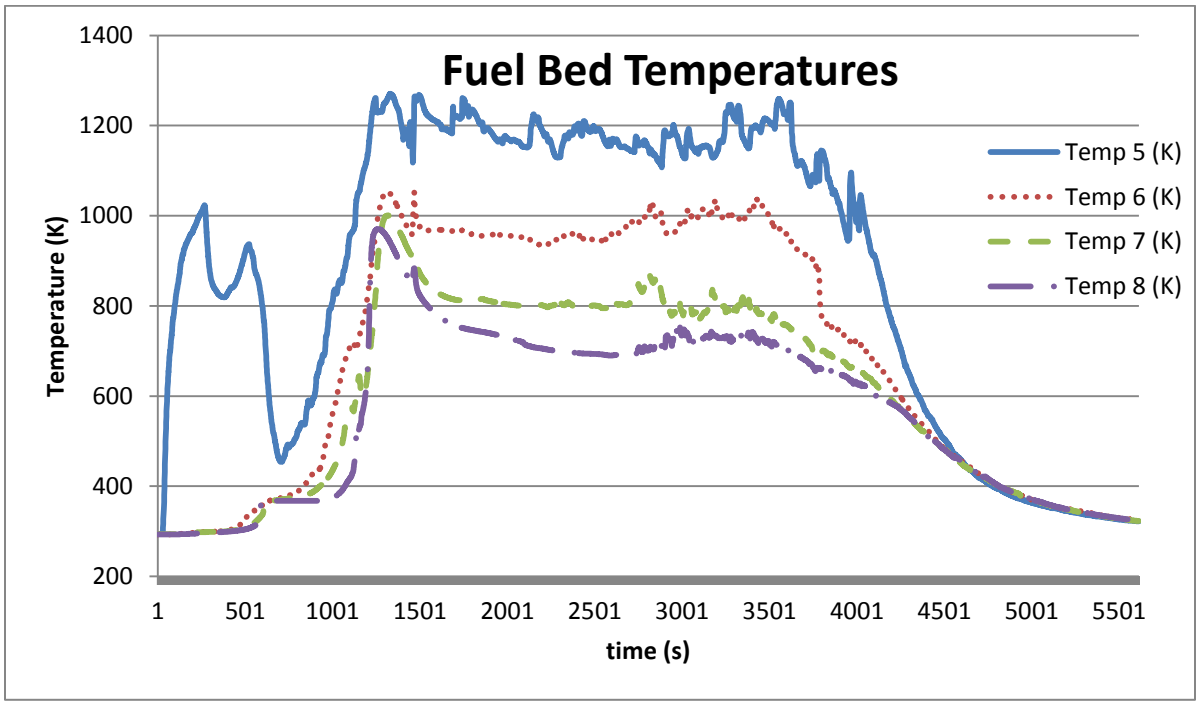

Figure 32. TC 5-8 of TRL 3.

The measurement of this experiment is shown in Figure 31 for the exhaust gas temperatures and Figure 32 for fuel bed temperatures. The x-axis of the graphs is time in seconds and y-axis of the graphs is temperature in kelvin. Exhaust gas temperatures would be the focus of the discussion of the result because this measurement showed a clear trend on different burning phases. From Figure 31, the burn phases can be separated into three phases, which are startup, volatile combustion, and charcoal combustion. Startup phase started when the fuel is ignited, and lasted for 10 minutes time frame. During this phase, combustion occurred at the bottom of the burner while the burner was slowly heating up. The phenomena can be observed through a rise T3 and T5, which are the closest measurement to the flame, while other measurement did not show temperature rise. As the overall burner temperature increased, the syngas combustion rate also increased. Temperature increased for a period of 20 minutes, close to 1300 K on T4. This phase is the volatile combustion, which produced a high firepower within a short period of time. The last phase that occurs in downdraft design was the charcoal oxidation. The charcoal oxidation phase occurred after all the volatile left burner, which is indicated by low fire power. Measurement of exhaust gas showed that after the burner reached the peak temperature, it decreased to about 800 K. However, the fuel bed temperature was shown to be higher for longer period of time.

The burner was designed with concentric exhaust with a purpose to pre-heat the incoming fuel. However, as the data has shown, the fuel bed temperature increased above 200 C (473 K), which is the starting of pyrolysis temperature. During volatile combustion, all the temperature measurements indicated that temperature reached an average of 1000 K. with this temperature environment, the fuel batch would have adequate energy to conduct pyrolysis, regardless of air flow, because there are enough energy to supply the endothermic reactions of pyrolysis.

After the experiment, the char leftover was weighted. The weighted leftover was significantly lower than TRL 2 leftover, which was about 20 grams. Low charcoal leftover occurs due to the different zones in the downdraft gasifier systems (see chapter 2). In downdraft, the fuel bed is forced to flow downwards by gravity. A phenomenon is observed where all the fuel has to pass through the combustion region located at the bottom. The charcoal that passes through the combustion zone will be smoldered and combusted.

In conclusion, an experiment was conducted to study the behavior of a downdraft semi-gasifier burner. The burner was equipped with rotameters and thermocouples. During the experiment, temperature measurement indicated that the combustion had different phases, which are startup, volatile combustion, and charcoal combustion. During volatile combustion, fuel was being consumed at the same time. Afterwards, the charcoal was combusted for a period of 70 minutes, which resulted in 20 grams leftover.

4.4 TRL 4

The experiment of TRL 3 showed that the downdraft burner performed in a more stable combustion than updraft burner. The next step was to refine the downdraft design such that the burner was able to perform the required task in the lab environment. This refinement included major changes of design and various experiments to reach an acceptable emission for the project. There are six subchapters that explained the development until the prototype was established.

1. Mass balance analysis
2. Energy balance analysis
3. Design and fabrication of TRL 4 prototype
4. Initial testing and result
5. Modifications on TRL 4
6. Final testing of air requirement and ignition sequence

4.4.1 **Mass Balance Analysis**

In order to optimize performance, a mass balance analysis was completed. This analysis gave predictions for analytical air flow rates. Mass balance analysis was conducted using 2 steps overall reactions of chemical kinetics [28]. This analysis was conducted to find an estimated air flow, which improves Modified Combustion efficiency. The first chemical equation shows the air quantity needed for the gasification process. The second chemical equation shows the air needed to combust the syngas that is produced by the first equation. The biomass presented in these equations is the CHO ratio with respect to C. They are not the actual molecules of the fuel. The equations are shown in equation 11 and 12, respectively.

(11) $$CH_{1.4}O_{0.6} + 0.4\,(O_2 + 3.76\,N_2) \rightarrow 0.7\,CO + 0.3\,CO_2 + 0.6\,H_2 + 0.1\,H_2O + 1.504\,N_2$$

(12) $$0.7\,CO + 0.3\,CO_2 + 0.6\,H_2 + 0.1\,H_2O + 0.65\,(O_2 + 3.76N_2) + 1.504\,N_2 \rightarrow CO_2 + 0.7\,H_2O + 3.95\,N_2$$

The stoichiometric condition to combust the fuel is about 1.05 moles of air. In Equation 4.11, the amount of air required for primary air flow rate is theoretically 0.4 of stoichiometric condition. In equation 4.12, the amount of secondary air mass flow rate is theoretically 0.65 of stoichiometric condition. With that as a foundation for the analysis, the mass air flow rate can be obtained by choosing a desired mass fuel flow rate. The details of the calculation can be obtained in appendix C. At standard temperature and pressure, the result shows that the flow rate of air needed for gasification is 0.63 CFM and for secondary air is 1.80 CFM. These flow rates are based on 400 gr/hr fuel consumption rate, which is the ideal burn rate for the burner. Throughout the paper, the ratio of secondary to primary air is used, and it is defined in equation 13 where $R_{Sec\ prim}$ is the ratio of secondary to primary air flow rate, $\dot{Q}_{sec\ air}$ is the volumetric flow rate of secondary air, and $\dot{Q}_{prim\ air}$ is the volumetric flow rate of primary air.

(13) $$R_{Sec\ prim} = \frac{\dot{Q}_{sec\ air}}{\dot{Q}_{prim\ air}}$$

4.4.2 **Energy balance analysis**

The next analysis is the energy balance analysis, which is based on the first law of thermodynamics. The purpose of this analysis is to estimate how much energy would be required

to dry the waste. The assumptions in this analysis would be that each person produces about 400 grams of feces everyday [55]. Calculations were conducted using equation 14.

(14) $$\dot{Q} = \dot{m}\, C_p\, \Delta T$$

Where $\dot{Q}$ is the total energy, $\dot{m}$ is the mass flow rate, C_p is the heat constant of the fuel, and ΔT is temperature rise. The equation was used on how much energy would be produced from the fuel, subtracted by the energy required to vaporize water. The result indicates that 40% of syngas combustion energy is needed for dehydration. Drying energy is divided into two sections. The larger fraction of drying energy is used in the dryer, while the smaller is used in the fuel hopper.

4.4.3 **Design of TRL 4 Prototype**

This section will discuss the reasoning behind component designs that were implemented in TRL 4. All design considerations were based on the information that had been obtained through TRL 3 experiments and the analyses that had been conducted on mass and energy balance.

In terms of geometry, the previous chamber was designed to hold 500 grams of dry fuel. As shown in Appendix C, 500 grams of wet fuel with 70% moisture content leads to roughly 167 grams dry of fecal material. Significant design requirement was changed during this time. The change was mainly on the number of daily user. Burner size was modified in TRL 4 to hold 2 kg of dry waste at a given time.

Even thou the size of the burner was increased, the diameter of the fuel load were not significantly changed. Hearth load [28] is the production rate of a gasifier, which is calculated by

dividing the gas production rate by the diameter of the chamber. In gasifier, the diameter of the combustor determined the fuel consumption rate of the burner. The previous design of TRL 3 consumed 500 grams of fuel within 1 hour period, which is the desired fuel consumption rate. Therefore, the diameter was only increased from 2.5" to 3".

With the increased size of the burner, some structural design considerations were thought, such that the burner would be structurally stable. The thickness of material was increased to 16^{th} gauge from 22^{nd} gauge for rigidity of the wall. Support system was developed at the bottom of the burner to increase the footing area. With the burner being rigid, it was difficult to do the ash management, and therefore ash tray was implemented for easy method of maintenance.

As previously tested on TRL 3, too much heat transfer to the fuel bed would cause thermal runaway to occur. A consideration was thought to create an air shroud around the bottom of the fuel bed to prevent direct exposure to the flame. A 4"diameter primary air inlet enveloped the 3" diameter fuel bed concentrically, and covered the bottom 6" of the fuel bed. As the shroud insulate the fuel bed from direct contact with the flame, the heat from the flame is transferred to pre-heat the primary air.

For secondary combustion in the burner, both oxidizer and fuel are in gaseous form. For gaseous fuel combustion, mixing is a crucial variable. Increased mixing rate can be achieved by implementing tangential air inlet to the burner. High mixing rate will increase the percentage of pre-mixed combustion. Pre-mixed combustion is more desirable due to the high Modified Combustion Efficiency. This consideration is applied to primary air and secondary air inlets.

The final design of the burner is shown on Figure 33. The burner was built with four detachable components. The first component at the top is the fuel chamber. The chamber is designed with a 45 degree elbow to easily interface to a drier. A square section under the elbow functions as gas path to preheat the incoming fuel. The fuel chamber has two flanges. The top flange that is connected to the exhaust chamber with bolts connected to it. The smaller flange is meant to be a stopper for the primary air shroud. The height of the vertical section of the chamber is 18" and its diameter is 3" OD. The second component is the primary air shroud. It has a 4" section in diameter with the height of 6". At the bottom of the part, the shroud necks down into a 2.5" section where the reduction zone is located. The reduction zone is designed to be smaller in order to reduce the fire power of the burner. The primary air shroud has the tangential air inlet to have more distributed air flow. The primary air comes in the gap between the shroud and the fuel chamber; it is about 0.25" vertical gap at the bottom of the fuel chamber where the air flow is introduced to the fuel.

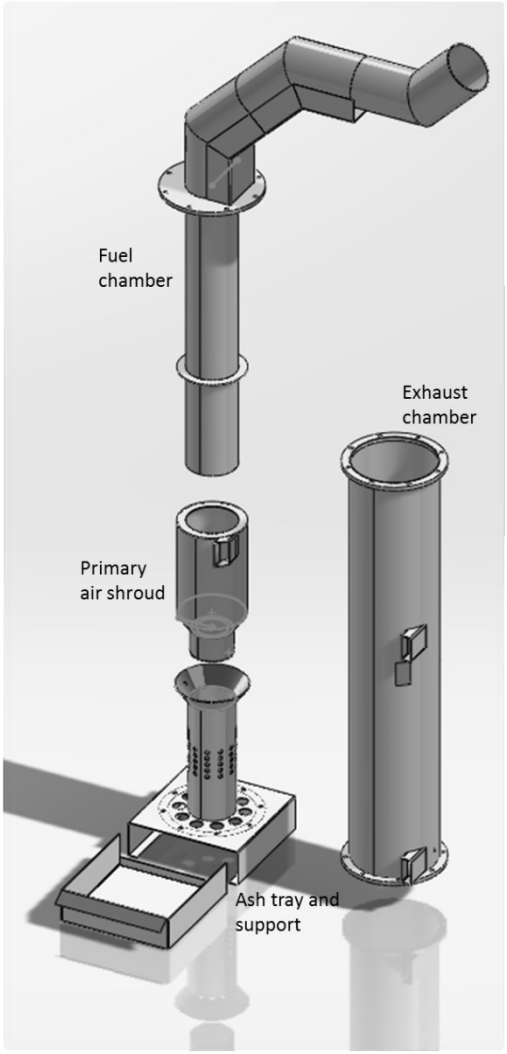

Figure 33. Exploded view of TRL 4.

Regarding previous discussion about support, an ash drawer was built. The ash drawer is designed to be emptied as a maintenance routine. The drawer is connected to a tubular support that locks the primary shroud and fuel chamber concentric with the flanges. The tube has of numerous holes for the gas flow. Inside the tube, there is a secondary igniter implemented. The placement of secondary igniter ensures that all the gas have to pass through the igniter. The last component is the exhaust chamber. This part connects the flange at the top and at the bottom,

assuring the concentric design of the burner. The exhaust chamber has some holes for the placement of glow plug and thermocouples.

After the design was completed, the operation was expected to be shown as Figure 34. The burner operates by taking the fuel and drops it to the reduction zone. In that zone, the glow plug heats up a small batch of fuel. The gas production started when the heated fuel is introduced to primary air. The produced gas exit through the holes on tubular support, and mixed with the secondary air flow. The mixture is heated with secondary igniter to start the combustion.

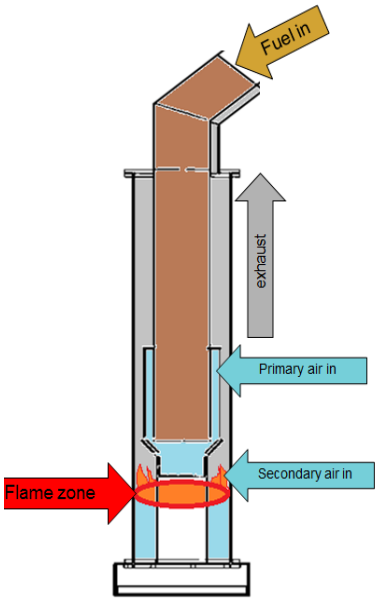

Figure 34. Cross section of TRL 4.

4.4.4 Initial Testing of TRL 4

After the design was completed and fabricated, some initial tests were conducted as visual quality experiments. These experiments were meant to be a preliminary method before more sophisticated tests could be conducted. Since the burner had no design comparison to other

products, the design features were purely experimental. The preliminary tests were meant to test the features whether it operates the way it's desired. These experiments were not measuring any temperature or emission, but rather focus on the visual measurement.

Different factors were observed during these preliminary timeframe. The initial burns with the completed design proved that the flame exit through the ash tray, because the ash tray have less pressure drop than the exhaust. In response to pressure drop, a negative pressure system was implemented to the exhaust of the burner. The leakage was significantly reduced, and all the flow was directed to the exhaust. However, the exhaust of the burner was observed to be similar to the exhaust on TRL 2 startup, which is a mixture of unburned syngas and air.

Figure 35. Initial experiment visual results.

A factor that was causing the mixture of unburned syngas and air was natural buoyancy. The secondary air inlet position was located below the gas production site, and the air temperature was lower than the produced syngas. By natural buoyancy, a higher temperature gas

would tend to rise faster than colder gasses. An argument was made that the syngas rose faster than the incoming secondary air, which would prevent mixing between the two components. When the mixture reached the exhaust, the gas temperature had decreased below ignition temperature. An experiment was conducted by cutting a section of the burner above the holes of gas outlet, and injecting the secondary air inlet at that location. The configuration of the experiment is shown in Figure 36.

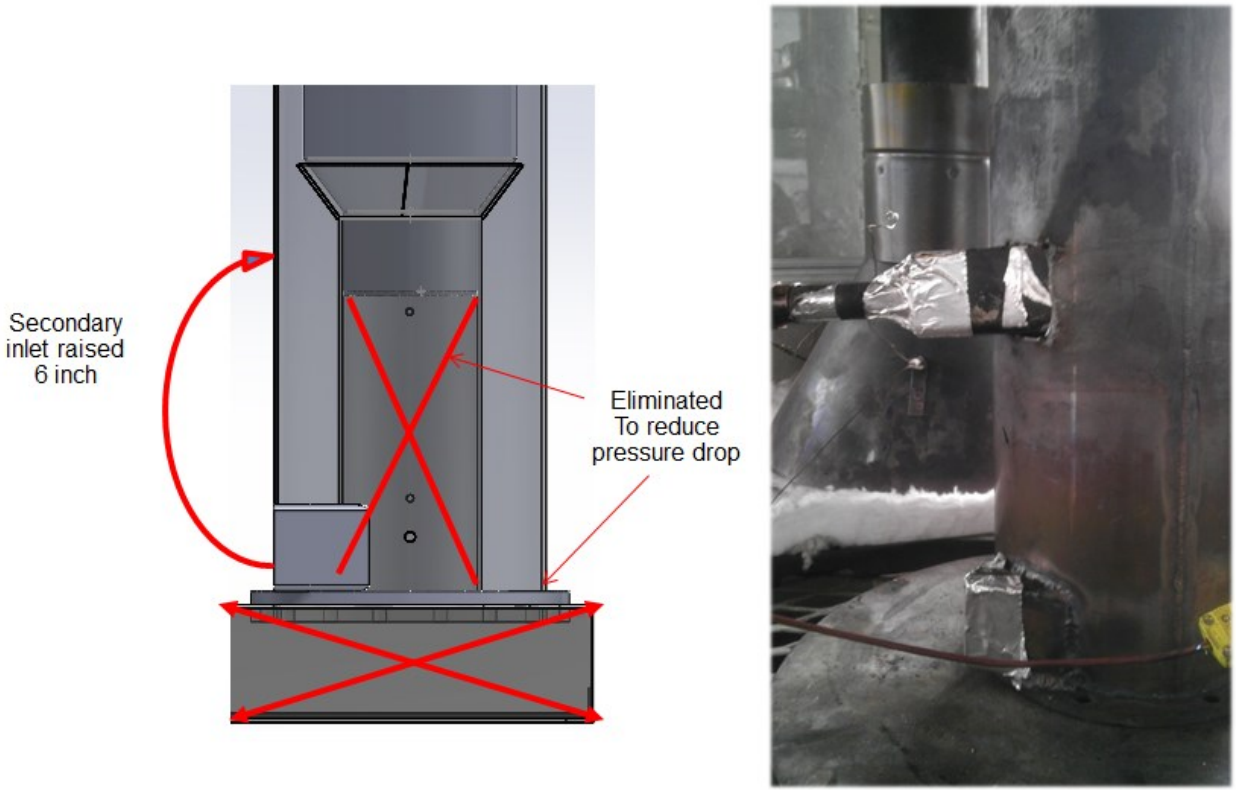

Figure 36. Raised secondary inlet.

The experiment was a success. The visual smoke production was less visible, and the flame was more stable than previous experiments. Therefore, more analysis was conducted on the following section. The analysis would consist of why this phenomenon occurs and how to optimize the performance.

4.4.5 **TRL 4 Modifications**

The experimentation led to several design enhancements. The first modification was the raised secondary inlet in order to comply with fourth experiment result. The secondary air manifold was optimized through analysis with CFD. As a result of geometry change from secondary air manifold, the original secondary igniter was no longer usable, and therefore, a new secondary igniter was developed as the second modification.

4.4.5.1 Secondary Inlet Modification

An analysis was conducted in order to understand the detail phenomenon inside the burner. The analysis was conducted by a simple CFD (Computational Fluid Dynamic) model with FLUENT®. This model did not simulate the flame or chemical kinetic, and only focused the analysis of fluid mixing. The presupposition of the phenomena is based on natural buoyancy, which is a fluid dynamic phenomenon. Therefore, it is acceptable not to model the chemical kinetic inside the burner. This model simulated the syngas as hot air, while the secondary air was modeled as cold air. All the air was modeled as incompressible ideal gas, which means that density difference will force a natural draft. The model was created with the geometry of the original TRL 4 without any ash tray at the bottom.

The geometry of the computational domain is a two dimensional axisymmetric mesh. The computational domain is shown in Figure 37. The number of cells in the computational domain is relatively coarse. However, there are five cells in the gap between the primary air shroud and the exhaust chamber. Five cells span allows the boundary layer to be captured by the computation. The flow model that was used is laminar, because the Reynolds number of the gas

inlet was calculated to be laminar. The model was assumed to be adiabatic to reduce the computational time.

The result of the model can be seen in Figure 38. It can be seen from the Figure that the hot gas did not mix with the cold air. The hot gas and the cold air formed a layer within the gap, which resulted only in diffusion mixing. Diffusion mixing have significantly lower rate than forced mixing. The gas that was exhausted did not combust because it was not mixed with the cold air. Both the air and the syngas exited the burner to create an unburned mixture of syngas and oxidizer.

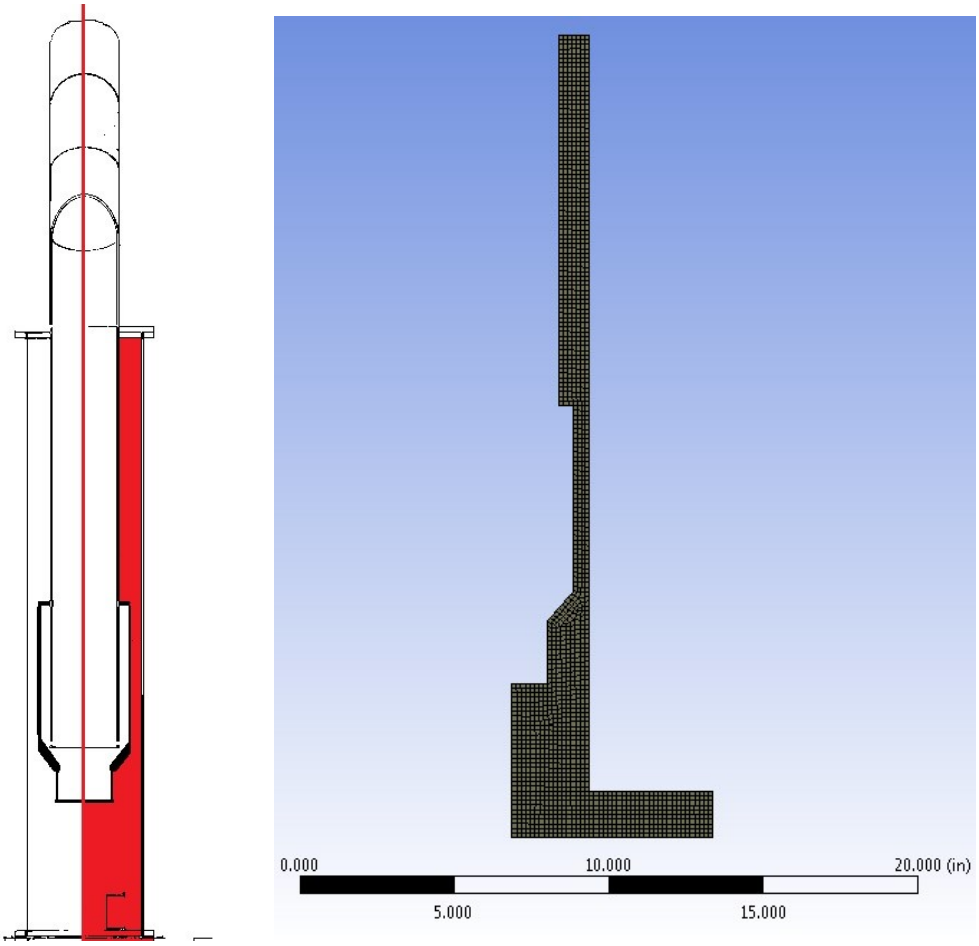

Figure 37. Computational domain of simulation.

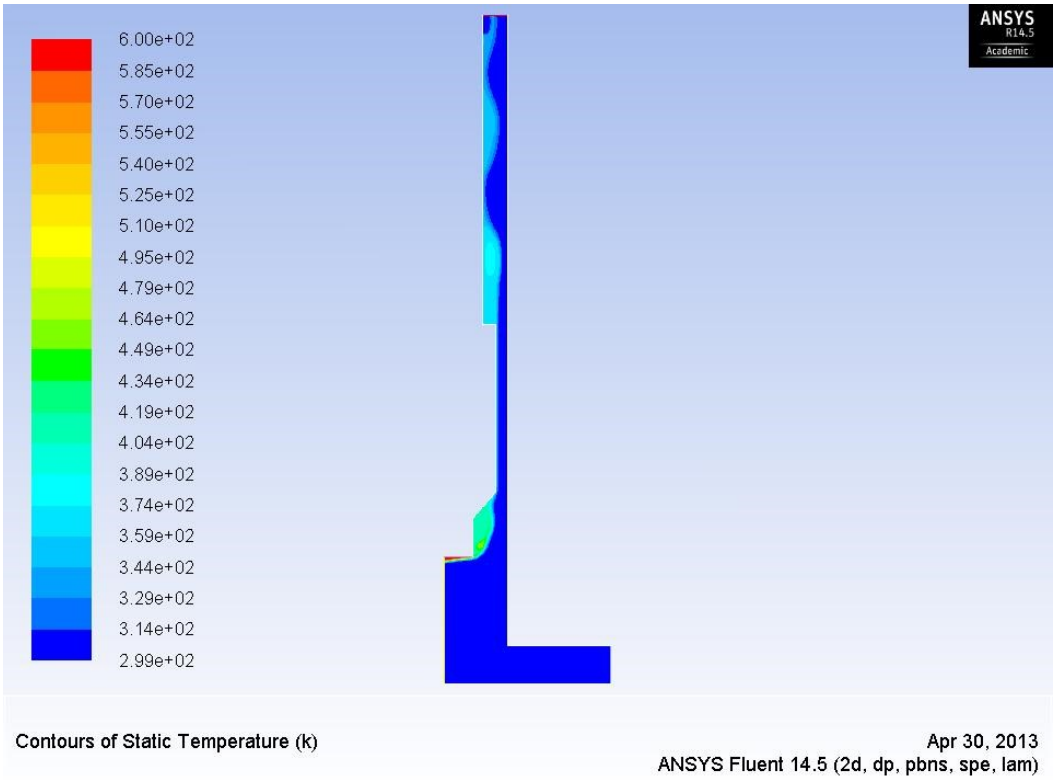

Figure 38. Computation result of 2D simulation.

To enhance mixing, the cold air inlet was raised above the hot gas inlet. Natural buoyancy worked in the favor of mixing since the hot syngas that rose will be mixed with cold air. To visualize the fourth initial experiment, another experiment was conducted. A high temperature rated glass was placed under the burner while the ash tray was removed. The gap between the glass and the burner was sealed to ensure no leakage from the bottom. The result of this visual experiment can be seen in Figure 39, which shows the view of the mirrored bottom of the burner looking up.

The flame in the picture was injected tangentially and showed to improve mixing inside the chamber. Through this experiment, tangential air was proven to enhance the mixing. Despite the spin, the shape of the flame was not uniform. The air had more momentum to spin in the

location close to the inlet. The flame was lifted from the inlet, and tended to have a more non-premixed shape. This concluded that to enhance mixing between the gas and the air, a distributed manifold was needed. The design of the manifold is shown in Figure 40.

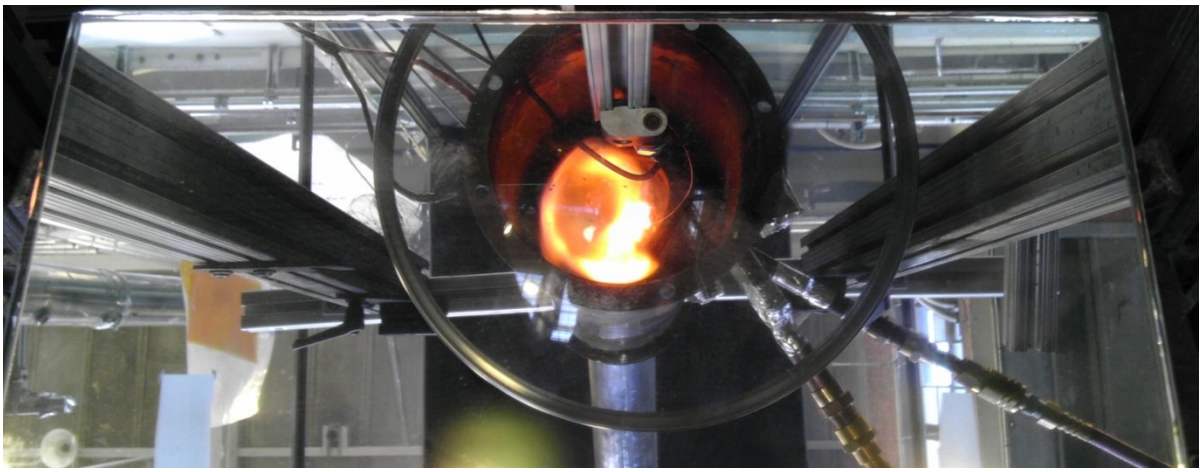

Figure 39. Visual experiment for raised secondary inlet.

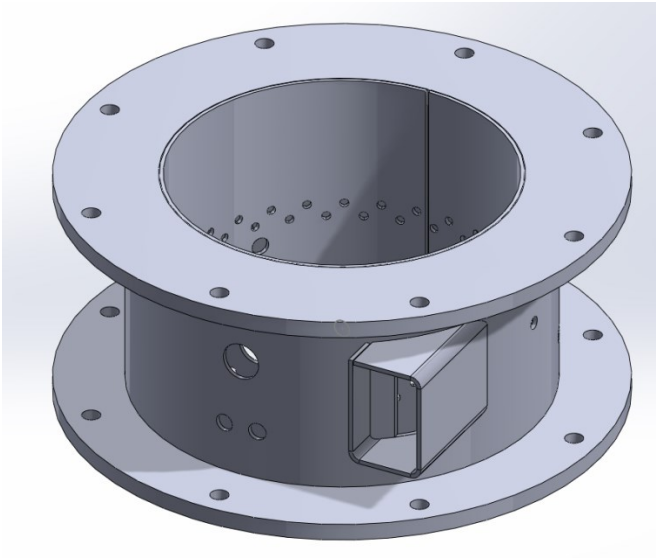

Figure 40 Secondary air manifold

The manifold was made from double stainless steel wall with distributed holes in the inside walls. Air came in tangentially through the square hole, then distributed to the small holes located on the inside walls. The holes in the inside were bent in the direction of the air flow, so the air did not come out perpendicular to the inside wall. To connect to the burner and to obtain the right height for the holes, the exhaust chamber shroud had to be cut to a length such that the holes would be in the correct position desired. The holes have a diameter of 0.125", and it was found that 0.125" diameter holes will give the highest velocity of air to balance the static pressure of DC fans (see appendix D). The flanges at the bottom were connected to a new ash tray that was going to be sealed properly instead of leaking like the original design of TRL 4.

The fabrication of the manifold was started by cutting and rolling the parts, and then the sections were welded. The part had to be aligned such that the outside walls and the inside walls of the manifold were concentric. Bending of the holes was another task in fabrication process. The tools to bend the holes were heated rod with equal diameter to the holes diameter. The heated rod was slip through the holes until the rod was halfway through. The rod was then tilted in the direction of desired air flow. As the rod was tilted, the holes were bent with the heat from the rod. The inside walls of the manifold had to be made with a thinner material in order for the holes to be bent. It was fabricated using 0.033" thick stainless steel. The completed manifold and the detailed picture of the holes are shown in the following Figures.

Figure 41. Completed secondary air manifold.

Figure 42. Detail view of the bended holes.

After the manifold was completed and implemented to the device, a visualization test was conducted to see the difference between before and after the manifold, and whether visually mixing is being enhanced. The result is shown in Figure 43. The image clearly shows improved mixing and homogeneous circular shape.

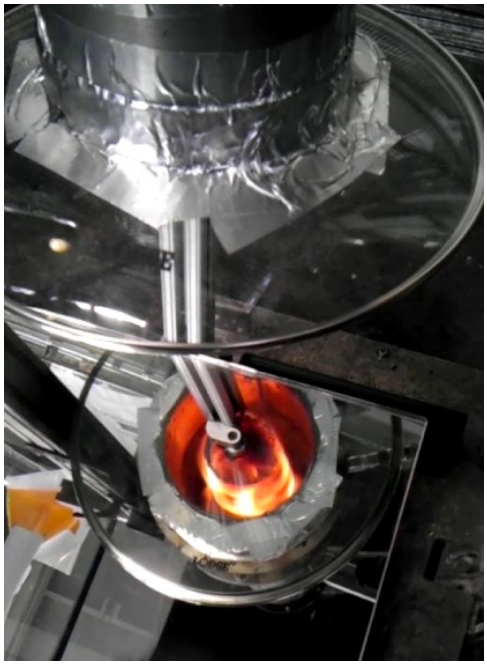

Figure 43. Visualization test with secondary air manifold.

4.4.5.2 Secondary Igniter Modification

Due to geometry change of the secondary air manifold, the bottom parts of the burner were unusable, including the secondary igniter. This proposed a need to develop a new configuration for secondary igniter. The proposed secondary igniter came from the bottom of the burner, and reached up close to the grate where the syngas exit. The components for this igniter were nichrome wire, high temperature cable, high temperature terminal block, and ceramic tube. The components can be seen in Figure 44. The left Figure shows the completed assembly of the igniters, and the right Figure shows the tested igniters seen from the top of the burner.

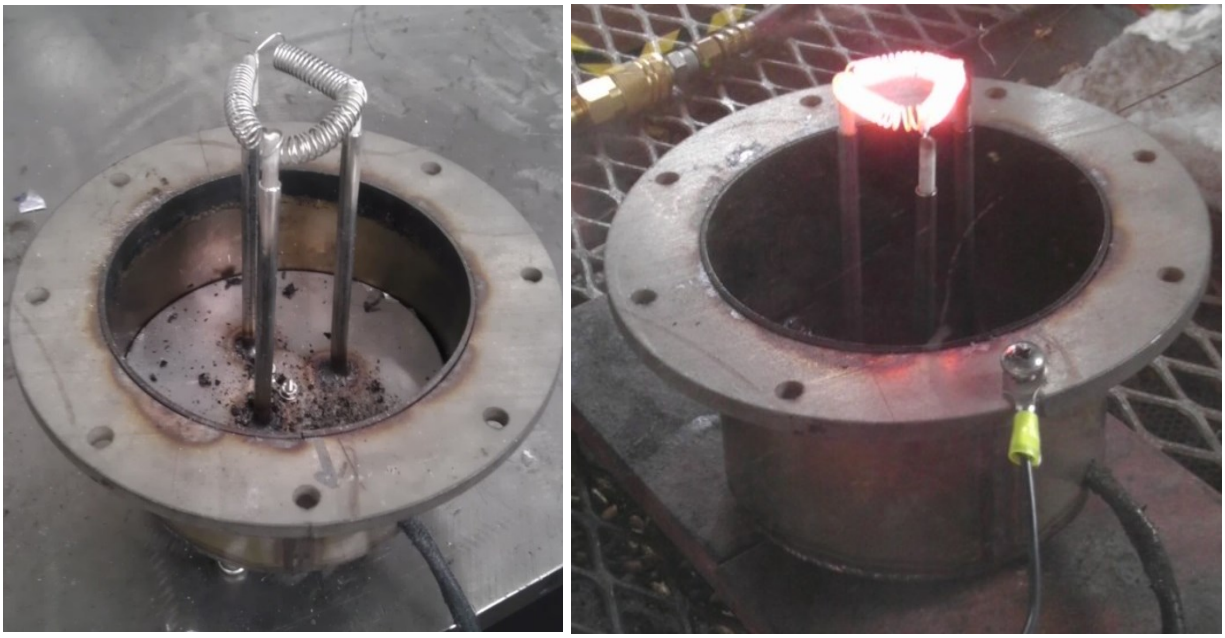

Figure 44. Secondary igniter assembly and test.

4.4.6 **Modified TRL 4 Testing**

After visual quality test had been completed, more sophisticated tests were conducted. The tests were meant to optimize the performance of the burner through more detail measurements, such as emission and temperature. Two major variables of the burner were studied through the tests, which are air flow and ignition sequence.

4.4.6.1 Air Requirement Experiment

4.4.6.1.1 Experimental Details

Operating conditions that could be optimized for the given design criteria were firepower and emissions. Optimized fire power and MCE were characterized during design criteria. The fire power of the burner was meant to low, a steady small flame, while MCE value was pre-determined to be above 95%. To optimize these operating conditions, two main variables could

be parametrically varied: primary and secondary air stream flow rates. Accordingly, experiments were conducted to perform in which primary and secondary air flow rates were varied to obtain optimum operation conditions. For these experiments, the following instrumentation was used. First, thermocouples were imbedded in the burner to measure oxidation and exhaust temperatures. Second, NDIR gas measurements were conducted to measure CO (ppm) and CO2 (%).

To begin each experiment, the fuel hopper was filled with 500 grams of wood pellets, and the fuel was added continually as needed to produce a steady state flame in the burner. For each experiment, the primary and secondary air was held constant. The device was then ignited using a diesel glow plug and hot wire igniter. Both of the igniters were turned on for 3 minutes. Keeping the air flow constant, temperature was observed to rise until it reached a steady state. Once the temperature reached steady state, the air flow rates were changed at 10 minutes intervals. Table 6 summarizes 3 cases of volumetric air flow rate once the burner reached a steady state. Each case consists of different volumetric flow rates, and each case differs with the ratio of secondary to primary air. Case 1, 2, and 3 have a secondary to primary air ratio of 3, 4, and 5, respectively.

Table 6. Air configurations matrix.

Total Air [CFM]	Case 1			Case 2			Case 3		
	Pri	**Sec**	**Ratio**	**Pri**	**Sec**	**Ratio**	**Pri**	**Sec**	**Ratio**
3	0.7	2.3	**3**	0.6	2.4	**3**	0.5	2.5	**3**
5	1.3	3.8	**4**	1.0	4.0	**4**	0.8	4.2	**4**
7	1.8	5.3	**5**	1.4	5.6	**5**	1.2	5.8	**5**

4.4.6.1.2. Temperature Data

In this section, the variation in combustion temperatures as a function of the air flow rates is presented. The purpose of obtaining temperature data was to evaluate the capability of the burner to perform the task of high MCE. It is well documented that at temperatures less than 1000 K the conversion of CO to CO_2 becomes very slow [12].

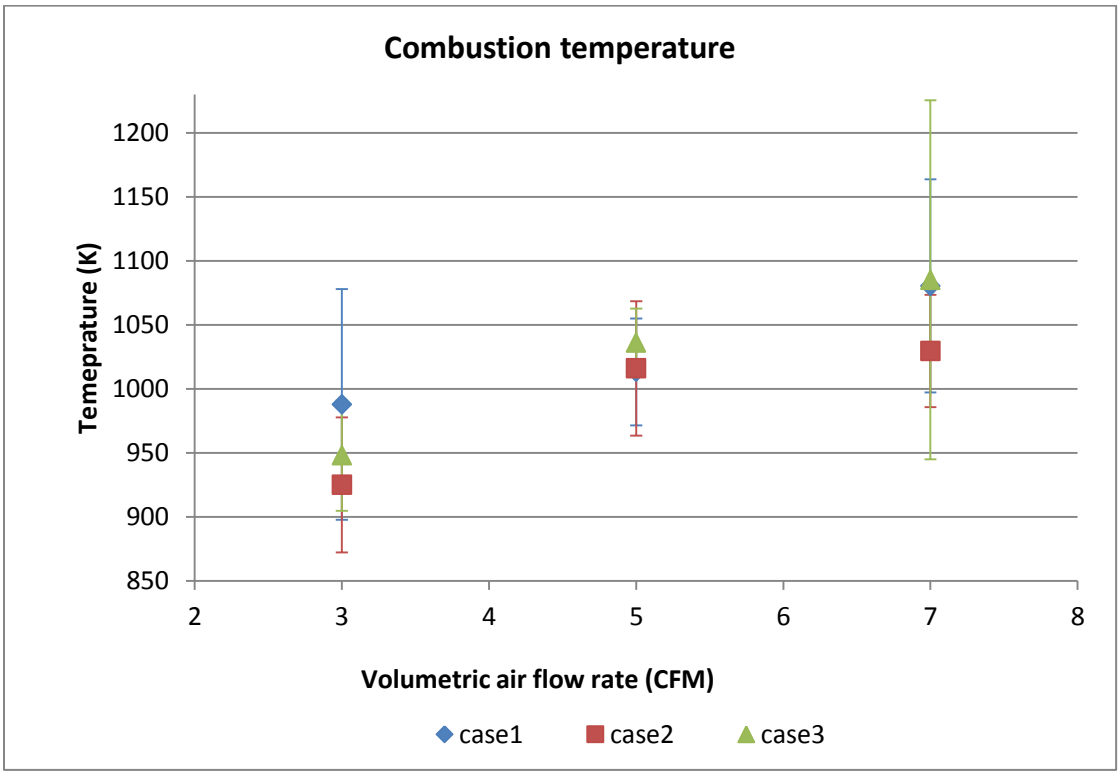

Figure 45. Measured combustion temperature at different air flow rates.

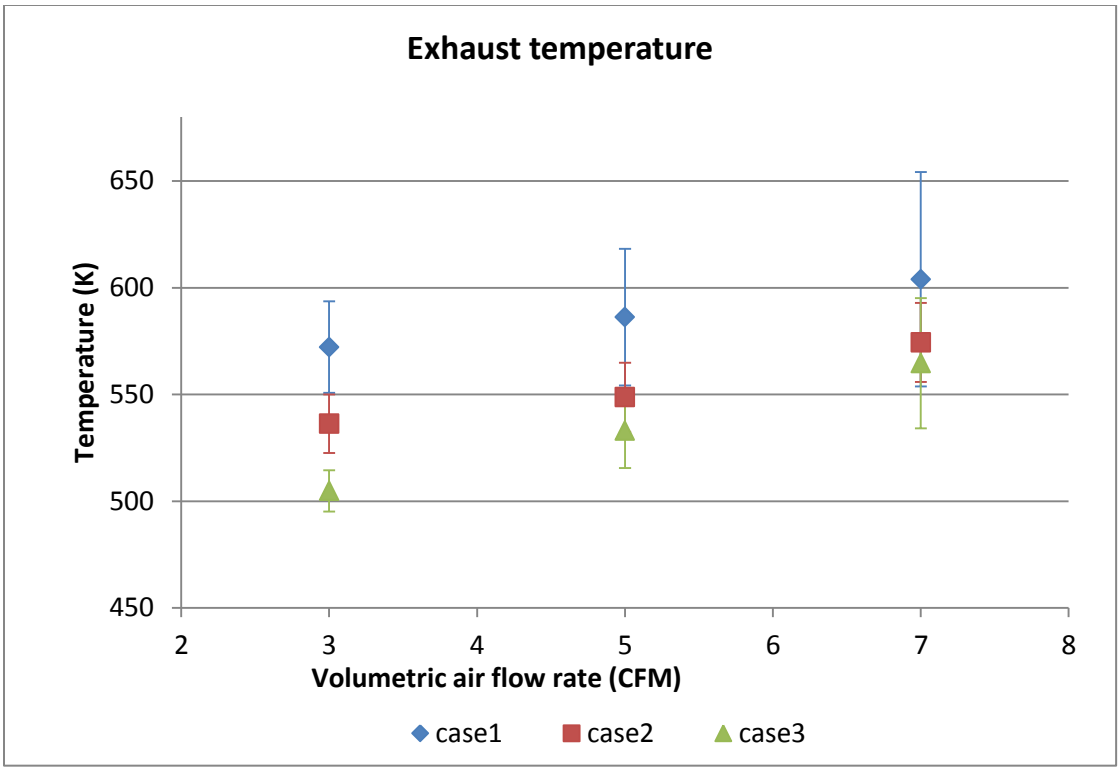

Figure 46. Measured Exhaust temperature at different air flow rates.

For the results presented here, the temperature data were time averaged throughout 10 minutes of each configuration. Two separate temperature measurements were made. The first measurement was the combustion temperature, which was hottest temperature of the burner. The second measurement was the exhaust temperature. The combustion and exhaust temperatures are plotted in Figs. 3 and 4, respectively, for all of the cases listed in Table 6. It can be seen from the Figures that as more air is introduced to the burner, both the combustion and exhaust temperatures increase.

Temperature increase is a consequence of the gasifier behavior. Primary air flow rate is the main variable to change the combustible gas production rate. A rise in primary air flow rate will result in the rise of combustible gas production. The gas then meets the secondary air, and it

creates a diffusion flame sheet. With more gas and more air mixing together at the sheet, the temperature of the sheet will increase which results in overall temperature rise. This phenomenon explains the increase of temperature with different air flow rates. It is also observed that temperature decrease with different cases where the secondary to primary air flow ratio increase. Higher ratio means there is more secondary air at room temperature being introduced to smaller gas production rate at high temperature. As more air meets smaller gas production rate, the flame sheet will be diluted and cooled down.

4.4.6.1.2 Modified Combustion Efficiency Result

As mentioned above, a major design criterion of the burner was that it must have low CO emission. In this section, the CO emissions data is presented for different volumetric air flow rates. By measuring CO and CO_2 concentration, it is also possible to calculate the modified combustion efficiency, which was presented on chapter 3. In general combustion, efficiency can be defined as the measured conversion of chemical energy to thermal energy in comparison to the ideal case of complete combustion, in which all carbon was converted to CO_2. In this case, the modified combustion efficiency is defined as CO_2 concentration divided by the sum of CO_2 and CO concentration.

From Figure 47, it can be seen that the combustion efficiency was greater than 97% for the majority of air flow cases. This result is consistent with the combustion efficiencies measured in improved rocket elbow stoves which have combustion efficiencies of greater than 94% [15]. It can also be seen that under some conditions, the combustion efficiency reached at 99%. These efficiencies were obtained with an overall volumetric air flow rate of 5 CFM and ratio of secondary to primary air flow rate of 3.

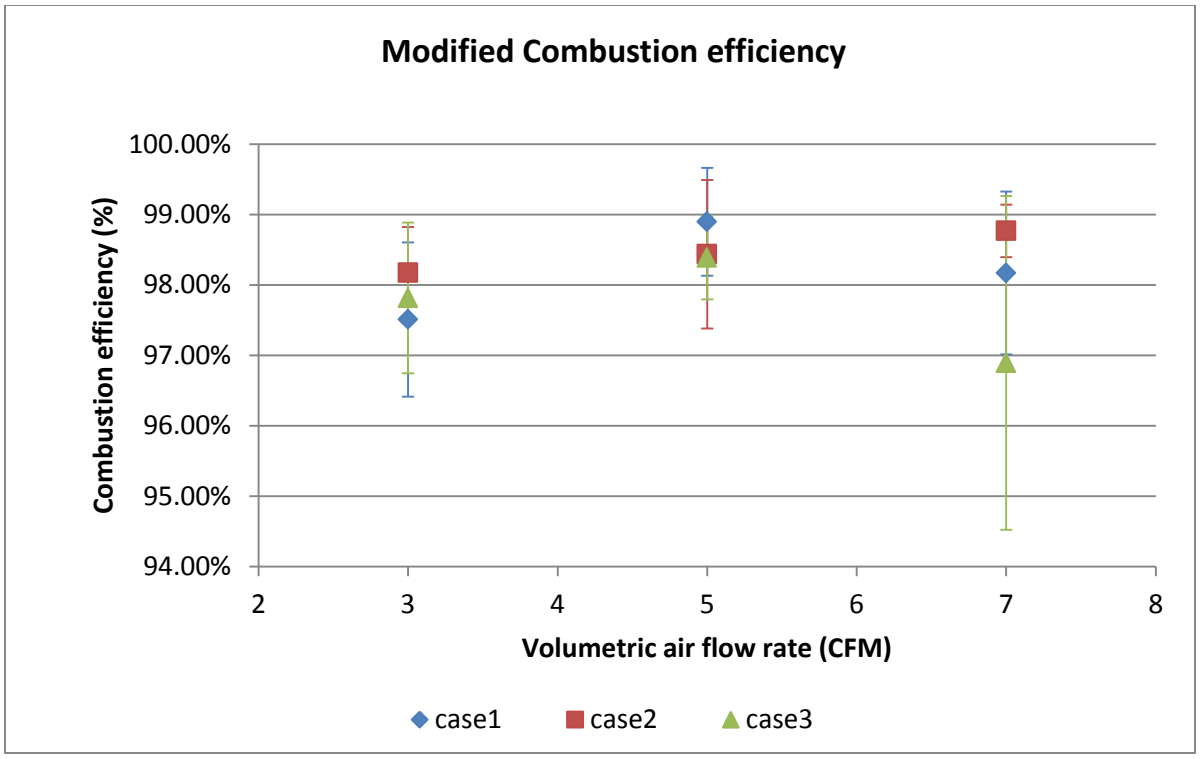

Figure 47. Measured modified combustion efficiency at different air flow rates.

4.4.6.1.3 Fire Power Result

Another design criterion was that it is preferable to perform the drying task with warm air flow and long residence time [14]. The criterion is based on the physical phenomena of drying where the presence of air flow is more critical than temperature. Burning the fuel at a lower rate will ensure longer residence time that to dry the material. In the following derivation, it will be shown how fuel consumption rate is related to firepower.

In this section, the method of calculating firepower and the carbon balance from CO and CO_2 emissions is presented. The carbon-balance was based on conservation of carbon (C) species. Given the percent of carbon in the fuel, which is roughly 50% [13], the mass flow rate of

the fuel could be obtained by measuring the CO and CO_2 in the exhaust. The firepower is then determined by multiplying the fuel mass flow rate and the fuel heating values.

The calculations assume that the fuel would be entirely converted into gas and all the charcoal consumed, which was a reasonable assumption. The amount of char remaining was observed to be insignificant compared to the CO and CO2 production. Figure 48 is a plot of fire power as a function of volumetric air flow rate for all of the cases presented herein.

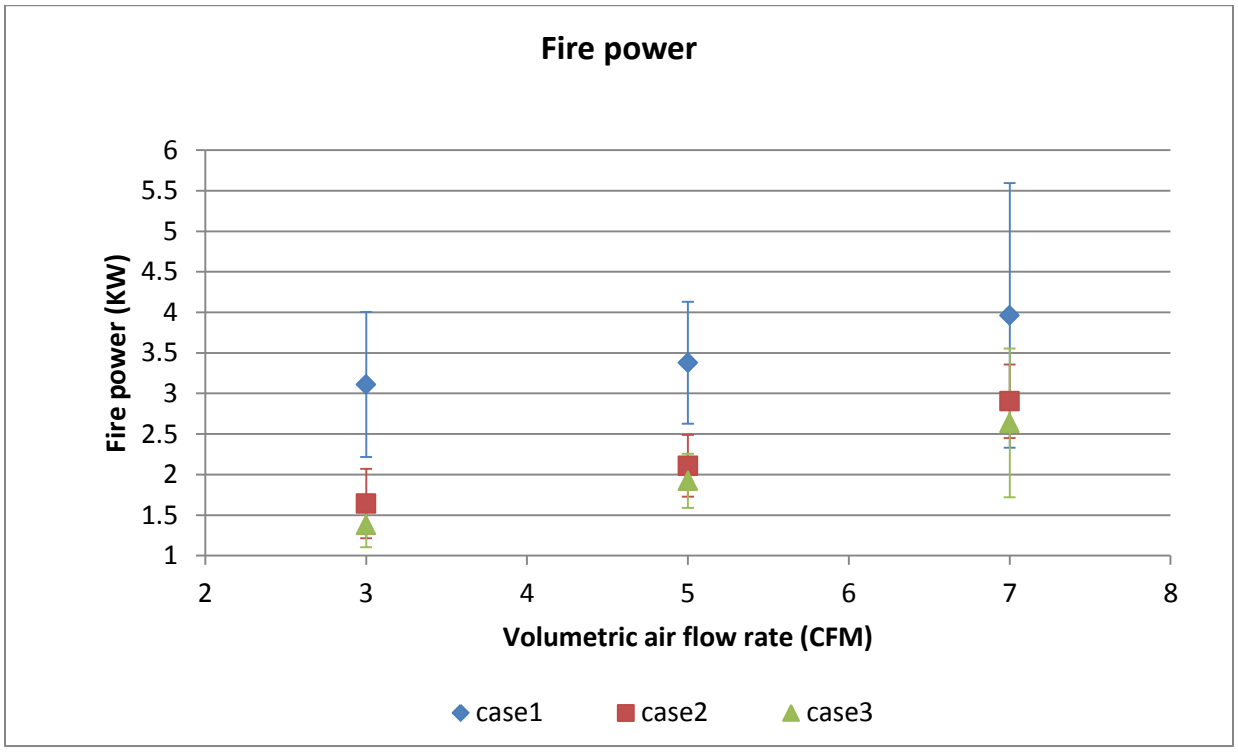

Figure 48. Measured Fire power at different air flow rates.

As it was explained in chapter 3, the gasifier will have a fuel consumption rate increase with the increased amount of primary air flow rate. From equation 2.6, it can be seen that fire power is fuel consumption rate multiplied by LHV. As the air flow rate was increased, the fire power, which is directly related to the fuel flow rate, also increased. The results suggest that the

fire-power in this system can be easily adjusted, which is an additional benefit of the system. Specifically, this unit suggests that the system could adjust to the transient operations of intermittent use inherent to a device.

4.4.6.2 Ignition Sequence Experiment

4.4.6.2.1 Experimental Details

The purpose of ignition experiment was to minimize net energy consumption, while in the same time produce consistent ignition. One of the major phases of energy consumption is ignition sequence, which needs to be reduced. There are five variables that are adjusted for each run in this experiment. They are:

1. Air flow rate for primary and secondary
2. Time for both air flows turn on
3. Time at primary igniter is turned on
4. Time of secondary igniter is turned on
5. Time of both igniter is turned off

In each run of this experiment, 200 grams of fuel was used, and the ultimate decision for each configuration was based on whether the flame was ignited and stable. Configurations were changed by trial and error, until stable ignition could be observed. With that configuration, the tests were repeated three times to reduce uncertainty. Final ignition sequence was obtained through repetition of 13 runs.

From the runs that were conducted, it was found that flame could be extinguished by a sudden increase of secondary air flow rates. A sudden increase on secondary air flow rates

indicated a sudden increase of mass that required heat. The newly ignited flame did not have enough thermal energy to take into account a sudden increase of heat load, which cause the flame temperature to drop. In some cases, the temperature dropped below ignition temperature and the flame was extinguished. To handle the changing, a ram increase with a span of 15 s was used instead of a step increase. The span provides the flame some time to adjust on higher heat load.

4.4.6.2.2 Ignition Data Results

Table 7. Ignition sequence result.

No.	Air Config (Prim, Note Sec(CFM))		Time air turned on	Primary igniter turned on	Secondary Igniter turned on	Igniters turned off	Stable??	NOTE
1	0.75	4	00:00	01:00	00:00	02:00	N	
2	1	4.5	00:00	00:30	00:00	03:00	N	Wire broke
3	1	4.5	01:00	00:30	00:00	03:30	Y	High volume of smoke
4	1	4.5	01:00	01:00	00:00	04:00	Y	Temp drop once igniters off
5	1	4.5	01:00	01:00	00:00	05:00	Y	
6	1	4.5	01:00	01:00	00:00	05:00	Y	
7	1	2	01:00	01:00	00:00	05:00	Y	Much closer to stable ignition
	1	4.5	05:00					
8	1	2	01:00	01:00	00:00	05:00	N	The step up in secondary ignition extinguish the flame
	1	4	05:00					
9	1	2	01:00	01:00	00:00	04:30	Y	
	1	4	04:00					
10	1	2	01:00	01:00	00:00	05:00	Y	
	2	6	04:00					
11	1	1	01:00	01:00	00:00	04:00	Y	Smoke still visible a little bit
	2	6	03:00					
	1	4	05:00					
12	1	1	01:00	00:30	00:00	04:00	Y	Needs to ramp up primary air slowly for a span of 15 s
	2	6	03:00					
	1	4	05:00					
13	1	1	01:00	00:30	00:00	04:00	Y	Smoke clears out much faster
	2	6	03:00					
	1	4	05:00					

Run 13 was selected to be the ignition sequence designated to the burner, because it is the most consistent configuration. Granted, run 13 consumed more energy than run 1, 2, and 3, because run 13 configurations have the igniters on for longer period of time. To choose between energy consumption and stability, stability was chosen because stability was a desired factor in the final product.

4.5 TRL 5

With the main burner fully operational, TRL 5 attempted to integrate the burner system with the drying system for the first time. The drying system was design by Research Triangle Institute). The tasks to fulfill TRL 5 qualification are integrated frame and adapter. After the burner and the dryer were integrated, they were tested with wood pellets and dog waste as the fuel.

4.5.1 **Integration Process**

The burner from TRL 4 was used for TRL 5. The burner was attached to galvanized parts that channeled the exhaust gas through a tee. Galvanized steel was used because the adequate temperature rating and easy assembly. The attachment to the burner is shown in Figure 49. The connector assembly consisted of a reducer and a tee. The reducer was meant to connect the outlet of the dryer into the fuel chamber, and the tee was meant to channel the exhaust gas to the inlet of the dryer.

Figure 49. galvanized steel attachment of the burner.

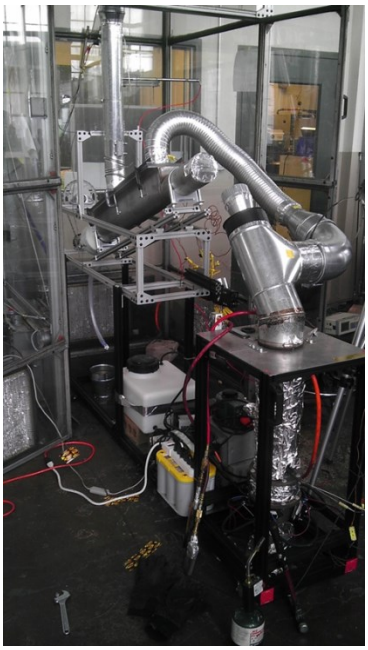

Figure 50. Completed TRL 5 integration.

The frame was built using extruded aluminum, shown in Figure 50. In the Figure, the inlet of the burner was disconnected from the outlet of the dryer, which was different from the original design. The gas that was produced in the burner flowed backwards when the inlet was connected to the dryer. The presence of syngas in the dryer would damage the dryer because it was not meant to hold syngas. In the future works, a valve could be implemented to segregate the two components.

4.5.2 **Emission Experiment of TRL 5**

With an integrated system, experiments were conducted to measure the drying and emission performance. Drying performance was measured by visual examination of a solid waste model that was placed on the dryer. Emission performance was measured by NDIR gas analyzer. In TRL 5, all the results from TRL 4 were implemented as standard burning conditions, both air

flows and ignition sequence. The experiments were conducted two times, with different fuels. The first experiment used wood pellets as the fuel, while the second experiment used dog waste. In each experiment, the fuel load is 500 grams dry.

After the experiments were conducted, the dryer was observed for drying result. The visual drying results were different between the two experiments. The first experiment with wood pellets showed that the wet solid waste in the dryer had a range of moisture content. The closest waste to the exhaust gas inlet was pyrolyzed on the surface, but inside, the waste was still wet. The furthest waste from the exhaust gas did not show any decrease on moisture content. The gradient showed that the dryer had unequal temperature distribution. The second experiment was proven to have a lower exhaust gas temperature in comparison to the previous burns, so there was no pyrolysis is observed. However, the fuel did not dry due to lower temperature. Along with the drying result, CO and CO2 emission were measured and converted to Modified Combustion Efficiency. The result of both experiments is shown in Figure 51. The y-axis shows the modified combustion efficiency in percent, while the x-axis shows the time of the experiment. The blue curve is the emission result with wood pellets while the red curve is the solid waste.

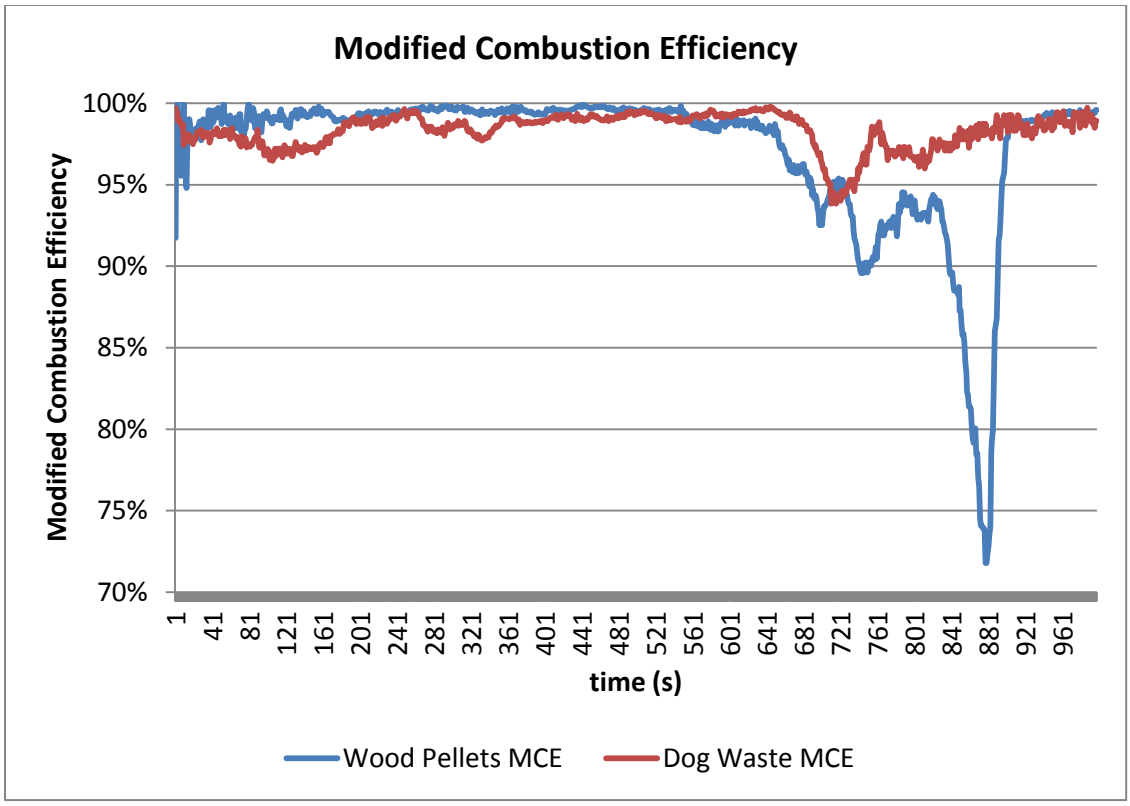

Figure 51. Measured Modified combustion efficiency of wood pellets in comparison to dog waste.

TRL 5 experimental results showed that the average of MCE for both experiments was above 95%. The average of wood pellets was 97.2%, and of dog waste was 98.3%. The data suggested that the fuel surrogates assumption was valid in terms of emission data. However, during the dog waste experiment, constant agitation needed to be applied to the burner throughout the whole experiment. Due to the high ash content, the grate of the burner tends to get covered with ash and causes the fuel to bridge. This issue was further studied on TRL 6. Towards the end of the burns the MCE for wood pellets dropped below 75%, which implied that CO emission spiked. This was a result of charcoal combustion phase, which required different air configurations to combust.

4.6 TRL 6

So far, TRL 4 and 5 based their operation on laboratory environment. Some components in the burner were still connected to external power source, which access would be limited on the field. TRL 6 was developed for the purpose of having a burner that would operate in a simulated field condition. The main goal of TRL 6 was to establish consistent operation with a single 12 Volt battery as a power supply. Air flows on previous TRL had been supplied by air compressor, and the igniters had been powered by 120 Volt electrical grid. These two major components were modified to operate with a 12 Volt battery.

4.6.1 **Fan Calibration**

In order to simulate the field environment, pressurized air was no longer used as an air supply for the burner. Instead, air was supplied with DC brushless fans. A Micronel® fan with a 6 Volt maximum voltage and 18 CFM flow rating was used for the primary air, and a DAYTON 12 Volt with a flow rate of 129 CFM was used for the secondary air. Unlike pressurized air, DC fans do not provide as much static pressure to overcome the pressure drop. Therefore, the fans were calibrated to ensure that their flow rates were equivalent to the flow rates provided by the pressurized air.

The calibration was conducted using an enclosure of known volume sealed into the outlet of the prototype. Air was channeled through the burner, and subsequently filled up the constant volume at the outlet. With a known volume and time the air took to fill the volume, average flow rates were acquired. The measurement of average flow rates from the pressurized air and the DC fans were matched to obtain the Voltage to SCFM conversion. This experiment was repeated

five times for both of the primary and secondary flows. The result of this experiment is shown on Figure 52. There were difficulties in monitoring low flow rates, so low flow rates were excluded.

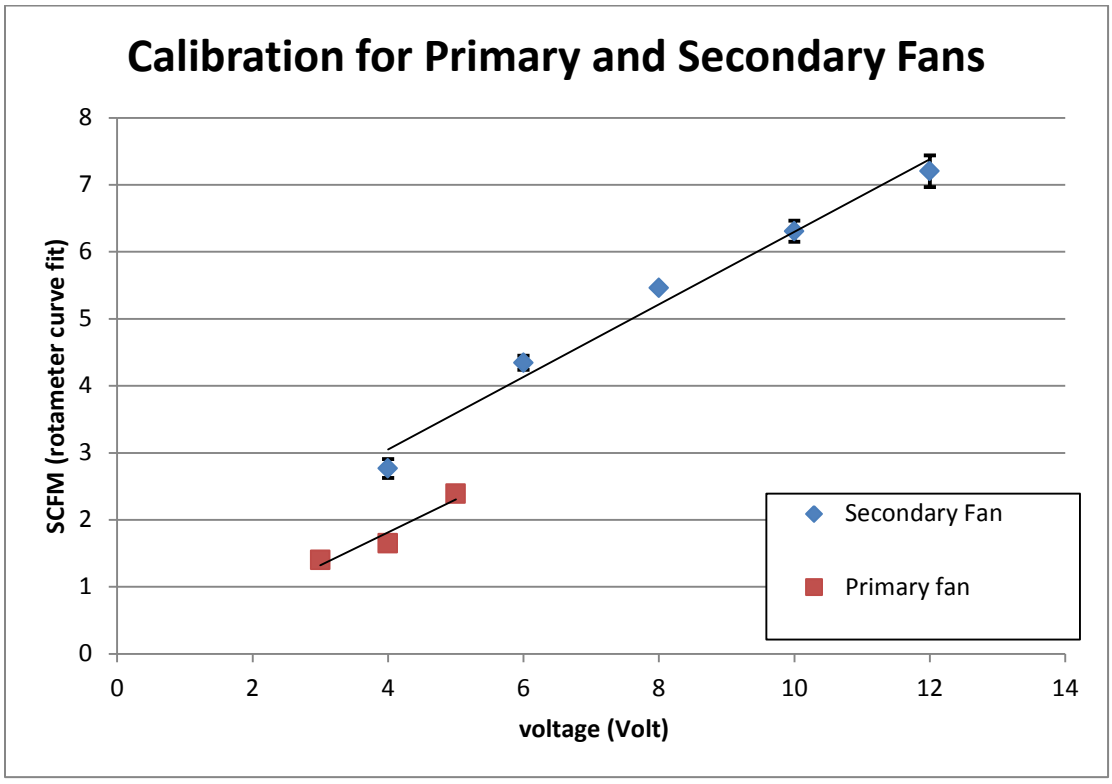

Figure 52. Curve fit conversion of voltage to SCFM of primary and secondary fan.

4.6.2 **Design of TRL 6**

Previous burner was proven to fulfill the required criteria. However, there were few improvements that were made to improve the burner performance even further. One major problem that was encounter on the previous prototype was thermal runaway with increased fuel load. When the fuel load in the previous burner was above the 6" primary air shroud, thermal runaway occurred continually. Change was conducted to raise the primary air shroud height to the top of the burner. Along with the raised primary air shroud, velocity of primary air through the shroud was calculated to check whether tangential flow in primary air was actually effective.

The analysis showed that the velocity through the concentric shroud was 0.099 $^{m}/_{s}$. The velocity was too low for tangential airflow to be significant, and therefore the inlet for primary air was changed into stainless steel pipe fitting.

Along with the primary shroud, a major overhaul was conducted at the flame front area. In this area, the glow plug was inserted from the side, but its body was exposed directly to the flame. A shroud was designed to prevent the glow plug from direct exposure. On top of the primary igniter, the secondary igniter was also modified. The wire diameter was increased to 0.065", which resulted in lower electrical resistance. Lower resistance would allow the igniter to be powered by 12 Volt battery. The modified secondary igniter is shown on Figure 53.

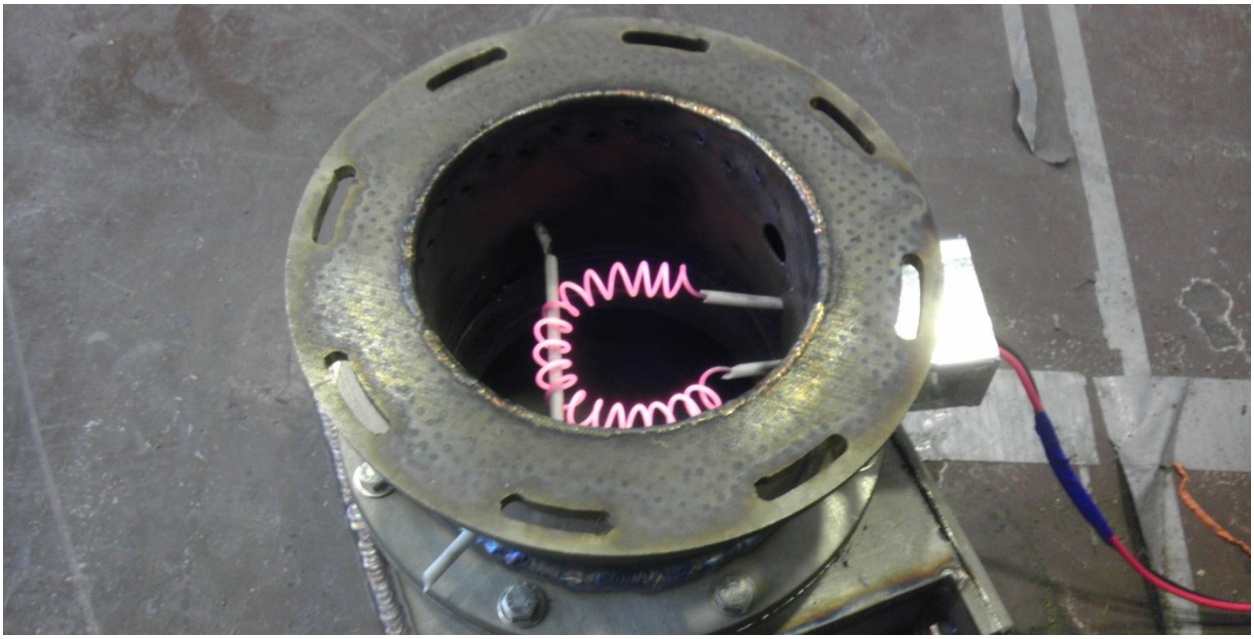

Figure 53. Floating secondary igniter for TRL 6 with 12 Volt battery as power supply.

TRL 5 experiment showed that in dog waste experiment, constant agitation was needed. To incorporate automatic agitation, a shaker mechanism was implemented to the burner, shown in Figure 54. The shaker mechanism was designed to be able to rotate with the power of a servo

motor. As the shaft turned, it rotated the cam back and forth against the wall of the shaker. The freely floating wall would create back and forth motion. Along with the shaker, the grate material was also improved using nickel alloy or Inconel.

Figure 54. Shaker mechanism for TRL 6.

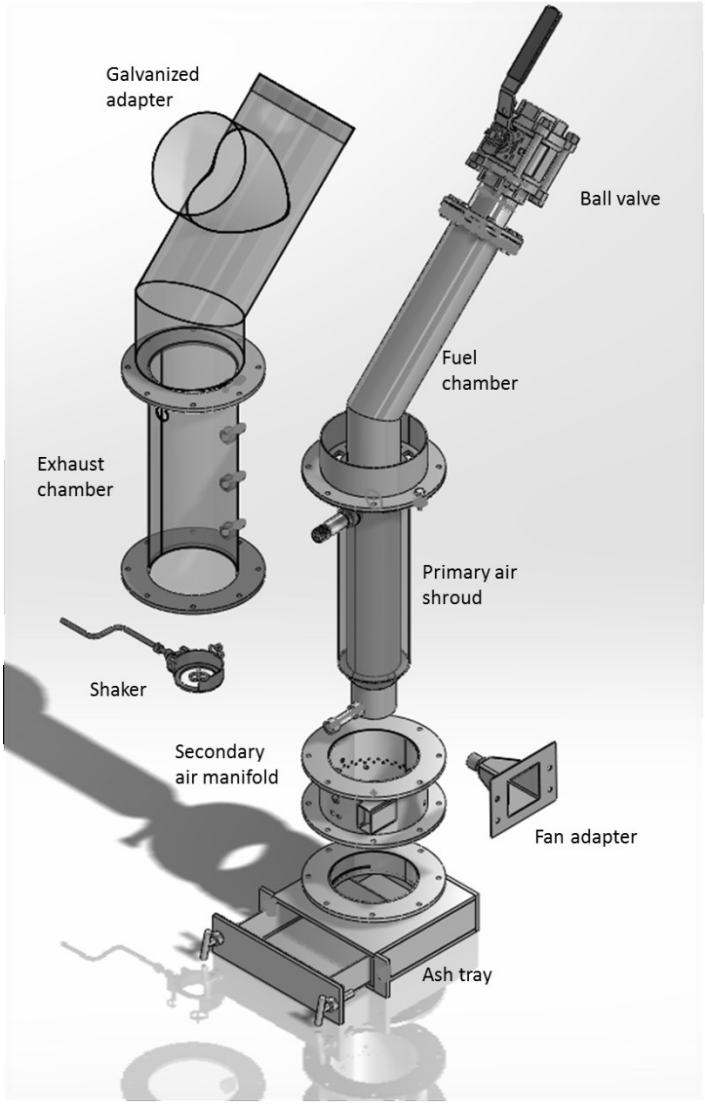

Figure 55. Overall design of TRL 6.

4.6.3 **TRL 6 Experiment : MCE Comparison of Air Hose and Fans**

4.6.3.1 Experimental Details

Previous experiment conducted the calibration of DC fans in respect to Pressurized air, and the result was the conversion between the DC fans voltage to the rotameter flow rate (SCFM). With the result of the conversion, combustion experiments were conducted to verify MCE stability between air hose and DC fans. Before the comparisons were made, however,

preliminary experiment was conducted in order to compare the performance between TRL 6 and TRL 4. The preliminary experiment used the air flow matrix in TRL 4 experiment to measure the performance of TRL 6 burner. CO and CO_2 emissions were measured along with exhaust gas temperatures were measured for this preliminary experiment. Afterwards, the comparison experiment between the fan and pressurized air was conducted.

4.6.3.2 Experimental Result

The preliminary experimental result using pressurized air is shown on Figure 56. In this Figure, two data lines are presented, MCE and Exhaust gas temperature. The temperature measurement location is shown to the left of the Figure, which is indicated by T4. The two data lines are represented in two different y-axes, with one for temperature, and one for MCE. On the other hand, the x-axis on this graph is time in seconds.

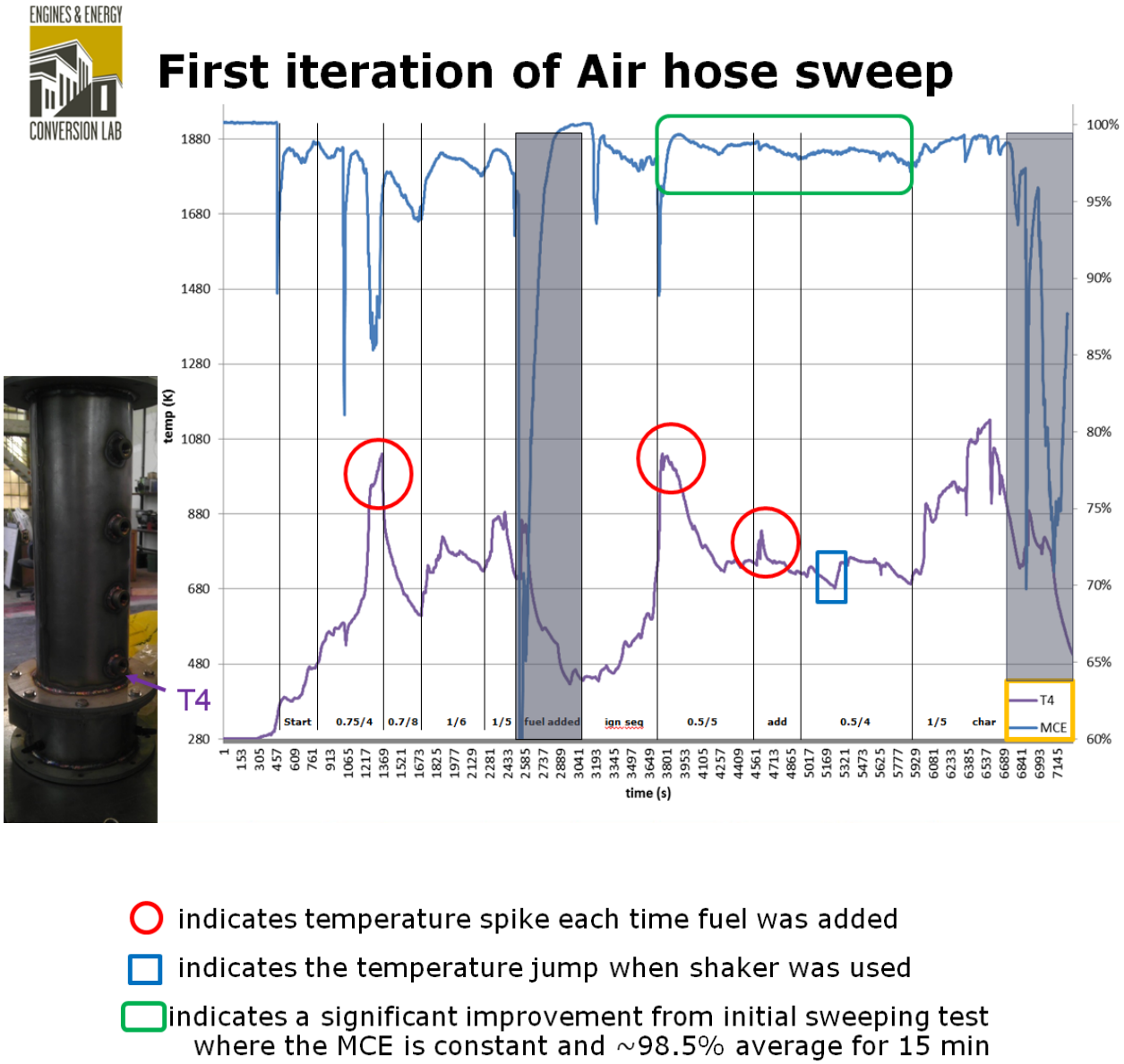

Figure 56. First iteration of experiment with air hose on TRL 6.

Analyzing the data was conducted by the markings in the Figure. The red circles indicated temperature spike that occurred in every fuel addition. The fuel produced high heat release in a short period of time, causing the temperature to spike and MCE to drop. This phenomenon was not noticeable in the previous prototype. The proposed cause for this phenomenon was the difference in grate height. The reduction zone that to convert the CO_2 back

to CO was significantly larger than TRL 4 zone. CO that came out from the reduction zone was combusted and produced more heat. The blue square in the Figure indicated the time when the shaker mechanism was activated. The temperature increased rapidly because the ash on the grate fell to the ash tray. As the ash fell through, the new incoming fuel occupied the space where the ash was. The temperature results indicated that the concept of agitator was proven to reduce fuel bridging. The green box indicated a consistent MCE above 98% during the experiment. In the first half of the experiment, the MCE was fluctuating between 98% and 80%. During the second half, a configuration of 0.5 CFM for primary air and 5 CFM for secondary air was able to produce a consistent result for 15 minutes. There was a small difference from the previous TRL 4 air flows, where the optimum air requirement was 0.75 CFM and 4 CFM. In this prototype, geometry difference might have caused higher thermal efficiency to oxidize CO.

With the result from preliminary experiment, the comparison experiment was conducted. The experiment consists of two tests, with different air supply methods. The data shown in Figure 57 was the test with pressurized air flow, while the data in Figure 58 was the test with DC fans. In the early section of both tests, The MCE values were above 95%, which were comparable to TRL 4. The temperature, however, did not look similar between the air hose and fans. The temperature in the fans experiment was decreasing after it ignites. The decreasing temperature indicated a net heat loss in the burner. The unstable temperature that kept decreasing eventually dropped the MCE value, because with lower temperature, the CO was not oxidized. The lower temperature towards the end of fans experiment caused the drop of MCE to about 70%. Visual smoke was seen exiting the burner which indicates that the firepower was too low.

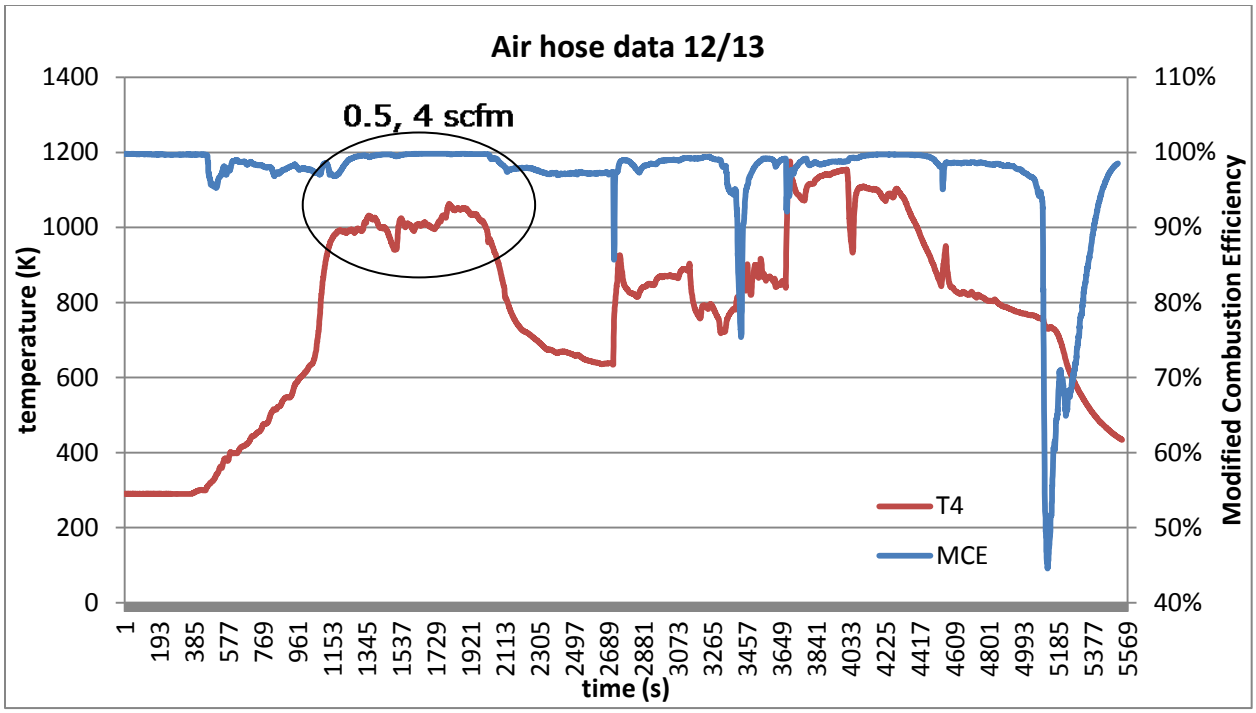

Figure 57. MCE and Temp of Air hose experiment in TRL 6.

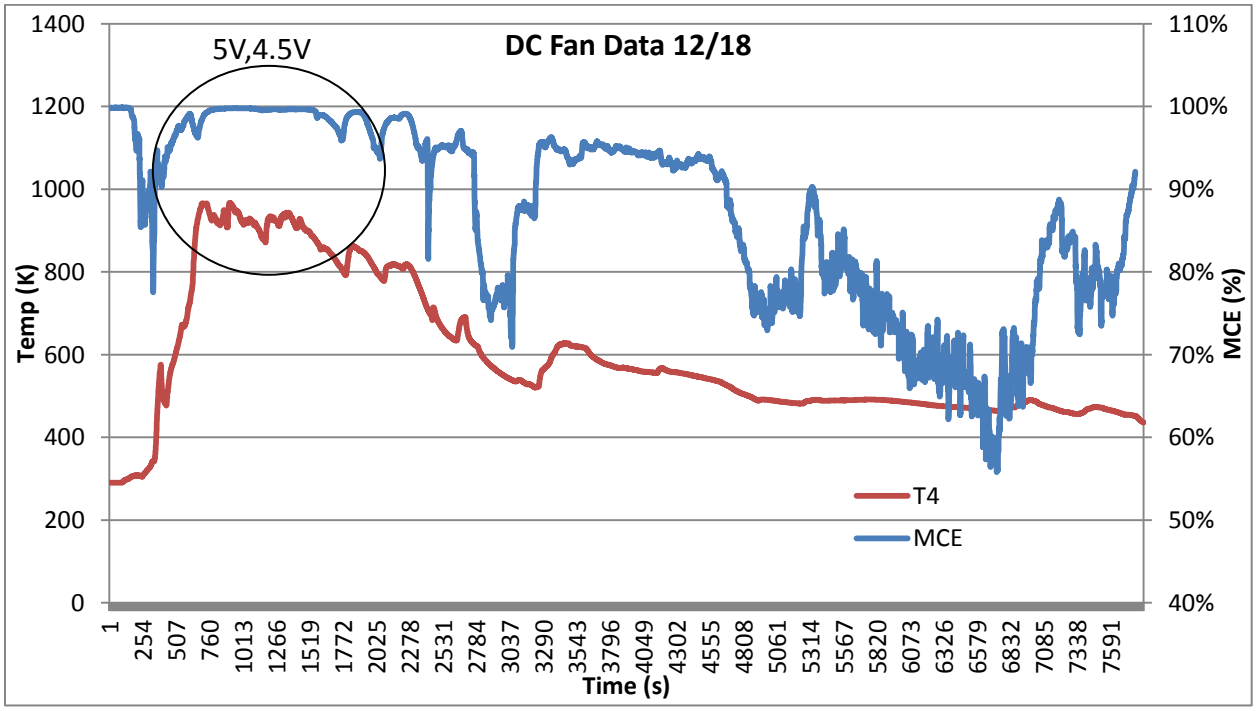

Figure 58. MCE and Temp of DC fans experiment in TRL 6.

5. CONCLUSION AND FUTURE WORKS

5.1 Conclusion

A downdraft semi-gasifier burner was developed for the sanitation of solid human waste through incineration. The burner was designed to be a component of an overall sanitation system that was developed by CSU and RTI. The system was meant to operate without any outside power source and able to self-sustain operations. The developed prototype reached TRL 6, which would be categorized as field simulated prototype in the lab.

The development was started with an updraft design for TRL 1 and 2, in which the fuel characteristics were studied. Combustion experiment was conducted and found that the solid waste were able to produce enough energy for the system to sustain itself. However, it was concluded that dried and shaped solid waste was able to optimize the performance of the burner. After the fuel was studied, a combustion experiment were conducted and measured visually. With the result of the combustion, it was found that the secondary igniter had to be implemented to shorten the time until ignition.

Downdraft designs were developed through the results from the updraft design. TRL 4 was able to combust the fuel with the performance that was required. The design was optimized with secondary air manifold with the purpose of tangentially channeled air to enhance mixing. CFD simulation using FLUENT was conducted in developing the right inlet size. Optimization of the burner was conducted for air flow and ignition sequence. Optimized air flow indicated that primary air required 1 CFM of flow while secondary air required 4 CFM of flow. The design was further optimized in TRL 6 to operate within a field environment. Air supply was switched

into DC brushless fans. The fan was calibrated to simulate the flow of pressurized air, and then the results were implemented into combustion experiment.

The completed prototype would be able to help the sanitation problem in this world, because it is able to operate in the place with no access to electricity or water. The device would be able to sanitize the solid waste of a household in less than a day. Sustainable operation will help to reduce children death due to poor sanitation access.

5.2 Future work

The future work of this application includes the further optimization of the burner size. The reduced size burner is shown in Figure 59, while the dimension in inches is shown in Figure 60. The reduced size burner would increase the portability of the device for transportation to rural area. On top of that, the cost of the device would be reduced due to less material used for each prototype.

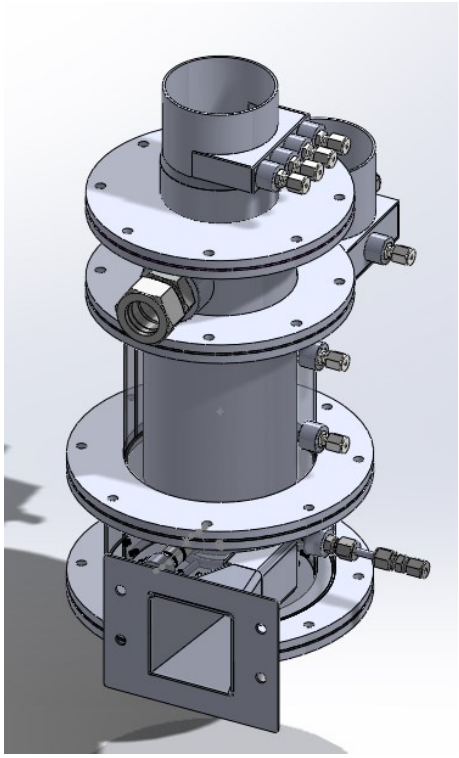

Figure 59. Reduced size downdraft semi-gasifier burner.

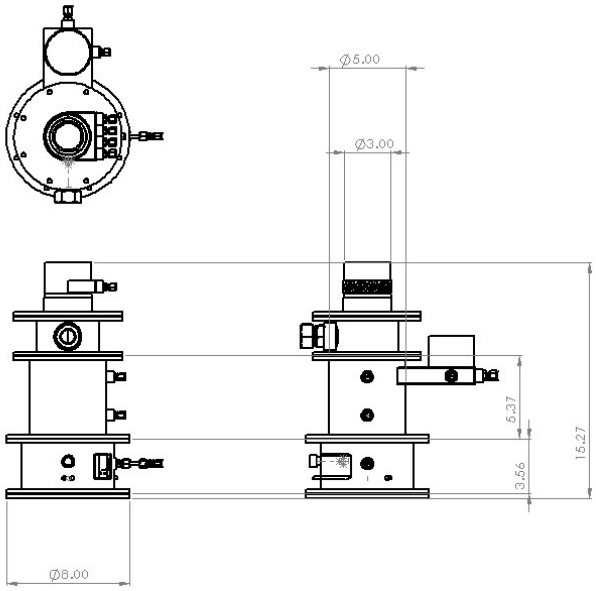

Figure 60. Dimension for reduced size prototype in Inches.

6. REFERENCES

1. United Nations Millenium Declaration
2. Langergraber, Günter, and Elke Muellegger. “Ecological Sanitation—a Way to Solve Global Sanitation Problems?” Environment International 31.3 (2005): 433–444. ScienceDirect. Web. 31 May 2013.
3. “Water, Sanitation & Hygiene - Bill & Melinda Gates Foundation.” Web. 31 May 2013.
4. Werner, Christine, et al. "Reasons for and principles of ecological sanitation." *2nd International Symposium on Ecological Sanitation, April 2003*. 2003.
5. Gorman, Christine. "A Brief History of the Toilet [Slide Show]: Scientific American." A Brief History of the Toilet [Slide Show]: Scientific American. N.p., 18 Aug. 2011. Web. 05 June 2013.
6. Otterpohl, Ralf. "Design of highly efficient source control sanitation and practical experiences." *Decentralised sanitation and reuse* (2001): 164-179.
7. Jönsson, Håkan, et al. Guidelines on the use of urine and faeces in crop production. EcoSanRes Programme, 2004.
8. Baumeyer, A. "New Toilets for Indian Slums-Nutrients Mass Balance of a Co-Composting Plant in Bangalore, India." (2003).
9. Gujer, W., and A. J. B. Zehnder. "Conversion processes in anaerobic digestion." Water Science & Technology 15.8-9 (1983): 127-167.
10. Nels, C. “Energy Recovery by Incineration of Solid Wastes in the Federal Republic of Germany.” Waste Management & Research 2.1 (1984): 37–51. ScienceDirect. Web. 3 June 2013.
11. Defeche, J. “Combustion, Corrosion and Fouling Aspect of Energy Recovery from Municipal Waste.” Waste Management & Research 1.1 (1983): 17–30. ScienceDirect. Web. 10 June 2013.
12. Werner, C., et al. "Overview of worldwide Ecological Sanitation Concepts and Strategies." (2004).
13. Balkema, Annelies J et al. “Indicators for the Sustainability Assessment of Wastewater Treatment Systems.” Urban Water 4.2 (2002): 153–161. ScienceDirect. Web. 3 June 2013.
14. Morris, M, and L Waldheim. “Energy Recovery from Solid Waste Fuels Using Advanced Gasification Technology.” Waste Management 18.6–8 (1998): 557–564. ScienceDirect. Web. 3 June 2013.
15. Vinnerås B. Possibilities for sustainable nutrient recycling by faecal separation combined with urine diversion. PhD thesis, Agraria 353, Swedish University of Agricultural Sciences, Uppsala, Sweden, 2002.
16. Lewis, S. J., and K. W. Heaton. "Stool form scale as a useful guide to intestinal transit time." *Scandinavian journal of gastroenterology* 32.9 (1997): 920-924.

17. "Phyllis2." - ECN Phyllis Classification. Nergy Research Centre of the Netherlands (ECN), 29 Apr. 2009. Web. 20 June 2013.
18. Barneto, Agustín García et al. “Kinetic Models Based in Biomass Components for the Combustion and Pyrolysis of Sewage Sludge and Its Compost.” Journal of Analytical and Applied Pyrolysis 86.1 (2009): 108–114. ScienceDirect. Web. 8 July 2013.
19. De Oliveira Silva, Jader et al. “Thermal Analysis and FTIR Studies of Sewage Sludge Produced in Treatment Plants. The Case of Sludge in the City of Uberlândia-MG, Brazil.” *Thermochimica Acta* 528 (2012): 72–75. *ScienceDirect*. Web. 14 June 2013.
20. Telmo, C., and J. Lousada. “Heating Values of Wood Pellets from Different Species.” Biomass and Bioenergy 35.7 (2011): 2634–2639. ScienceDirect. Web. 14 June 2013.
21. Nummer, Brian A., Ph.D. "Historical Origins of Food Preservation." National Center for Home Food Preservation. National Center for Home Food Preservation, May 2002. Web. 11 July 2013. <http://nchfp.uga.edu/publications/nchfp/factsheets/food_pres_hist.html>.
22. Luboschik, Ulrich. “Solar Sludge Drying — Based on the IST Process.” Renewable Energy 16.1–4 (1999): 785–788. ScienceDirect. Web. 9 July 2013.
23. Mathioudakis, V.L. et al. “Extended Dewatering of Sewage Sludge in Solar Drying Plants.” Desalination 248.1–3 (2009): 733–739. ScienceDirect. Web. 9 July 2013.
24. Deng, Wen-Yi et al. “Measurement and Simulation of the Contact Drying of Sewage Sludge in a Nara-type Paddle Dryer.” Chemical Engineering Science 64.24 (2009): 5117–5124. ScienceDirect. Web. 12 July 2013.
25. Kalderis, D., M. Aivalioti, and E. Gidarakos. “Options for Sustainable Sewage Sludge Management in Small Wastewater Treatment Plants on Islands: The Case of Crete.” Desalination 260.1–3 (2010): 211–217.
26. Basu, Prabir. Biomass gasification and pyrolysis: practical design and theory. Academic press, 2010.
27. Reed, Thomas B., and Agua Das. Handbook of biomass downdraft gasifier engine systems. Biomass Energy Foundation Press, 1998.
28. "Reinventing the Toilet." University of Colorado Boulder. Regents of the University of Colorado, n.d. Web. 30 Sept. 2013. <http://www.colorado.edu/engineering/college-news/reinventing-toilet>.
29. Conesa, J.A. et al. “KINETIC STUDY OF THE PYROLYSIS OF SEWAGE SLUDGE.” Waste Management & Research 15.3 (1997): 293–305. ScienceDirect. Web. 12 June 2013.
30. Xiong, Sijiang et al. “Effect of Moisture Content on the Characterization of Products from the Pyrolysis of Sewage Sludge.” Journal of Analytical and Applied Pyrolysis n. pag. ScienceDirect. Web. 12 July 2013.
31. Fonts, Isabel et al. “Sewage Sludge Pyrolysis for Liquid Production: A Review.” Renewable and Sustainable Energy Reviews 16.5 (2012): 2781–2805. ScienceDirect. Web. 12 July 2013.
32. Boráň, Jaroslav, Lucie Houdková, and Thomas Elsäßer. “Processing of Sewage Sludge: Dependence of Sludge Dewatering Efficiency on Amount of Flocculant.” Resources, Conservation and Recycling 54.5 (2010): 278–282. ScienceDirect. Web. 10 June 2013.

33. Coovattanachai, Naksitte. “Biomass Gasification Research and Field Developments by the Prince of Songkla University, Thailand.” Biomass 18.3–4 (1989): 241–271. ScienceDirect. Web. 31 May 2013.
34. Li, Jianfen et al. “Hydrogen-rich Gas Production by Steam Gasification of Palm Oil Wastes over Supported Tri-metallic Catalyst.” International Journal of Hydrogen Energy 34.22 (2009): 9108–9115. ScienceDirect. Web. 4 June 2013.
35. Higman, Christopher, and Maarten Van der Burgt. Gasification. Access Online via Elsevier, 2011.
36. Klass, 1998, p. 276.
37. Knoef, 2005, p. 15.
38. Zainal, Z.A et al. “Experimental Investigation of a Downdraft Biomass Gasifier.” Biomass and Bioenergy 23.4 (2002): 283–289. ScienceDirect. Web. 23 May 2013.
39. Balu, Elango, and J.N. Chung. “System Characteristics and Performance Evaluation of a Trailer-Scale Downdraft Gasifier with Different Feedstock.” Bioresource Technology 108 (2012): 264–273. ScienceDirect. Web. 19 Nov. 2013.
40. Simone, Marco et al. “Assessment of Syngas Composition Variability in a Pilot-scale Downdraft Biomass Gasifier by an Extended Equilibrium Model.” Bioresource Technology 140 (2013): 43–52. ScienceDirect. Web. 12 Oct. 2013.
41. Law, Chung K. Combustion physics. Cambridge University Press, 2006.
42. Turns, Stephen R. An introduction to combustion. Vol. 499. New York: McGraw-Hill, 1996.
43. Ernst, Armin, and Joseph D. Zibrak. “Carbon Monoxide Poisoning.” New England Journal of Medicine 339.22 (1998): 1603–1608. Taylor and Francis+NEJM. Web. 19 Nov. 2013.
44. Li, Juan et al. “An Updated Comprehensive Kinetic Model of Hydrogen Combustion.” International Journal of Chemical Kinetics 36.10 (2004): 566–575. Wiley Online Library. Web. 19 Nov. 2013.
45. Tydén-Ericsson, I. “A New Pyrolyzer with Improved Control of Pyrolysis Conditions.” Chromatographia 6.8-9 (1973): 353–358. link.springer.com. Web. 19 Nov. 2013.
46. (28)Reed, Thomas B., and Agua Das. Handbook of biomass downdraft gasifier engine systems. Biomass Energy Foundation Press, 1998.
47. Mass and Energy balance of Downdraft Gasifier
48. Dogru, Murat, Adnan Midilli, and Colin R Howarth. “Gasification of Sewage Sludge Using a Throated Downdraft Gasifier and Uncertainty Analysis.” Fuel Processing Technology 75.1 (2002): 55–82. ScienceDirect. Web. 4 June 2013.
49. Kim, Young Doo et al. “Air-Blown Gasification of Woody Biomass in a Bubbling Fluidized Bed Gasifier.” Applied Energy 112 (2013): 414–420. ScienceDirect. Web. 14 Jan. 2014.
50. Stanley, Doris. "Induced Heat Resistance in E. Coli." USDA-ARS Food Safety Research Unit, July 1998. Web. 23 Sept. 2013.
51. Venkatasubramanian, Rama et al. “United States Patent: 7838760 - Trans-Thermoelectric Device.” 23 Nov. 2010. Web. 29 Jan. 2014.

52. Miller-Lionberg, Daniel David. “A Fine Resolution CFD Simulation Approach for Biomass Cook Stove Development.” COLORADO STATE UNIVERSITY, 2011. gradworks.umi.com. Web. 30 Jan. 2014.
53. "ECOM CN." ECOM EN2. ECOM America, n.d. Web. 29 Jan. 2014.
54. Zube, Daniel Joseph. “Heat Transfer Efficiency of Biomass Cookstoves.” (2010): n. pag. digitool.library.colostate.edu. Web. 31 Jan. 2014.
55. Burkitt, D. Po, A. R. P. Walker, and N. S. Painter. "Dietary fiber and disease." Jama 229.8 (1974): 1068-1074.

APPENDIX A. DOG WASTE MODEL CALCULATION

November 29th Dry stack with wet top

$m_{dry} := 100gm$

$m_{wet} := 87gm$ moisture_content := .5

$m\_moisture := m_{wet} \cdot moisture\_content = 43.5 \cdot gm$ $ash_{residual} := 47gm$

Energy required to burn off wet moisture

$Q_{temp\_increase\_1} := m\_moisture \cdot C_{p\_water} \cdot \Delta T = 13.657 \cdot kJ$

$Q_{vaporization\_1} := m\_moisture \cdot \Delta h_{vap.water} = 98.31 \cdot kJ$

$Q_{total\_required\_burn} := Q_{temp\_increase\_1} + Q_{vaporization\_1} = 111.967 \cdot kJ$

$q_{dry} := m_{dry} \cdot Q_{comb\_pico\_feces} = 1.531 \cdot MJ$

Order of magnitude more energy than was needed to dry wet material.

Dec 3 densities for ground Jack poop - 50% moisture

$\rho_{wet} := 74\frac{gm}{200mL} = 0.37 \cdot \frac{gm}{mL}$

$\rho_{dry} := 59\frac{gm}{200mL} = 0.295\frac{gm}{mL}$

$\frac{\rho_{dry}}{\rho_{wet}} = 0.797$ $.5 \cdot .797 = 0.399$

Volume needed per day of fecal mass - 50% moisture and geometry manipulated (ground)

$daily_{mass} = 2kg$

$V_{daily\_fecal\_output\_wet} := \frac{daily_{mass}}{\rho_{wet}} = 5.405L$ $V_{daily\_fecal\_output\_wet} = 1.428gal$

$V_{daily\_fecal\_output\_dry} := \frac{daily_{mass} \cdot percent\_moisture}{\rho_{dry}} = 4.746L$ $V_{daily\_fecal\_output\_dry} = 1.254gal$

$$\frac{V_{daily\_fecal\_output\_dry}}{V_{daily\_fecal\_output\_wet}} = 0.878 \qquad reduction := 1 - \frac{V_{daily\_fecal\_output\_dry}}{V_{daily\_fecal\_output\_wet}} = 0.122$$

Pelletizing Shape

Assume 2 x 2 x 2 cm cube

$l := 2cm \qquad w := 2cm \qquad h := 2cm$

$V_{cube} := l \cdot w \cdot h = 8 \cdot mL$

Total number of cubes needed

$$V_{total} := \frac{m_{dot\_dry}}{\rho_{dry}} = 2.034L$$

$$quantity := \frac{V_{total}}{V_{cube}} = 254.237$$

Five Gas Data Processing to produce Fire Power and MCE

Instruction

1. using the icon on HOME tab, IMPORT DATA
2. Find the excel file in your data
3. Pop-up window will appear and select the two column of CO2 and CO
4. Do NOT select the first row which are the title in excel
5. Import emission as a matrix (first column is CO2 and second is CO)
6. rename the emission data to 'emission'
7. save matrix as RAW.mat wherever in the same location as this program
8. Check and adjust constant
9. RUN / PUBLISH

Assumptions

1. ideal gas
2. assuming that the data will start as ambient condition for the first 30s
3. ambient pressure is obtained from daily weather data in fort collins
4. blower speed depends on test, so make sure it is correct, and displacement per volume is as indicated
5. substracting the concentration values from ambient condition to give us actual produced concentration

```
clc

clear

load('RAW.mat')

%specify font_size

font_size = 15;
```

Emission RAW

```
%CO2 and CO in volume concentration

CO2_ind = emission(:,1)./100 ;

CO_ind = emission (:,2)./1000000;




%CO plot

Figure (1)

plot(emission(:,2));

set(gca,'FontSize',font_size);

xlabel('Time (s)','FontSize',font_size);

ylabel('CO(ppm)','FontSize',font_size);

title ('CO vs time');

grid on;


%CO2 plot

Figure (2)

plot(emission(:,1));

set(gca,'FontSize',font_size);

xlabel('Time (s)','FontSize',font_size);

ylabel('CO2(%)','FontSize',font_size);

title ('CO2 vs time');   grid on;
```

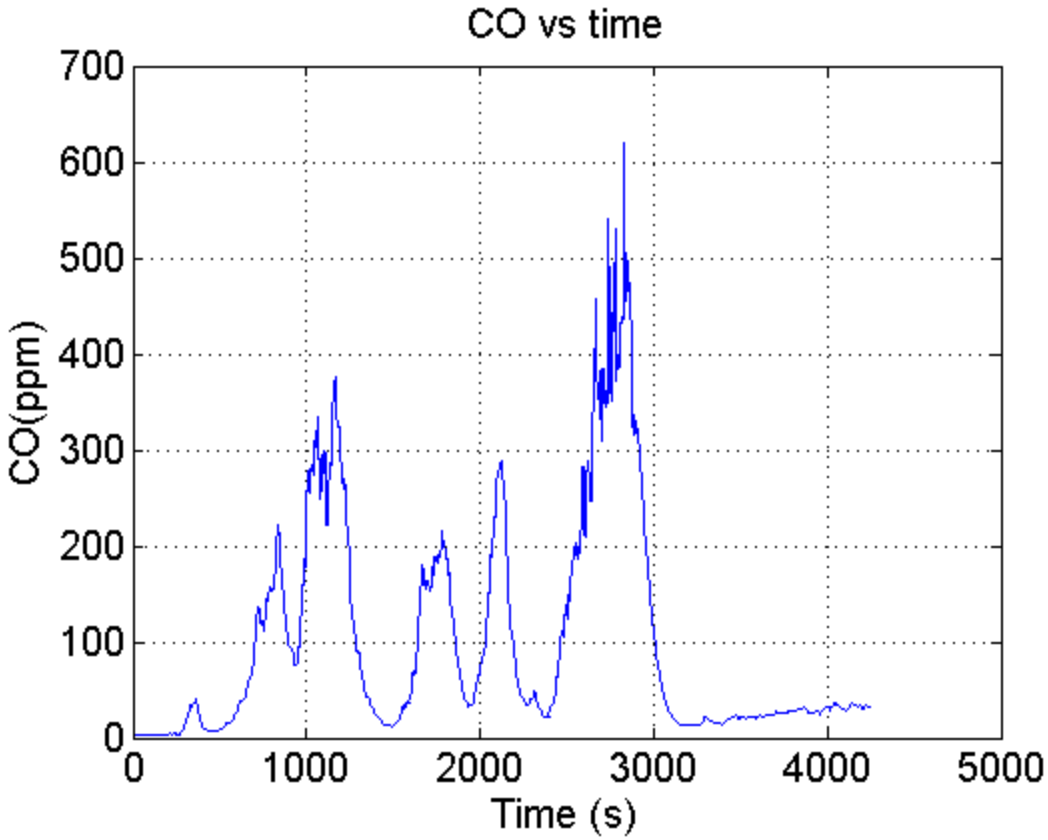
CO vs time
CO(ppm)
Time (s)
0
100
200
300
400
500
600
700
0
1000
2000
3000
4000
5000

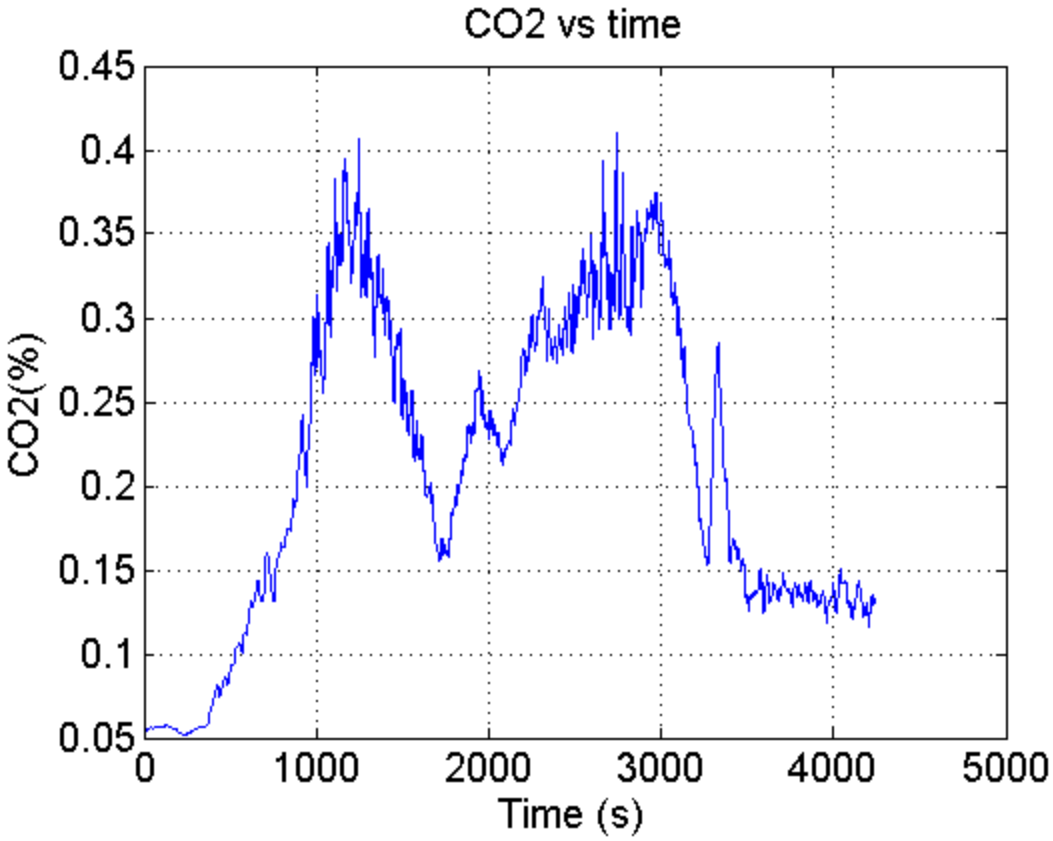
CO2 vs time
CO2(%)
Time (s)
0.05
0.1
0.15
0.2
0.25
0.3
0.35
0.4
0.45
0
1000
2000
3000
4000
5000

Constant

```
V_blower = 1500; %RPM

Q_blower_per_Rev = 0.004813;%m^3/rev

Q_blower = V_blower * Q_blower_per_Rev / 60 ; % m^3/s

R = 8.314 ; % J / mol K

Cp_H2O = 4.186 ; % (J/g c)

MW_CO = 28.01 ; %g/mole

MW_CO2 = 44 ; %g/mole

MW_C = 12.01; %g/mole

MW_air = 28.97 ;

Carbon_percent_fuel = 0.5 ;

LHV = 16.2;
```

Ambient Constant

```
time_amb = 30; %s

P_amb = 85000 ; %Pa

T_amb = 292; %K

CO2_amb = mean(CO2_ind(1:time_amb));

CO_amb = mean(CO_ind(1:time_amb));
```

Densities (kg/m^3)

```
%PV = NRT

% m/V = P * MW / R / T(K)
```

```
rho_CO = P_amb * MW_CO / (R *(T_amb)) / 1000; %kg/g conversion%

rho_CO2 = P_amb * MW_CO2 / (R *(T_amb)) / 1000;

rho_air = P_amb * MW_air / (R *(T_amb)) / 1000;
```

MCE calculation

```
CO_act = CO_ind - CO_amb;

CO2_act = CO2_ind - CO2_amb;



for zz = 1: length(CO_act)

   if CO_act(zz)<0

      CO_act(zz) = 0;

   end

end

for zz = 1: length(CO2_act)

   if CO2_act(zz)<0

      CO2_act(zz) = 0;

   end

end



%MCE is in percent

MCE = CO2_act./(CO_act+CO2_act) .*100;



Figure (3)
```

```
plot(MCE);

set(gca,'FontSize',font_size);

xlabel('Time (s)','FontSize',font_size);

ylabel('MCE (%)','FontSize',font_size);

title ('Modified Combustion Efficiency');

ylim ([50 100]);

grid on;
```

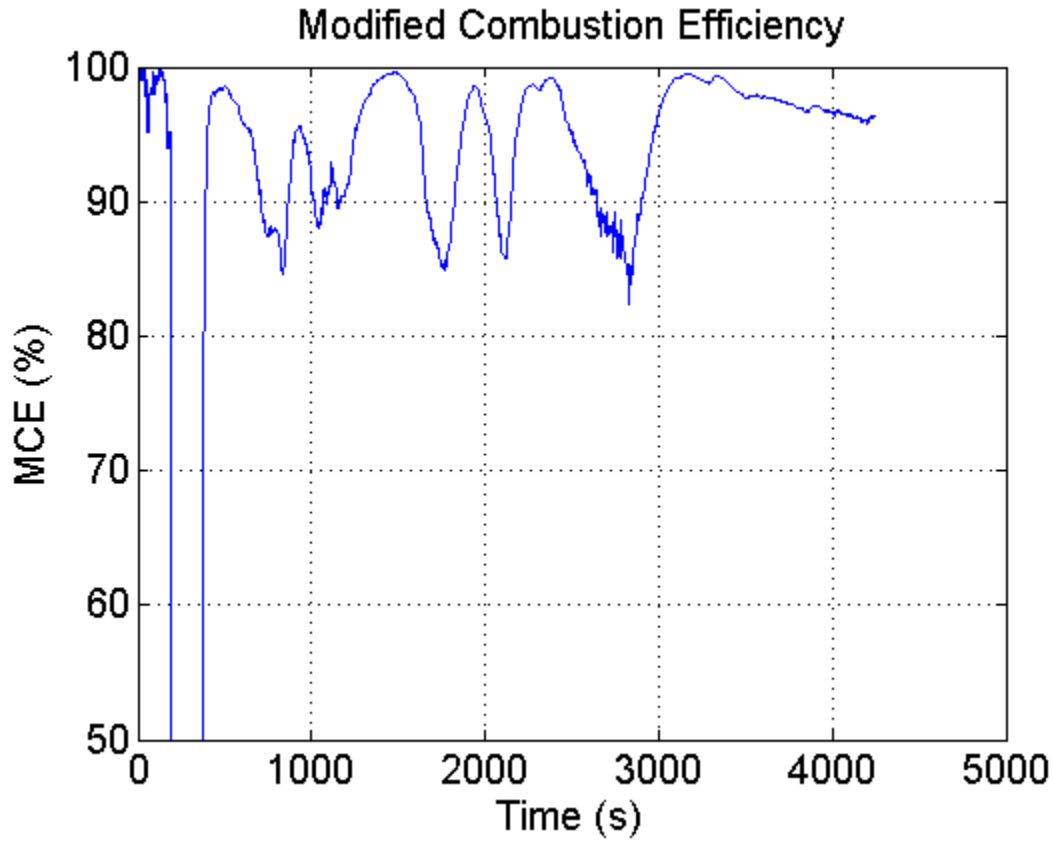

Fire Power Calculation

```
CO_mdot = CO_act .* rho_CO ./rho_air .* Q_blower *1000 ; % g/s

CO2_mdot = CO2_act .* rho_CO2 ./rho_air .* Q_blower *1000 ; % g/s
```

```
C_mdot = (CO_mdot .* MW_C ./ MW_CO) + (CO2_mdot .* MW_C ./ MW_CO2); %g/s

fuel_mdot = C_mdot ./ Carbon_percent_fuel; % g/s

fire_power = fuel_mdot * LHV ;



Figure (4)

plot(fire_power);

set(gca,'FontSize',font_size);

xlabel('Time (s)','FontSize',font_size);

ylabel('Fire Power (kW)','FontSize',font_size);

title ('Fire Power');

grid on;
```

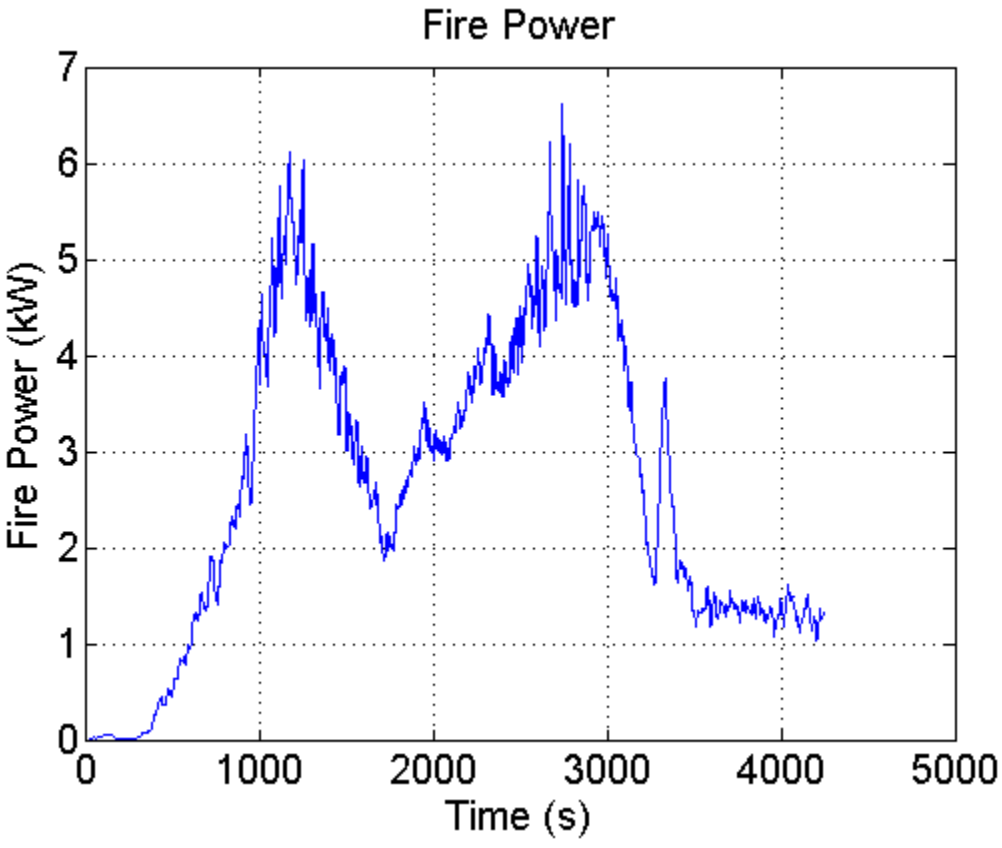

Published with MATLAB® R2012b

APPENDIX C. MASS AND ENERGY BALANCE ANALYSIS

Mass Balance Analysis

$$0.7\ CO + 0.3\ CO_2 + 0.6\ H_2 + 0.1\ H_2O + 0.65\ (O_2 + 3.76N_2) + 1.504\ N_2 \rightarrow CO_2 + 0.7\ H_2O + 3.95\ N_2$$

$$CH_{1.4}O_{0.6} + 0.4\ (O_2 + 3.76\ N_2) \rightarrow 0.7\ CO + 0.3\ CO_2 + 0.6\ H_2 + 0.1\ H_2O + 1.504\ N_2$$

The desired fuel consumption rate = **400 gr/hr**

Mole flow rate

$$\dot{n}_{fuel} = \frac{\dot{m}_{fuel}}{MW_{fuel}} = 17.39 \frac{mole}{hr}$$

Mole air required for primary air and secondary air

Primary air and secondary air

$$\dot{n}_{prim\ air} = 0.4 * (4.76) * \dot{n}_{fuel} = 33.11 \frac{mole}{hr}$$

$$\dot{n}_{sec\ air} = 0.65 * (4.76) * \dot{n}_{fuel} = 53.8 \frac{mole}{hr}$$

Finding the mass flow rate of air required

Primary air and secondary air

$$\dot{m}_{prim\ air} = \dot{n}_{prim\ air} * MW_{air} = 959.28 \frac{gr}{hr}$$

$$\dot{m}_{sec\ air} = \dot{n}_{sec\ air} * MW_{air} = 1558.836 \frac{gr}{hr}$$

Finally, find the volumetric air flow rate at Standard Temperature and Pressure

$$\dot{Q}_{prim\ air} = \frac{\dot{m}_{prim\ air}}{\dot{\rho}_{\ air}} = 17.7\ LPM$$

$$\dot{Q}_{sec\ air} = \frac{\dot{m}_{sec\ air}}{\dot{\rho}_{air}} = 51.96\ LPM$$

Ratio of secondary to primary flow rate

$$R_{Sec\ prim} = \frac{\dot{Q}_{sec\ air}}{\dot{Q}_{prim\ air}} = 2.9$$

First law drying analysis

$$m_{dot\_deuce} := .4\frac{\frac{kg}{person}}{day}$$

Density of wet Human feces from (Site Source)

$$\rho_{wet} := 1200\frac{kg}{m^3} \qquad moisture_{content} := 70\%$$

Assume after drying shape remains constant- (We do know there is a volume contraction but we leave it out here)

$$\rho_{dry} := \rho_{wet}\cdot\left(1 - moisture_{content}\right) = 360\frac{kg}{m^3}$$

Daily wet versus dry

$$m_{dot\_dry} := \left(1 - moisture_{content}\right)\cdot daily_{mass} = 0.6\,kg$$
$$m_{dot\_water} := moisture_{content}\cdot daily_{mass} = 1.4\,kg$$

Energy required to raise moisture from ambient to 100C

$$C_{p\_water} := 4.186\frac{J}{gm\cdot\Delta°C} \qquad T_i := 25°C \qquad T_f := 100°C$$
$$\Delta T := T_f - T_i = 75K$$

$Q_{temp\_increase} := m_{dot\_water} \cdot C_{p\_water} \cdot \Delta T = 439.53\,kJ$

Energy Required to vaporize moisture

$\Delta h_{vap.water} := 2.260\frac{kJ}{gm}$

$Q_{vaporization} := m_{dot\_water} \cdot \Delta h_{vap.water} = 3.164\,MJ$

Total energy required to dehydrate feces (does not include Cp of feces) per number of people and mass from above

$Q_{total\_required} := Q_{temp\_increase} + Q_{vaporization} = 3.604\,MJ$

Total energy available

$Q_{comb\_pico\_feces} := 15.312\frac{kJ}{gm}$

$Q_{available} := m_{dot\_dry} \cdot Q_{comb\_pico\_feces} = 9.187\,MJ$

$\frac{Q_{total\_required}}{Q_{available}} = 0.392$

A minimum of 39.2% of all the combustion energy is needed for the dehydration.

1 gram of dry can dry how many additional grams of wet

$percent\_moisture := .7 \quad mass\_dry := 1gm \quad available := Q_{comb\_pico\_feces} \cdot mass\_dry = 15.312\,kJ$

Guess

$mass_{wet} := 1gm$

Given

$available - mass_{wet} \cdot percent\_moisture \cdot \left(C_{p\_water} \cdot \Delta T + \Delta h_{vap.water}\right) = 0$

$Find\left(mass_{wet}\right) = 8.498\,gm$

$Q_{\Delta T} := mass_{wet} \cdot percent\_moisture \cdot \left(C_{p\_water} \cdot \Delta T\right) = 0.22\,kJ$

$Q_{vap} := mass_{wet} \cdot percent\_moisture \cdot \left(\Delta h_{vap.water}\right) = 1.582\,kJ$

$Q_{total} := Q_{\Delta T} + Q_{vap} = 1.802\,kJ$

Chemical Kinetic analysis from 2 steps overall reaction

Gasification Process

Gasification Temperature ~ 400 C

```
%general equation

%CH1.4O0.6 + n_air(O2 + 3.76 N2) => n CO + n CO2 + n H2 + n H2O + n O2 +

%n N2

%mole

n_biomass = 1;

n_air_prime = 0.4 ;

n_CO = 0.7 ;

n_CO2 = 1*n_biomass - n_CO;

n_H2 = 0.6;

n_H2O = 1.4*n_biomass/2 - n_H2;

n_O2 = (n_air_prime*2 + n_biomass*0.6 - n_CO - n_CO2*2 - n_H2O)/2;

n_N2 = n_air_prime * 3.76;

%humidity

rh = 0 ; % relative humidity

%heat of formation is taken from Combustion by Stephen R. Turns

%heat of formation @ 298 K

HHV_biomass = 15.312; %Kj/gr

MW_biomass = 12+1.4+0.6*16; %gr/mole

hf_biomass = HHV_biomass*MW_biomass *1000; %Kj/kmole

hf_O2 = 0;
```

```
hf_N2 = 0;

hf_CO = -110541; %Kj/kmole

hf_CO2 = -393546;

hf_H2 = 0;

hf_H2O= -241845;



%difference of heat of formation at 400 C (gasification)for products

dhf_CO = 12029;

dhf_CO2 = 17749;

dhf_H2 = 11749;

dhf_H2O = 14209;

dhf_N2 = 11942;

dhf_O2 = 12503;

%sum of mole*hf or reactants and products

nh1_in = -hf_biomass + n_air_prime*(hf_O2 + 3.76*hf_N2);

nh1_out = n_CO*(hf_CO + dhf_CO) + n_CO2*(hf_CO2+dhf_CO2) + n_H2*(hf_H2+dhf_H2) +
n_H2O*(hf_H2O+dhf_H2O) + n_O2*(hf_O2+dhf_O2)+n_N2*(hf_N2 + dhf_N2);

%combustion equation nh1 = (mole. entalphy) for 1st process(gasification)

q_gas = nh1_out - nh1_in
```

```
q_gas =

   1.7273e+05
```

Combustion Process

```
%general Solution

%n CO + n CO2 + n H2 + n H2O + n O2 + n N2 +n_air_sec(O2 + 3.76 N2) => n CO2 + n H2O + n O2 + n_N2

%mole

n_CO2_comb = n_CO + n_CO2;

n_H2O_comb = n_H2 + n_H2O;

n_air_sec = 0.65;

n_O2_comb = (n_CO + 2* n_CO2 + n_H2O + 2*n_air_sec -2*n_CO2_comb - n_H2O_comb)/2;

n_N2_comb = n_N2 + n_air_sec*3.76;

%difference of heat of formation at 1000 C

dhf_CO2_comb = 50149;

dhf_H2O_comb = 38963;

dhf_N2_comb = 31510;

dhf_O2_comb = 33350;

%sum of mole*hf of reactants and products

%the inlet to the second reaction is plus the air at gasification temp

nh2_in = nh1_out + n_air_sec*(dhf_O2 +3.76*dhf_N2);
```

```
nh2_out = n_CO2_comb*(hf_CO2 +dhf_CO2_comb) + n_H2O_comb*(hf_H2O + dhf_H2O_comb) +
n_O2_comb*(dhf_O2_comb) + n_N2_comb*(dhf_N2_comb);

q_comb= nh2_out - nh2_in

q_overall = q_comb + q_gas
```

```
q_comb =

  -2.1888e+05
```

```
q_overall =

  -4.6150e+04
```

Result per grams of fuel (KJ)

```
q_gas_grfuel = q_gas /1000 /(12+1.4+0.6*16)

q_comb_grfuel = q_comb/1000 /(12+1.4+0.6*16)

q_overall_grfuel = q_overall/1000 /(12+1.4+0.6*16)
```

```
q_gas_grfuel =

    7.5098

q_comb_grfuel =

   -9.5163

q_overall_grfuel =

   -2.0065
```

APPENDIX D. HOLE SIZING OF SECONDARY AIR MANIFOLD

In the making of secondary air manifold, the hole size within the manifold needs to be determined. The key to hole size is pressure drop. The holes within the secondary manifold have to have the right amount of pressure drop. Too high of pressure drop will cause the flow to be restricted, and on the other hand if pressure drop is too low, the flow won't be distributed equally.

CFD model was created with 2D laminar model. Since the purpose of this model is only to find the right size hole, air is modeled as constant properties. There is no hot gas inlet. The inlet pressure is modeled as the pressure inlet that is equal to maximum fan static pressure. The hole is modeled as a gap between the thin walls. Velocity was measured on what is the deepest penetration possible. The Figure below shows the contour of velocity and pressure between three different gaps. It was found that the optimum gap for the hole would be 0.125 inch or 1/8".

Contour of pressure

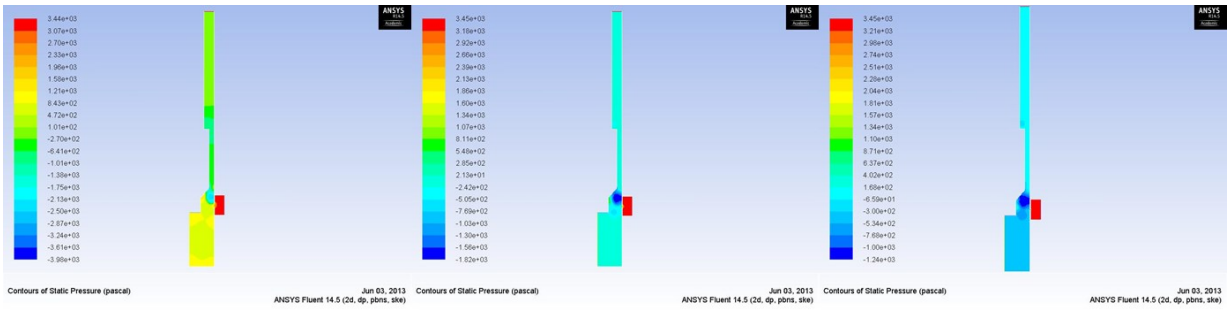

0.5 inch 0.25 inch 0.125 inch

- **Current Igniter design**
  - R = 2.5 Ω
  - V = 30 Volts
  - D (wire diameter) = 0.025“

$$Power\ of\ igniter = \frac{(30\ V)^2}{2.5\ \Omega} = \mathbf{360\ Watts}$$

- **ρ (resistivity of nichrome) = 1.1 *10^-6 Ωm**
  - Roberston, Ian. *Electronics for Electricians and Engineers*. New York, NY: Industrial Press, 1987: 34
- **Calculation of 12 V igniter**

$$P1 = P2$$
$$\frac{V1^2}{R1} = \frac{V2^2}{R2}$$
$$360\ Watts = \frac{12^2}{R2}$$
$$\boldsymbol{R2 = 0.4\ \Omega} \qquad \boldsymbol{R = \frac{\rho * L}{A}}$$

Assuming that the same wire is used which implied equal resistivity, and have equal length (roughly) , what is the diameter required to output the same power with 12 V battery supply?

$$\frac{R1}{R2} = \frac{\frac{\rho L}{A1}}{\frac{\rho L}{A2}} = \frac{A2}{A1} = \frac{\frac{\pi}{4} * D2^2}{\frac{\pi}{4} * D1^2} = \frac{D2^2}{D1^2}$$
$$\frac{2.5\Omega}{0.4\Omega} = \frac{D2^2}{0.025^2}$$
$$D2 = \sqrt{0.025^2 * \frac{2.5}{0.48}} = \mathbf{0.0625"}$$

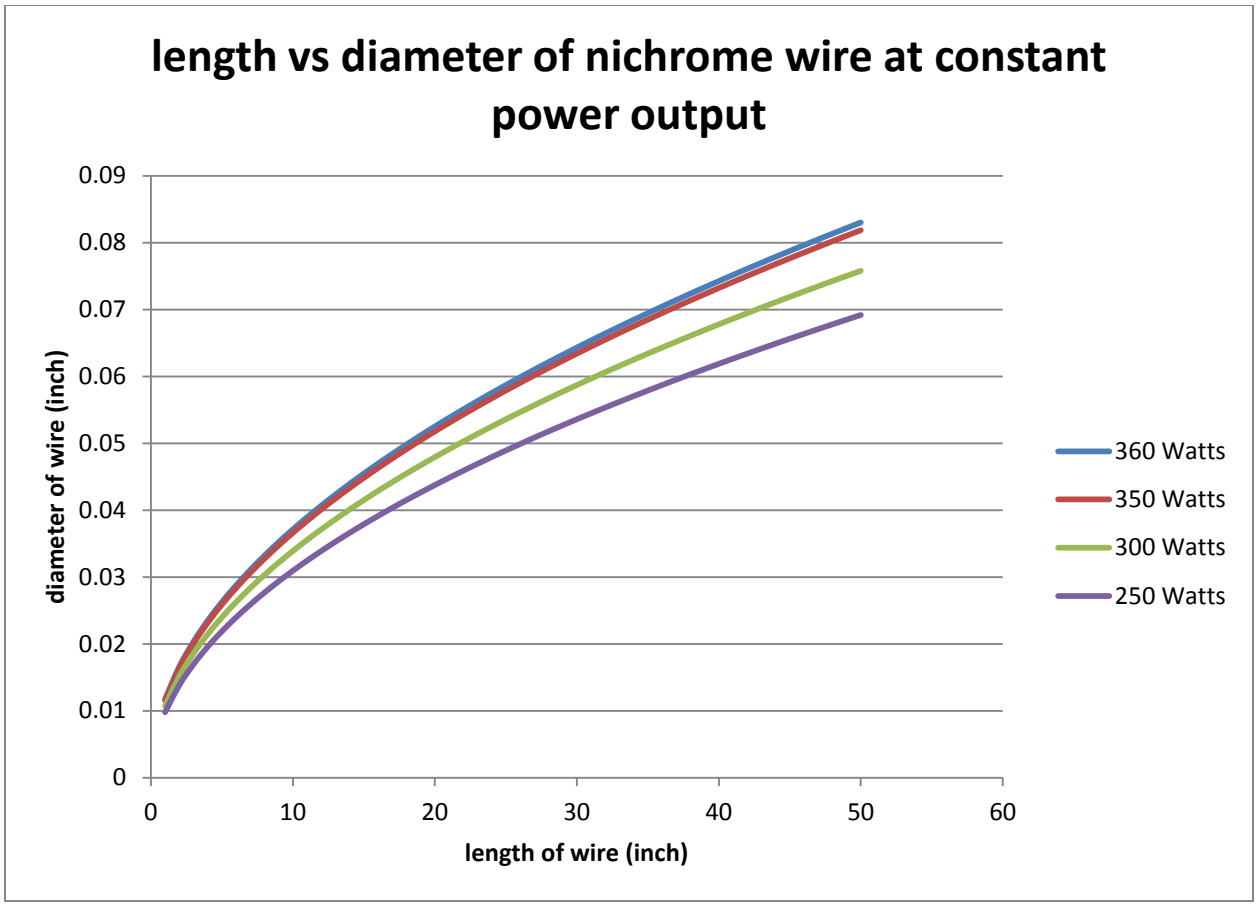
length vs diameter of nichrome wire at constant power output
diameter of wire (inch)
0.09
0.08
0.07
0.06
0.05
0.04
0.03
0.02
0.01
0
0
10
20
30
40
50
60
length of wire (inch)
360 Watts
350 Watts
300 Watts
250 Watts

APPENDIX F. ANEMOMETER CALIBRATION

Transitioning to DC electric fans means the flow measurement could no longer be done using rotameter. Instead it was to be done with the hot wire anemometer. A rotameter is the volumetric flow rate measurement device that measure SCFM, while an anemometer is a device that measures the velocity and temperature of the air. These two devices have different characteristics and therefore need to be calibrated. In order to calibrate the anemometer with the rotameter, the mass flow rates of both devices have to be same by conservation of mass. The rotameter was located on the inlet of the flow hooked up to the pressurized air, while the anemometer was located on the 4" galvanized exhaust duct. All the experiment was done on the cold flow where there is no chemical reaction took place.

$$\dot{m}_{inlet} = \dot{m}_{outlet}$$

Rotameter

measures the volumetric flow rates of SCFM needs to be converted to mass flow rate (kg/s)

$$\dot{m}_{inlet}\left(\frac{kg}{s}\right) = \dot{Q}_{rota}(SCFM) * \rho_{air}\left(\frac{kg}{m^3}\right) * 4.7195 * \frac{10^{-4}\left(\frac{m^3}{s}\right)}{1\,SCFM}$$

Where:

1. m_inlet = inlet mass flow rate of the compressed air
2. Q_rota = indicated volumetric flow rate of rotameter
3. P_air = density of air

Where the air density were obtained by ideal gas law

$$\rho_{air} = \frac{\left(P_{amb}(kPa) * MW_{air}\left(\frac{kg}{mol}\right)\right)}{R_u\left(\frac{J}{mol\,K}\right) * T_{amb}(K)}$$

Where:

1. P_amb = ambient pressure obtained from weather data
2. MW_air = 28.97 kg/mol
3. R_u = 8.314 J/mol K
4. T_amb = ambient temperature obtained from thermocouple

Anemometer

Measures the velocity and temperature of the air and it should be converted into mass flow rate

$$\dot{m}_{outlet}\left(\frac{kg}{s}\right) = v_{air}\left(\frac{m}{s}\right) * A_{duct}(m^2) * \rho_{air}\left(\frac{kg}{m^3}\right)$$

Where:

1. m_outlet = outlet mass flow rate
2. v_air = anemometer air velocity reading
3. A_duct = cross sectional of 4" dia galvanized duct
4. P_air = Density of air calculated using equation 3 with temperature data from the anemometer

Initial result

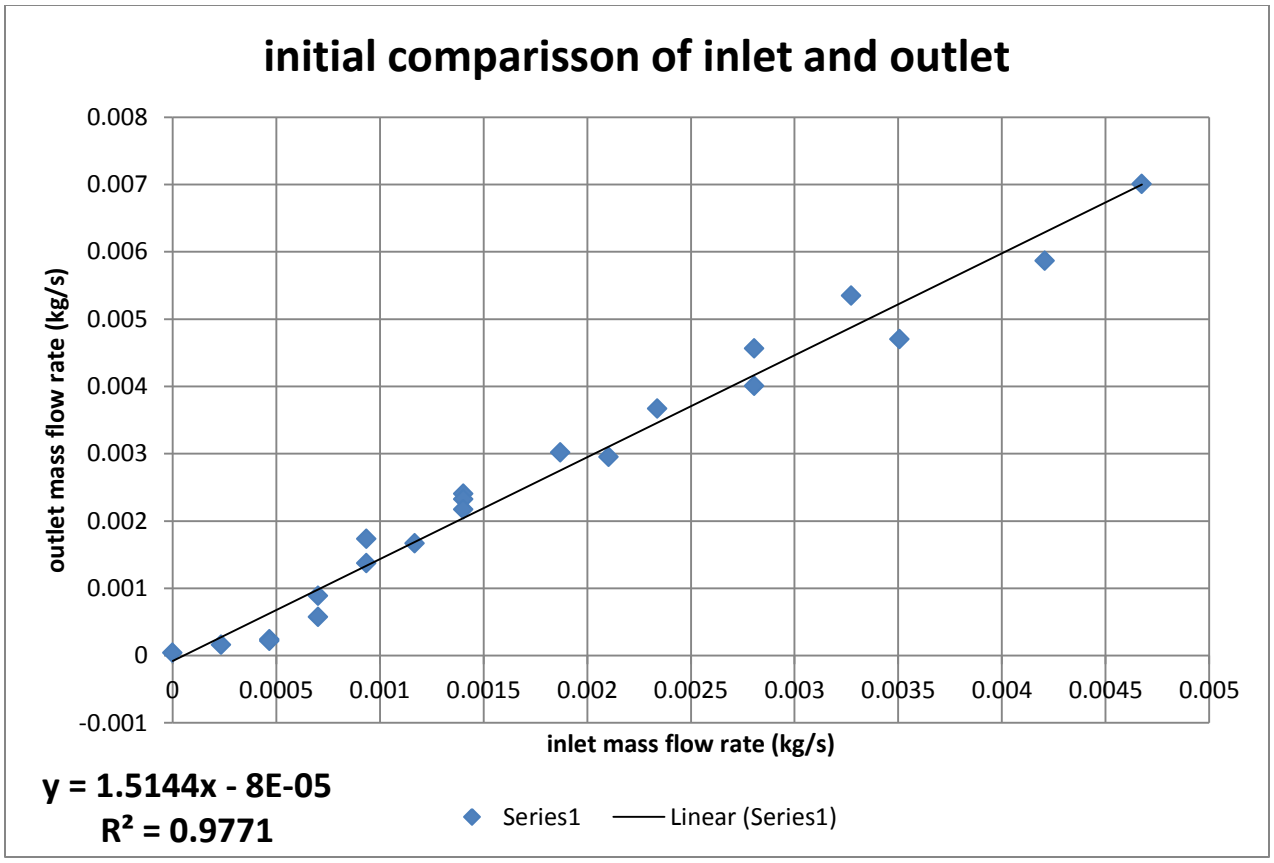

The trend shows that the outlet mass flow rate has a factor of 1.5144 times more the inlet mass flow rate. Ideally, the trend should follow the conservation of mass

$$outlet\ (y) = inlet\ (x) + 0$$

There has to be some mistake within the calculation. After all variables were checked, the variable that was not able to be justified was the cross sectional area of the exhaust duct. Initially, the assumption was that the duct had a perfect circle with 4" in diameter. In reality, the shape of the galvanized duct was not a perfect circle and the 4" diameter of the duct was nominal instead of exact.

Adjustment was made on the value of the cross sectional area through iterative process until the trend lines up with the ideal case.

Initial area (in^2)	Adjusted area (in^2)	Percent difference (%)
12.567	8.298	40.918

Justifications were made by tracking the area into solidworks and found the area to be 12.12

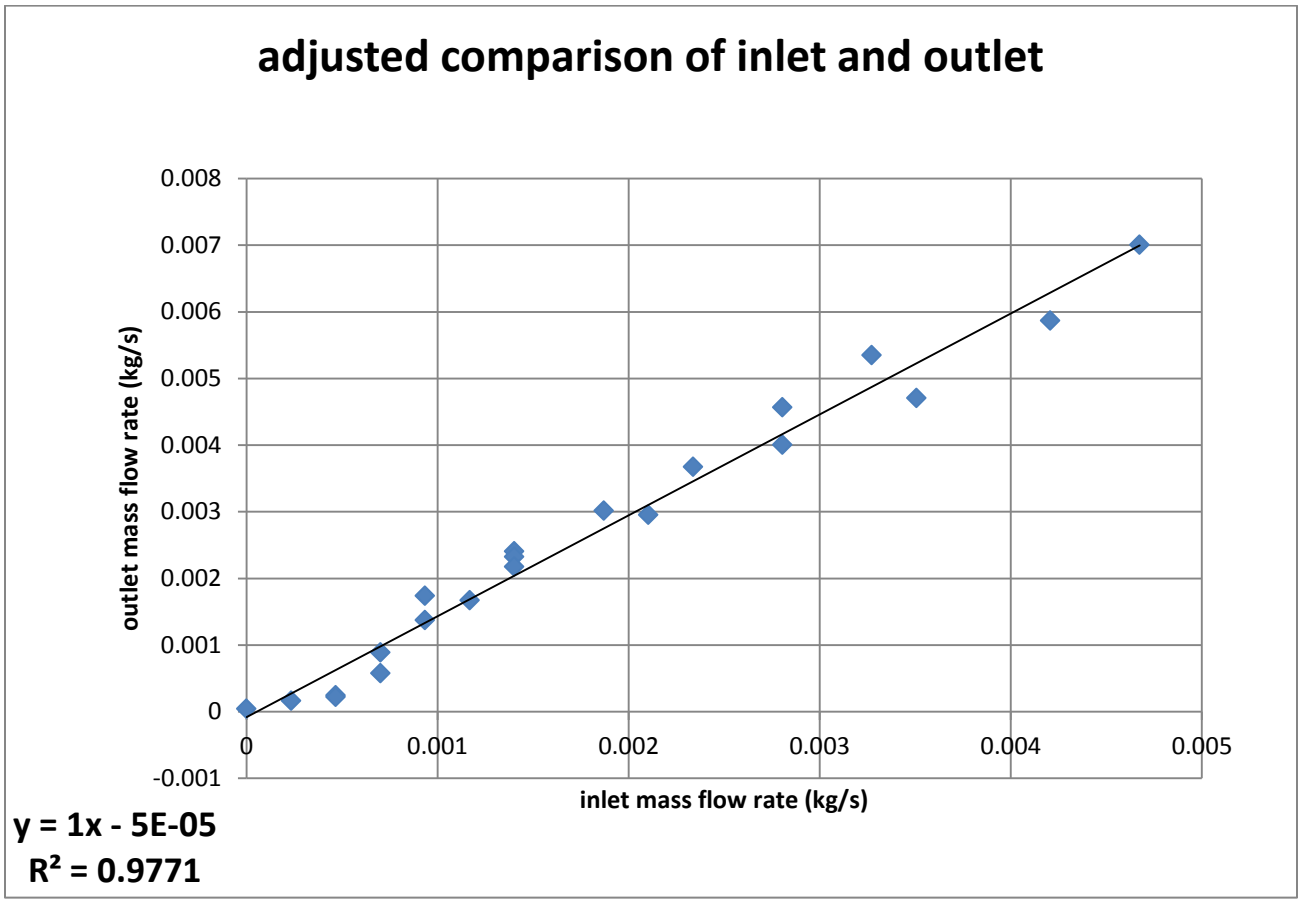

Conservation of mass

From the conservation of mass

APPENDIX G. EXPERIMENTAL APPARATUS

Rotameters

As it was explained on section 2.5, the semi-gasifier burner has two air inlets for primary and secondary air. The flow rate for both primary and secondary are crucial variables to its performance. Rota-meters were used to measure the flow rate of primary and secondary air. The rotameter measures the volumetric flow rate in cubic feet per minute (CFM). The rotameters for this application are shown in Figure 13.

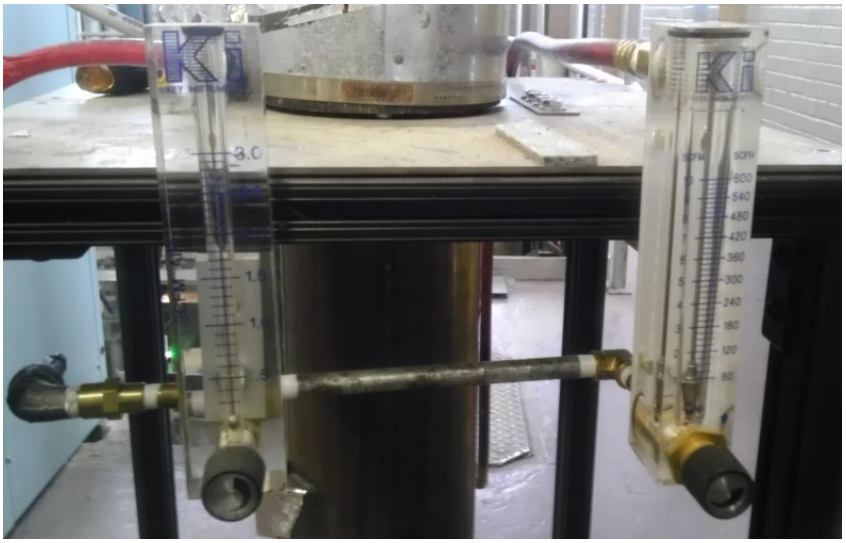

Non Dispersive Infrared Sensor (NDIR) gas analyzer

NDIR is a gas analyzer device that provides gas emissions in real time. An infrared sensor measures the infrared light absorption by the gas molecules. In this case, CO and CO_2 absorptions are measured. The device itself needs to be calibrated by the span gas that is available in the lab. Lionberg [52] did the calibration test needed for this application. The calibration showed that the device measurement is delayed for about 30 seconds. The data obtained from the fume hood also have to be calibrated for dilution factor. The following Figure

is the device of Siemens Ultramat 6 NDIR that measures the emission that comes from the fume hood.

ECOM-CN gas analyzer

ECOM is portable equipment to measure CO and CO_2 emission using electrochemical process. Since the ECOM is portable, it is capable to measure emission from the stack without any dilution factor. This device is primarily used as a comparison study against the NDIR. The following Figure is ECOM® with CN model.

Analysis Software

Various software were used for analysis throughout the development.

- SolidWorks : 3D modeling
- Fluent : CFD simulation software
- Matlab : math processing
- MathCad : math processing

APPENDIX H. TRL 3 GASIFIER EXPERIMENT

Another experiment that was conducted for this TRL version was the gasification experiment. This experiment was conducted as a test for the burner to operate as a gasifier. The purpose of this experiment is to understand the effect of secondary air to the performance of the burner. Temperature data was collected for this experiment to see how the temperature differs from the combustion temperature.

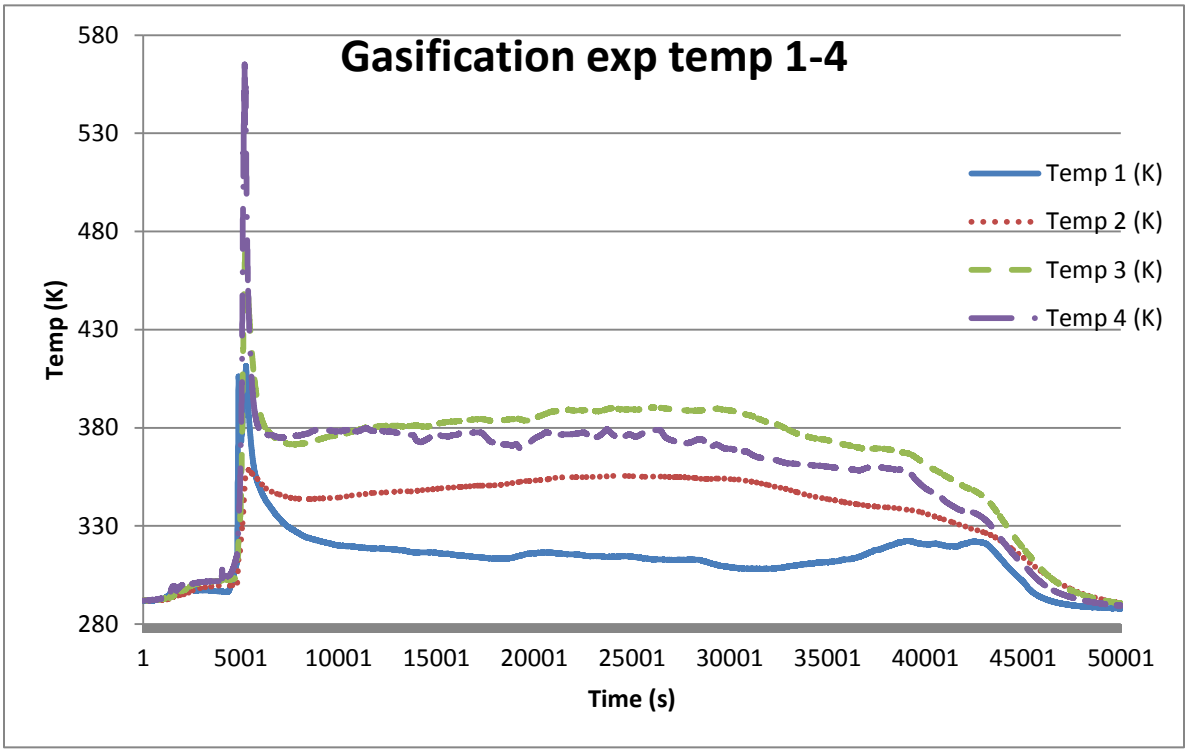

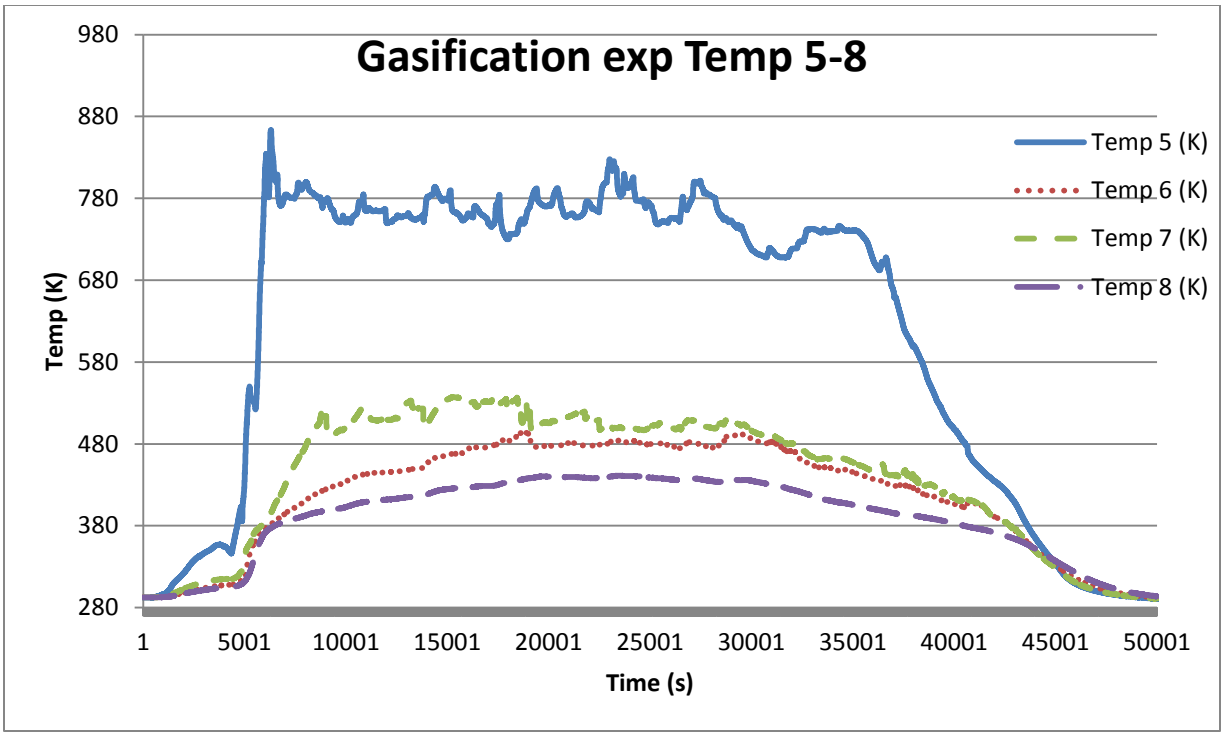

This experiment was conducted by igniting the fuel using the glow plug and intake of primary air. After the gas was produced, secondary air was not turned on. This resulted in a gas production that was oxygen deprived. The gas did not combust and cooled down by the concentric exhaust. The experiment was conducted for a period of time until the temperature indicated back at room temperature. It took about 14 hours until the temperature decreased back to room temperature. The temperatures on all the thermocouples stayed constant on most of the experimental period. This constant temperature showed that the fuel was not consumed at the same time. Thermocouple 8, which measured the top of fuel bed temperature, indicated that the temperature was below 473K. This meant that pyrolysis did not occur at the top of the fuel bed.

Despite the temperature result that fulfilled the temperature criterion, there are two major problems that resulted from the experiment. First is the charcoal leftover. After the whole night the experiment was left behind, the leftover was about 20% of the initial weight. This implied that the whole 14 hours, the experiment stops after de-volatilization was completed, and did not

go into charcoal region. Fuel bridging might be an issue with charcoal leftover inside the fuel bed. The second problem is the emission. The emission from the gasifier experiment is all syngas. Because there is no combustion, all the syngas cannot be converted to CO2 and H2O. This resulted in a highly visible smoke with high concentration of CO and H2.